

**PETROGENESIS AND STRUCTURAL CONTROL OF  
PEGMATITES AROUND KWARRA AREA: IMPLICATIONS ON  
RARE METAL MINERALIZATION, PART OF KURRA SHEET  
189 SW, NORTH CENTRAL NIGERIA**

**BY**

**SUNDAY, Adedeji Ebenezer B.Sc Geology (NSUK), 2010  
(P14SCGL8004)**

**IN PARTIAL FULFILLMENT OF THE REQUIREMENTS FOR THE  
AWARD OF THE DEGREE OF MASTER OF SCIENCE IN GEOLOGY  
(MINERAL EXPLORATION)**

**DEPARTMENT OF GEOLOGY  
FACULTY OF SCIENCE  
AHMADU BELLO UNIVERSITY, ZARIA  
NIGERIA**

**OCTOBER, 2019**

## DECLARATION

I, Sunday Adedeji Ebenezer, with registration number P14SCGL8004 declare that the work in this thesis entitled “**Petrogenesis and Structural Control of Pegmatites Around Kwarra Area: Implications on Rare Metal Mineralisation**” Part of KurraSheet 189 NW, North Central Nigeria” has been carried out by me in the Department of Geology. The information derived from the literature has been duly acknowledged in the text and a list of references provided. No part of this thesis was previously presented for another degree or diploma at this or any other institution.

.....

.....

.....

Name of student

Signature

Date

## CERTIFICATION

This work entitled “**Petrogenesis and Structural Control of Pegmatites Around Kwarra Area: Implications on Rare Metal Mineralisation**” Part of Kurra Sheet 189 NW, North Central Nigeria” by Sunday Adedeji Ebenezer meets the regulations governing the award of the degree of Masters of Science in Geology (Mineral Exploration) of Ahmadu Bello University, Zaria and is approved for its contribution to knowledge and the literary presentation.

Sunday Adedeji Ebenezer .....

Signature

Date

DR. A.A Ibrahim

Chairman Supervisory Committee .....

Signature

Date

DR. B.A. Jolly

Member, Supervisory Committee .....

Signature

Date

Prof. T. Najime

Head of Department .....

Signature

Date

Prof. Sani A. Abubakar

Dean, School of Postgraduate Studies .....

Signature

Date

## **DEDICATION**

I dedicate this work to the memory of my late sisters, Omoniyi Ajayi and Omotayo Ajayi

## ACKNOWLEDGEMENT

I thank God almighty without whom I can do nothing.

My heartfelt gratitude goes to my supervisors Dr. A.A Ibrahim and Dr. B.A. Jolly my external examiner Prof. Saidu Baba and my internal examiners Prof. Ogunleye Paul and Dr. Magaji for their immense contribution to the success of this work. Thanks for your support and guidance.

I specially appreciate my parents Mr. and Mrs. Sunday Ajayi and my family members Olabisi, Oluwafunmilayo, Victoria, Víctor, Pst. Abdul, Tosin, Seyi, Daniella, Zenith and Excel for their support and encouragement.

Special thanks to my dear friend Susan Zarafi for her care and immense support.

I also greatly appreciate my Pastor and General Overseer Apostle Abayomi Adekoya for his support and prayers. My sincere gratitude also goes to Pst. Felix Emmanuel and the entire members of Wisdom for Life and Power Church Farin Gida, for their prayers and encouragement. Joy Adava, Japhet Haruna, Raliya Hayatu, Sa'eed Adekoge, Usman Abdulraman, Ibrahim Waziri, Adeyinka Akanbi, Brenda Agidi, Lukman Adamu and Prestige Business Centre to mention a few for their encouragement and support.

I am very grateful for the Mai Angwa of Abu community Mr. P Jatau for the warm welcome and support shown to me during my field mapping. I also appreciate Mr Abbas for the warm hospitality given to me during my stay in Kwarra.

## ABSTRACT

The study area is underlain by Basement Complex rocks and Younger Granites. The Basement Complex rocks comprise amphibolite, migmatite gneiss, banded gneiss, granite gneiss and albitised granite, while the Younger Granite rock is alkali granite. Pegmatites and dolerites represent the minor rocks types in the study area. The pegmatites are grouped into two types; the quartz-muscovite-pegmatite and quartz-feldspar-pegmatite. The principal stress directions in the study area are N-S, NE-SW, and NNE-SSW with minor ENE-WSW, E-W trends. The quartz-muscovite-pegmatites are relatively rich in HFS elements such as Zr, Ga, and Nb and Ta, having values above the average crustal abundance of 165ppm, 17ppm, 25ppm and 2.2 ppm respectively. It is highly concentrated in lithophile element Rb but depleted in Sr and Ba. By contrast, the quartz-feldspar pegmatite is depleted in HFS elements namely Zr, Ga, and Nb and Ta and the LILE Sr and Ba but enriched in Rb although not up to the level of the quartz-muscovite-pegmatites. The quartz-muscovite-pegmatite is of the rare metal class akin to the LCT type and has higher concentration of Be, Cu, Ga, Nb, Sn, Ta, Ti, V, W, Y, Zn and Zr compared to the quartz-feldspar-pegmatite which is of the barren class. The pegmatites and albitized granite have been affected to varying degrees by sodic metasomatism which led to the replacement of K by Na in the feldspars and increase in the uranium concentration. The albitized rock types have low  $\sum$ REE, Sr and Ba while Rb is progressively depleted with increasing degree of albitisation. Although the rare metal pegmatites lack clearly defined development of Ta and Cs minerals and columbite-tantalite series, it is relatively high Sn concentration (up to 798 ppm), amounts high enough to be associated with a cassiterite mineralization. Based on the trace element concentration of the pegmatites, the petrogenesis of the rare metal pegmatite can be taken to be as a result of the partial melting of a deeply buried S-type fertile granite while the barren one (quartz-feldspar-pegmatite) is simply derived from late stage residual melts of less evolved granitic parent and trace element leached due to the intense effect of metasomatism.

## Contents

DECLARATION.....	i
CERTIFICATION.....	ii
DEDICATION.....	iii
ACKNOWLEDGEMENT.....	iv
ABSTRACT.....	v
TABLE OF CONTENT.....	vi
CHAPTER ONE.....	1
INTRODUCTION.....	1
1.1 Location and Accessibility of the Study Area.....	1
1.2 Climate and Vegetation.....	2
1.3 Relief and Drainage.....	3
1.4 Statement of Research Problem.....	4
1.5 Aim and Objectives.....	5
1.6 Scope of the Study.....	6
CHAPTER TWO.....	7
LITERATURE REVIEW.....	7
2.1 Regional Geology.....	7
2.2 The Basement Complex.....	8
2.3The Migmatite – Gneiss Complex (MGC).....	10
2.4The Schist Belt (Metasedimentary and Metavolcanic Rocks).....	11
2.5The Older Granites (Pan African Granitoids).....	12
2.5.1Nigerian Pegmatites.....	12
2.5.2Barren and Rare Metal Pegmatites.....	14
2.5.3Structural and Geochemical characterisation of Nigerian pegmatites.....	16
2.5.4Evolution of pegmatites from a granitic melt.....	17
2.6 Undeformed Acid and Basic Dykes.....	19
2.7 Younger Granites.....	19
CHAPTER THREE.....	22
MATERIALS AND METHODS.....	22
3.1 Introduction.....	22
3.2Desk Study.....	22

3.3	Field Method.....	22
3.4	LABORATORY ANALYSES.....	23
3.4.1	Petrographic Methods .....	23
3.4.2	Sample Preparation for Geochemical Analysis.....	24
3.4.3	Analytical Technique .....	24
CHAPTER FOUR.....		26
RESULTS.....		26
4.1	Field Geology and Petrology .....	26
4.1.2	Albitised Granite .....	30
4.1.3	Granite Gneiss.....	32
4.1.4	Banded gneiss .....	35
4.1.5	Migmatite Gneiss .....	37
4.1.6	Amphibolite .....	39
4.1.7	Pegmatite .....	42
4.1.8	Dolerite.....	45
4.2.2	Foliation .....	46
4.2.3	Joints	48
4.2.4	Veins	49
4.2.5	Folds	52
4.2.6	Pinch and Swell .....	53
4.2.7	Fault	54
4.3	Lineament analysis.....	55
4.4	GEOCHEMISTRY .....	59
4.4.1	Introduction.....	59
4.4.2	Major Element Geochemistry.....	59
4.4.	Trace Element Geochemistry.....	70
4.4.5	Rare Earth Element (REE) Geochemistry .....	76
4.4.5	Tectonic Discrimination Diagram .....	85
CHAPTER FIVE.....		88
DISCUSSION .....		88
5.1	Field Relationship .....	88
5.2	Geochemistry and Structural Geology of the Polycyclic Basement Rocks .....	89
5.3	Geochemistry and Structural Geology of the Granites .....	92

<b>5.3.1 Alkali Granites</b> .....	92
<b>5.3.2 Albitised Granite</b> .....	93
<b>5.4 Geochemistry and mineral potential of the pegmatites</b> .....	95
<b>5.5 The Role of Hydrothermal Alteration on the Geochemistry and Mineralogy of the Granitoids</b> . .....	99
<b>5.6 Petrogenesis</b> .....	102
<b>CHAPTER SIX</b> .....	107
<b>CONCLUSION AND RECOMMENDATION</b> .....	107
<b>6.1 Conclusion</b> .....	107
<b>6.2 Recommendation</b> .....	109
<b>6.3 Contribution to Knowledge</b> .....	109
<b>REFERENCES</b> .....	110

## **List of Tables**

Table 1: Major oxide compositions of the rocks in the study area.....	60
Table 2: CIWP Norm for the granitic rocks of the study area.....	61
Table 3: Concentration of some selected trace elements and some important elemental ratios in the rocks of the study area.....	71
Table 4: Concentration of rare earth elements in the rocks of the study area-----	.72
Table 5: Average abundances and ranges of some trace elements, rare earth elements and selected ratios from upper continental crust values.....	73

## List of Figures

Fig 1: Topographical map of the study area parts of Kurra sheet 189SW .....	2
Fig. 2: Relief map of the study area.....	3
Fig 3: Drainage Map of the study area.....	4
Fig 4: Simplified map of the geology of Nigeria.....	8
Fig 5: Location of the Nigerian Basement Complex between the West African and Congo Cratons and in relation to Hoggar and Borborema Provinces.....	9
Fig. 6: Geological map of Nigeria showing the locations of barren and rare-metal pegmatites.....	13
Fig. 7: Geological Sketch map of central and south-west Nigeria showing the location of the Wamba pegmatite field (study area) and the distribution of Pan-African Older Granites and pegmatites.....	14
Fig 8: Geological map of the study area.....	27
Fig 9: Rose diagram of foliation in the banded gneiss of the study area.....	47
Fig 10: Rose diagram of joints in the rocks of the study area.....	49
Fig 11: Rose diagram of pegmatite veins in the study area showing the NE-SW dominant trend.....	51
Fig. 12: Rose diagram of quartzo-feldspathic veins showing the NE-SW dominant trend in the banded gneiss of the study area.....	52
Fig. 13: Structural lineament map of the study area.....	56
Fig. 14: Lineament density map of the study area (the denser lineaments are indicative of the intensity of rock fracturing).....	57
Fig. 15: Rose diagram of structural lineament trends of the study area.....	58
Fig. 16: Harker plot of Al <sub>2</sub> O <sub>2</sub> , CaO, K <sub>2</sub> O and Na <sub>2</sub> O against silica (SiO <sub>2</sub> ) for the granite suites in the study area.....	64

Fig. 17: A/CNK – A/NK plot for the granitoids in the study area.....	66
Fig. 18: Fe (total)/(Fe (total)+MgO) versus SiO <sub>2</sub> .....	67
Fig 19: Na <sub>2</sub> O + K <sub>2</sub> O-CaO versus SiO <sub>2</sub> .....	67
Fig. 20: Na <sub>2</sub> O+K <sub>2</sub> O vs. SiO <sub>2</sub> for the granite suites in the study area.....	68
Fig. 21: Ternary normative Ab-Or-An diagram for the rocks in the study area.....	69
Fig. 22: A/CNK vs SiO <sub>2</sub> plot of rocks from the study area.....	70
Fig. 23: Spider diagrams for all the rocks samples normalized to average crust.....	74
Fig. 24: Chondrite normalized plot showing rare elements (REE) pattern in the metamorphic rocks from the study area.....	78
Fig. 25: Chondrite normalized plot showing rare elements (REE) pattern in the Pegmatites in the study area.....	79
Fig. 26: Chondrite normalized plot showing rare elements (REE) pattern in the granites from the study area.....	79
Fig. 27: Plot of Rb-Ba-Sr for the granitic rocks in the study.....	80
Fig. 28: Modified Triangular Ti-Sn-(Nb+Ta) Plot for albitized granite and pegmatites in the study area.....	81
Fig. 29: Plot of Rb vs Na/K showing the progressive depletion of Rb with the advancing albitisation of K-feldspar.....	81
Fig. 30: Plot of Ta Versus Cs tor The Muscovites of the pegmatites in the study area.....	82
Fig. 31: Plot of Ta Versus K/Cs For The Muscovites of Pegmatites in the study area.....	83
Fig. 32: Plot of Ta versus Ga for the pegmatites in the study area.....	83
Fig. 33: Plot of K/Rb versus Cs for the pegmatites in the study area.....	84
Fig. 34: Classification of the pegmatites using the plots of K/Rb versus Cs.....	84
Fig. 35: Nb/Ta versus Zr/Hf diagram differentiating the barren granites and granites hosting ore deposits.....	85
Fig. 36: Rb vs. Y+Nb tectonic discrimination diagram.....	86

Fig. 37: Plot of  $\text{FeO}_t / \text{Mgo}$  vs.  $\text{Zr+Nb+Ce+Y}$  for discriminating A-type granites.....86

Fig. 38: Triangular plot of Nb-Y-Ce for distinguishing the alkali granites in the study area into A1 and A2 granite.....87

## List of Plates

Plate 1: Photograph of a hand specimen of the alkali granite in the study area.....	29
Plate 2: Photomicrograph of alkali granite under (a) Cross Polarized Light (XPL) and (b) Plane Polarized Light (PPL).....	29
Plate 3: Photograph showing albitised granite outcropping in the study area.....	31
Plate 4: Photomicrograph of Albitised granite under (a) (XPL) and (b) (PPL).....	32
Plate 5: Photograph showing a granite gneiss outcrop.....	34
Plate 6: Photomicrograph of granite gneiss under (a) PPL and (b) XPL.....	34
Plate 7: Photograph of banded gneiss with quartz and quartzo-feldspathic veins.....	36
Plate 8: Photomicrograph of banded gneiss under (a) PPL and (b) XPL.....	36
Plate 9: Photograph of migmatite gneiss with ptygmatitic folding.....	38
Plate 10: Photograph of migmatite showing pre-migmatisation structures.....	38
Plate 11: Migmatite gneiss under (a) (XPL) and (b) (PPL).....	39
Plate 12: Photograph of a hand Specimen of amphibolite rock in the study area.....	41
Plate 13: Photomicrograph of amphibolite under (a) (XPL) and (b) (PPL).....	41
Plate 14: a. Photograph of quartz-feldspar-pegmatite intrusion into migmatite gneiss.....	43
Plate 14: b. Photograph showing a narrow zone of tourmalinisation around the contact between quartz-feldspar-pegmatite and the host rock.....	43
Plate 15: (a) Photograph showing quartz-muscovite-pegmatites boulder in the study area..	44
Plate 15: (b) Photograph showing a whitish quartz-muscovite-pegmatites intrusion in granite gneiss.....	44
Plate 16 (a): Photograph of highly deformed quartz-muscovite-pegmatites trending NE.....	44
Plate 16 (b): Photograph showing the deformed nature of the quartz-muscovite-pegmatites in uplifted region.....	44
Pate 17 (a): Photograph of dolerite dikes intrusion into granite gneiss.....	45
Plate 17 (b): Photograph of dolerite dike intrusion into Migmatite gneiss in the study area.....	45

Plate 18: Photograph of foliation structure in the banded gneiss of the study area.....	47
Plate 19: Photograph of joints in the granite gneiss of the study area.....	48
Plate 20: (a) Pegmatite veins that intruded the migmatite gneiss of the study area.....	50
Plate 20 (b): Photograph showing quartzo-feldspathic veins in the banded gneiss within the study area.....	50
Plate 21: (a) Photograph of asymmetrical folding observed on the banded gneiss.....	52
(b) Photograph of ptygmatic folding on the migmatite gneiss.....	52
Plate 22: Phototgraph of a pinch and swell structures in biotite gneiss.....	53
Plate 23: Photograph showing dextral fault of quartz veins in the banded gneiss.....	54

# CHAPTER ONE

## INTRODUCTION

### 1.1 Location and Accessibility of the Study Area

The study area lies between longitudes  $8^{\circ}30'00''\text{E}$  and  $8^{\circ}45'00''\text{E}$  and between latitudes  $9^{\circ}00'00''\text{N}$  and  $9^{\circ}8'00''\text{N}$  (Fig. 1). The area covers parts of Kurra Sheet 189 SW, in the North-Central part of Nigeria (Fig. 1). It has an overall land area of  $410.7\text{ km}^2$  that includes part of Sanga Local Government Areas of Kaduna state and Wamba Local Government Area of Nasarawa State. Major settlements in the area include Kwarra, Arum, Kanje, Marhai, Abu and Ragga. The area is accessible through five minor roads, namely; Abu –Ragga Gari road, Ragga–arimaw road, Gwongwon-Arum, Arum-Kwarra, Kwarra-Marhai, Kanje-Mangar. There is also a network of footpaths and cattle tracks which makes the study area very accessible by foot and by vehicle.

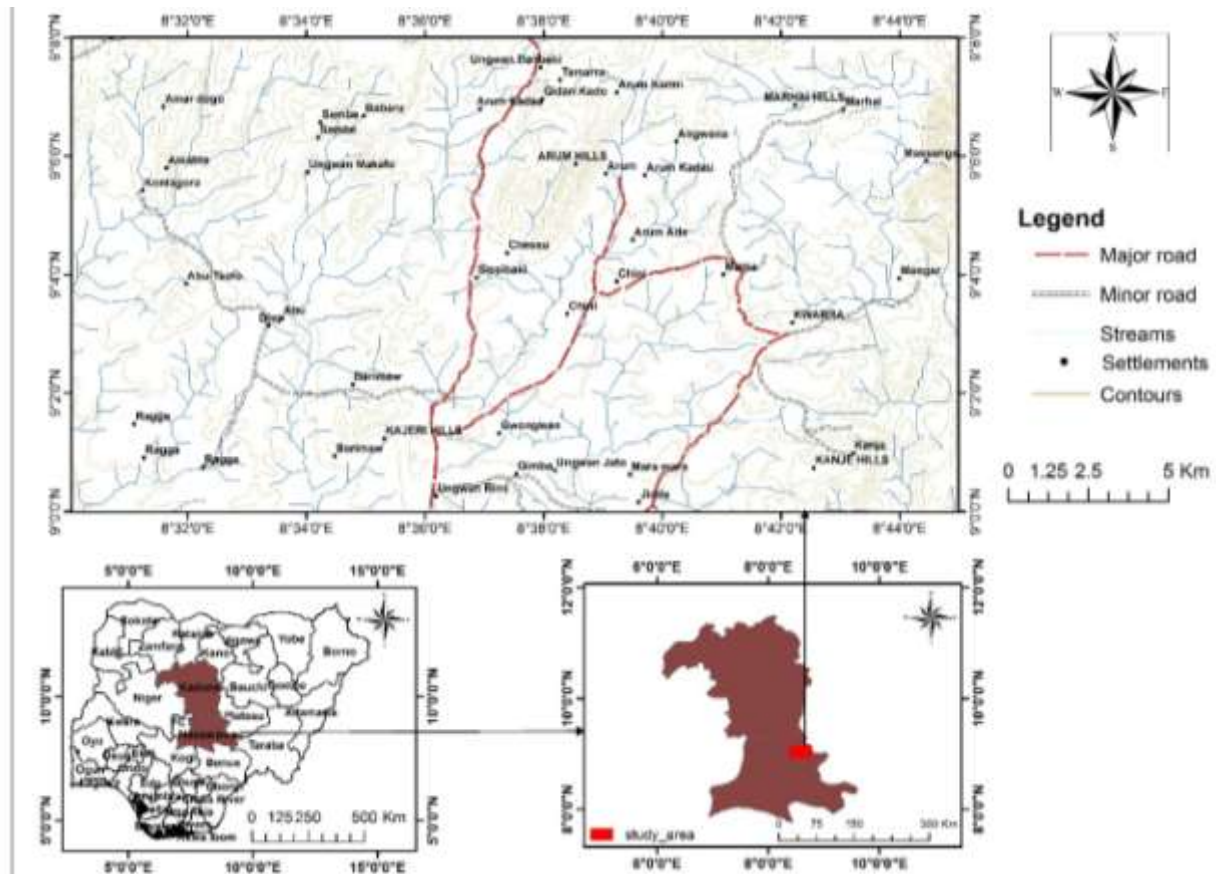


Fig. 1: Topographical map of the study area parts of Kurra sheet 189SW modified after Fed. Surveys, Nigeria 1967

## 1.2 Climate and Vegetation

The climate of Nasarawa is predominantly tropical with an average temperature of 30°C and an average rainfall of 1300mm. There are two major seasons, wet and dry season. The former begins from April and terminates in October with August and September as the wettest months. The latter starts from November and ends in March, with February and March as the hottest months.

The study area falls under the Sudan Savanna vegetation belt of Nigeria characterized by the coexistence of trees and grasses. Dominant tree species are combretaceae, caesalpinioideae and acaciaspecies are also important. The dominant grass species are usually andropogoneae, especially the genera andropogonand hyparrhenia, on shallow soils also loudetiaand aristida.

### 1.3 Relief and Drainage

The elevation of the region above mean sea level ranges from 250 m to over 780m (Fig. 2). The highest elevation occurs in the north-eastern portion and decrease both southwards and westwards. Generally the northern region of the area has a higher elevation than the southern area. The Arum hills in the northern part and the Kajeri and Kanje hills in the southern part form prominent topographic units in the area. The most pronounced topographical unit made up of a long stretch of high rising hills is located in the north-eastern part of the area and is an extension of the pankshin hills from Plateau State.

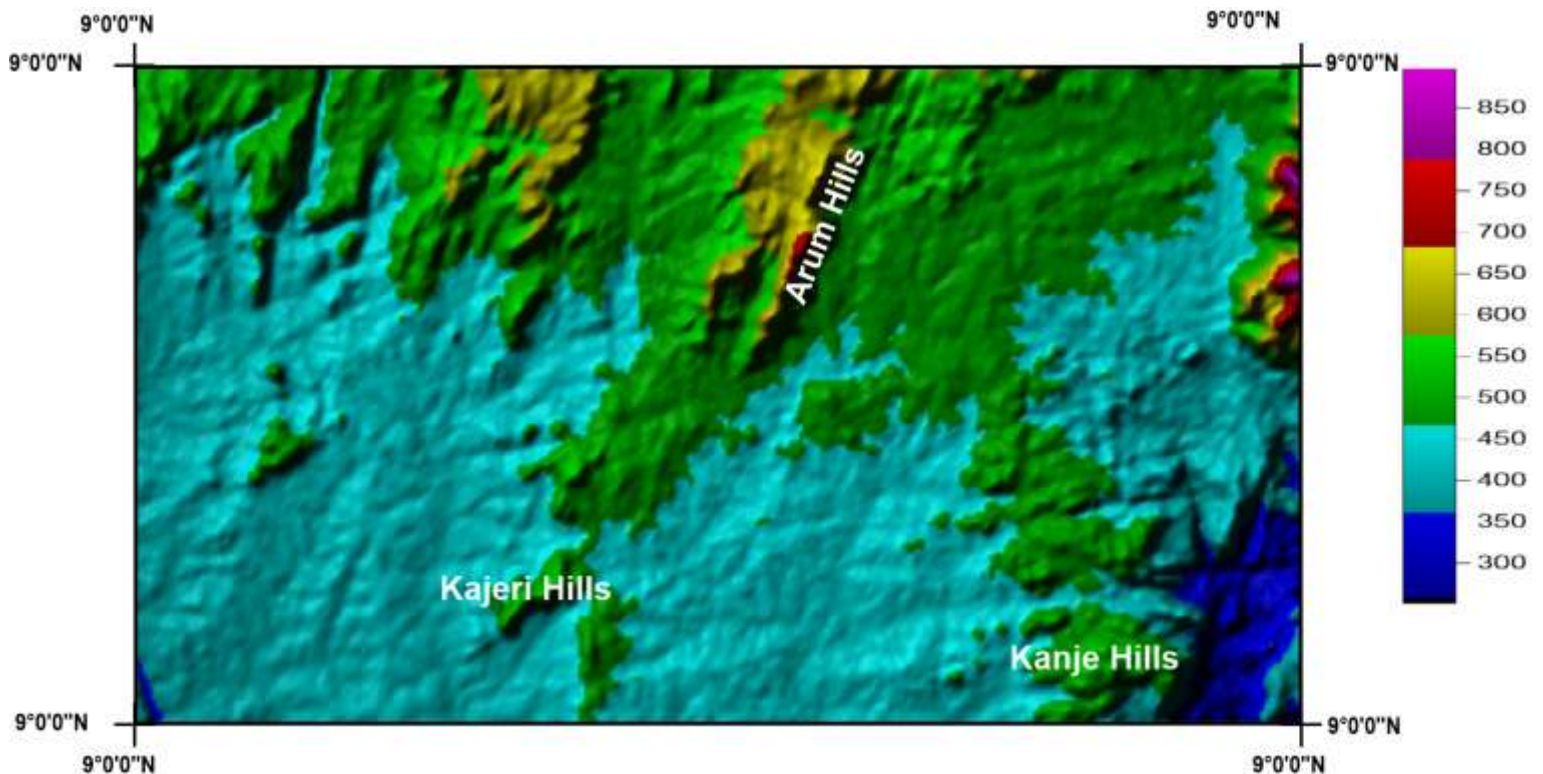


Fig. 2: Relief map of the study area

The study area is well drained and is characterized by Magama river on the west and Farin Ruwa River in the east with other smaller rivers and streams all flowing from north southward. The drainage pattern is dendritic (Fig. 3).

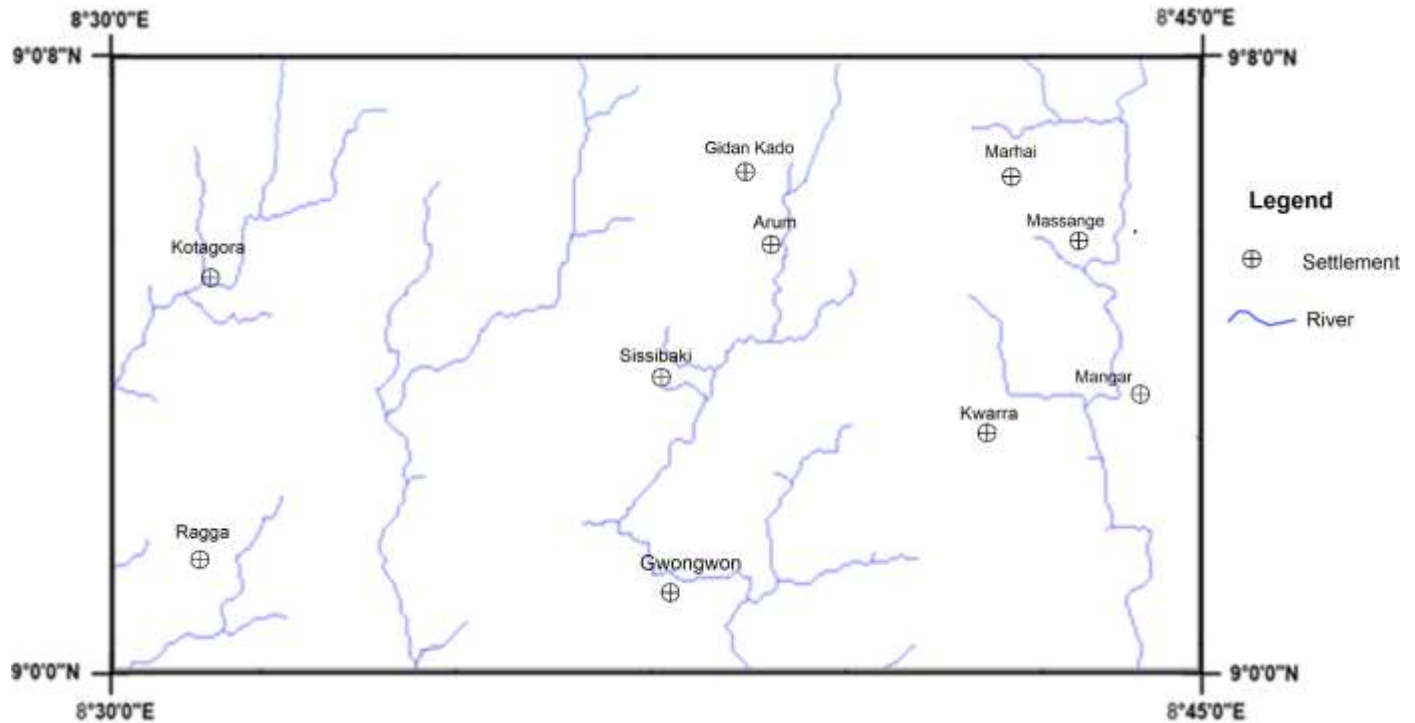


Fig 3: Drainage Map of the study area

#### 1.4 Statement of Research Problem

Recent studies by Okunlola, (2005) defined the metallogeny of the rare metal (Ta-Nb) pegmatites of Nigeria outlining seven (7) broad fields namely Kabba-Isanlu, Ijero-Aramoko, Keffi-Nasarawa, Lema-Ndeji, Oke Ogun, Ibadan- Oshogbo and Kushaka-Birnin Gwari. The pegmatites around Kwarra area falls within the Keffi-Nasarawa field where other members namely Wamba and Keffi pegmatites are currently being exploited for both metallic and gem minerals such as cassiterite, columbite, tantalite, tourmaline and beryl. Published work on the pegmatites around Kwarra area is rare and has mostly been captured on a regional scale as in the works of Kuster, 1990; Matheis and Caen-Vachette 1983; and Matheis, 1987. The available data on the rocks suggests a genetic relationship with the well-studied Wamba pegmatites (Jatau et al., 2012). Pegmatites in the Kwarra area are therefore going to be studied

with the aim of elucidating their petrogenetic and structural features and thus understanding their implication on rare metal mineralization.

## **1.5 Aim and Objectives**

This research aims to study the petrogenesis and structural control of the pegmatites in Kwarra area in order to evaluate their implication on rare metal mineralisation.

The objectives of this work are to:

- I. Produce a detailed geological map of the study area, differentiating the different rock types, determine their petrographic characteristics and to study the structural trends of the pegmatites in the area,
- II. Determine the geochemical characteristics of the rocks by studying the concentration of major and trace elements,
- III. Carry out petrogenetic evaluation using trace elements Rb, Ba, Sr, Zr, Y, Nb and the rare earth elements.
- IV. Classify the pegmatites based on their relationship to host rock, minor element content, magma genesis and tectonic setting
- V. Carry out structural analysis of the pegmatites and host rocks in the study area to establishing the relationship between their trends and geochemistry.
- VI. To update the mineralogical and geochemical information of the area

## **1.6 Scope of the Study**

The scope of work involves:

- Geological mapping of the study area on a scale of 1:50,000
- Petrographic studies of the rock samples collected using a petrological microscope.
- Whole rock geochemical analyses of the host rocks, quartz-feldspar-pegmatite and muscovite extracts from quartz-muscovite-pegmatite using ICP-MS.
- Structural analysis of the pegmatite and host rocks in the area.

## CHAPTER TWO

### LITERATURE REVIEW

#### 2.1 Regional Geology

The Nigerian Pan-African basement is part of an Upper Proterozoic-Lower Phanerozoic mobile belt situated between the West African and Congo cratons (Garba 2003). This mobile belt extends from Algeria across the Southern Sahara into Nigeria, Benin and Cameroon. Rocks of the Nigerian Basement Complex which is part of the Pan African Mobile Belt are intruded by Mesozoic ring complexes of Jos area and overlain unconformably by Cretaceous to Quaternary sediments forming the sedimentary basins (Akintola and Adekeye, 2008).

The Geology of Nigeria is made up of three major geological components (Fig. 4):

- I. Basement Complex
- II. Younger Granites
- III. Sedimentary Basins

The geology of the study area falls within the framework of the North-Central Basement Complex of Nigeria, which is underlain by Basement Complex rocks and parts of the Younger Granites.

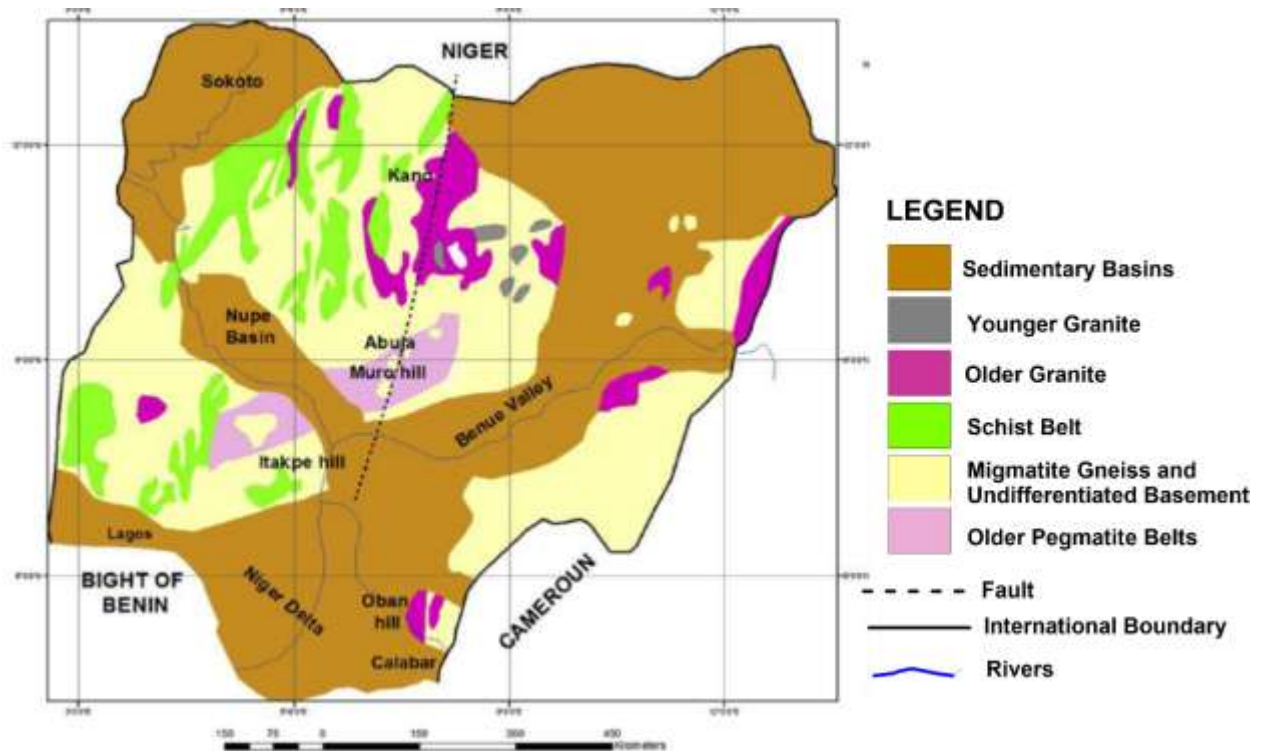


Fig 4: Simplified map of the geology of Nigeria after Okunlola, (2005).

## 2.2 The Basement Complex

Nigerian basement complex forms a part of the Pan-African mobile belt and lies between the West African and Congo Cratons (Fig. 5) and south of the Tuareg Shield (Black, 1980). It is intruded by the Mesozoic calc-alkaline ring complexes (Younger Granites) of the Jos Plateau and is unconformably overlain by Cretaceous and younger sediments.

The Nigerian basement (Fig. 5) was affected by the 600 Ma Pan-African orogeny and it occupies the reactivated region which resulted from plate collision between the passive continental margin of the West African craton and the active Pharusian continental margin (Burke and Dewey, 1972; Dada, 2006).

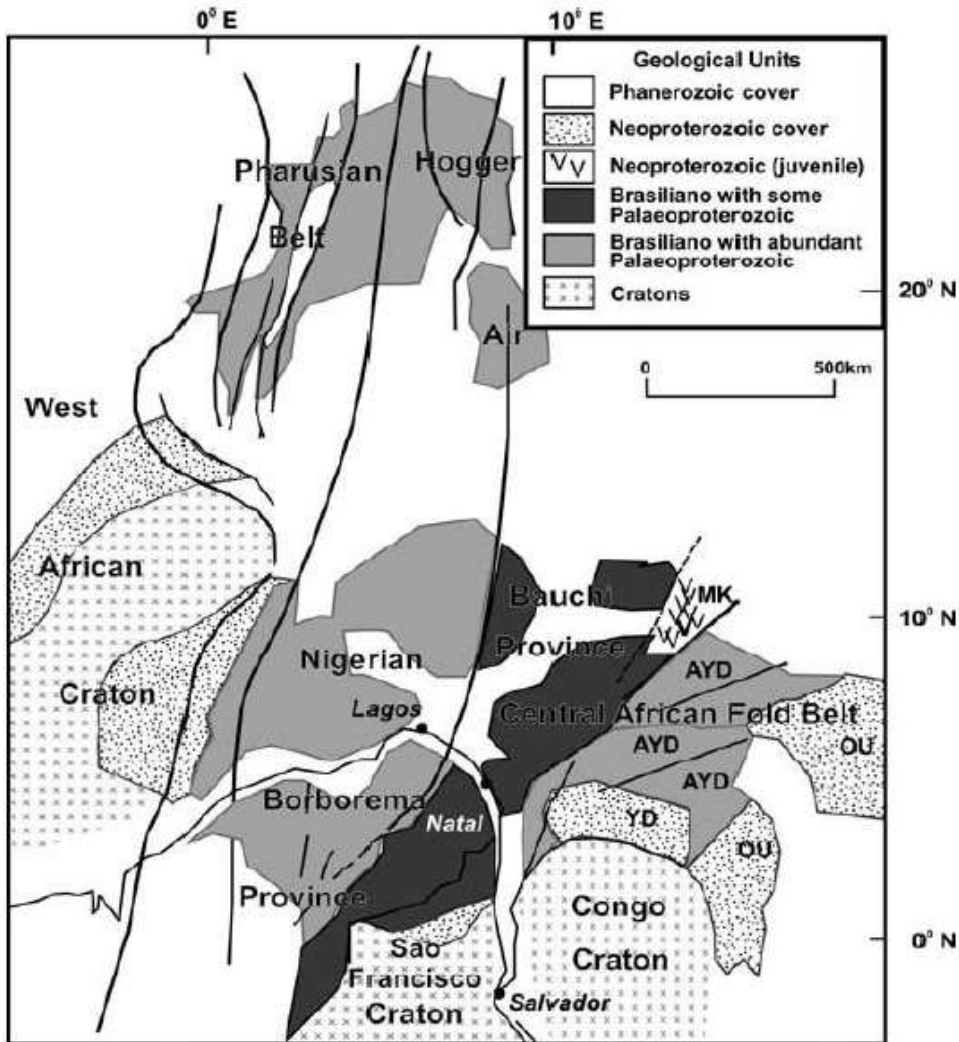


Fig 5: Location of the Nigerian Basement Complex between the West African and Congo Cratons and in relation to Hoggar and Borborema Provinces (adapted from Dada, 2008).

The basement rocks are believed to be the results of at least four major orogenic cycles of deformation, metamorphism and remobilisation corresponding to the Liberian (2,700 Ma), the Eburnean (2,000 Ma), the Kibaran (1,100 Ma), and the Pan-African cycles (600 Ma) (Obaje, 2009). The first three cycles were characterized by intense deformation and isoclinal folding accompanied by regional metamorphism, which was further followed by extensive migmatitisation. The Pan-African deformation was accompanied by a regional metamorphism, migmatitisation and extensive granitisation and gneissification which produced syntectonic

granites and homogeneous gneisses (Abaa, 1983). Within the basement complex of Nigeria four major petro-lithological units are distinguishable, namely:

1. The Migmatite – Gneiss Complex (MGC)
2. The Schist Belt (Metasedimentary and Metavolcanic rocks)
3. The Older Granites (Pan African granitoids)
4. Undeformed Acid and Basic Dykes

### **2.3 The Migmatite – Gneiss Complex (MGC)**

It is the most widespread of the component units in the Nigerian basement, covering about half of the Nigerian Basement; they are quartzo-feldspathic rocks that often contain hornblende and biotite. They strongly resemble the tonalite trondhjemite- granodiorite (TTG) suites of Archean and Early Proterozoic terrains elsewhere in the world (Dada *et al.*, 1993). The migmatite-gneiss complex also described as the polymetamorphic gneiss-migmatite complex by Garba, (2003) has ages ranging from Liberian (~2800 Ma) to Pan-African (~600Ma). Metamorphism is generally in the amphibolite facies grade (Garba, 2003). It has a heterogeneous assemblage comprising migmatites, orthogneisses, paragneisses, and a series of basic and ultrabasic metamorphosed rocks (Obaje, 2009).

These rocks record three major geological events (Rahaman and Lancelot, 1984); the earliest, at 2,500 Ma, involved initiation of crust forming processes (e.g. the banded Ibadan grey gneiss of mantle origin) and of crustal growth by sedimentation and orogeny; next came the Eburnean,  $2,000 \pm 200$  Ma, marked by the Ibadan type granite gneisses; this was followed by ages in the range from 900 to 450 Ma which represent the imprint of the Pan-African event.

## **2.4 The Schist Belt (Metasedimentary and Metavolcanic Rocks)**

The Nigerian schist belts are thought to have been deposited in back-arc basins which developed after the onset of subduction at the West African cratonic margin at about 1000 Ma. The schist belts are made up of mainly N–S to NNE–SSW trending belts of low grade (mainly greenschist facies) supracrustal (and minor volcanic) assemblages (Garba, 2003). The Schist Belts are best developed in the western half of Nigeria, west of 8°E longitude, though smaller occurrences are found to the east but only sporadically. The belts are confined to a NNE-trending zone of about 300 km wide. These belts are considered to be Upper Proterozoic supracrustal rocks which have been infolded into the Migmatite-Gneiss Complex (Obaje, 2009). The Schist belts zone is flanked by migmatites – gneisses – granites terrain, to the East and West, and the same terrain separate the individual belts within the zone (Turner, 1983; Ajibade et al., 1987).

These belts are intruded by granitic plutons belonging to the Pan – African magmatic suite. They are dated at approximately 1,100 Ma and are thought to belong to the Kibaran ensialic processes (Fitches et al. 1985).

The lithological variations of the schist belts include coarse to fine grained clastics, pelitic schists, phyllites, banded iron formation, carbonate rocks (marbles/dolomitic marbles) and mafic metavolcanics (amphibolites). The schist belts have been mapped and studied in detail in the following localities: Maru, Anka, Zuru, Kazaure, Kuseriki, Zungeru, Kushaka, Isheyin Oyan, Iwo, and Ilesha where they are known to be generally associated with gold mineralisation (Obaje, 2009).

## **2.5 The Older Granites (Pan African Granitoids)**

The Pan-African granitoids in Nigeria are referred to as the Older Granites to distinguish them from Mesozoic anorogenic granite ring complexes (the Younger Granites) (Garba, 2003). The Older Granites are Pan-African orogeny-related, range from syn- through late to postorogenic granitoids of upper Proterozoic to Lower Paleozoic age. They represent a varied and long lasting (750–450 Ma) magmatic cycle associated with the Pan-African orogeny (Obaje, 2009). The Older Granites are intrusions emplaced by stopping and diapiric processes (Fitches et al., 1985). The Older Granites suite is notable for its general lack of associated mineralisation although the thermal effects may play a role in the remobilisation of mineralizing fluids (Obaje, 2009).

The Older Granites occur intricately associated with the Migmatite-Gneiss Complex and the Schist Belts into which they generally intruded. Older Granite rocks therefore occur in most places where rocks of the Migmatite-Gneiss Complex or of the Schist Belt occur (Obaje, 2009).

### **2.5.1 Nigerian Pegmatites**

The Nigerian pegmatites belong to the terminal stage of the Pan-African magmatism between 562 and 534 Ma, indicating emplacement related to the end of the Pan-African magmatic activity (Garba, 2003; Rahaman et al., 1988). Prograde metamorphism and partial melting of country rocks at the close of Pan-African plutonism played major roles in pegmatitisation. (Adetunji et al., 2016). The ages, mineralogy, and composition of these pegmatite units appear to be analogous to those of the pegmatites environment in Brazil, Canada and Australia (Akintola and Adekeye, 2008). Both barren and mineralized pegmatites exist in the Nigerian Basement (Fig. 6). The pegmatites of the study area fall within the North Central

pegmatite province of Nigeria extending from Abuja to Jos Plateau (Fig. 7) and are emplaced mainly into the gneissic basement. Albitisation is a dominant feature of the rare metal pegmatites of the area, which is notably rich in tin (Matheis, 1987). The pegmatites in the study area is in close spatial relationship with the Pankshin anorogenic ring complex. Rb/Sr dating for the Gwon-Gwon pegmatite in the study area gave age of 555 +/-5 Ma and three muscovite model ages range from 537-522 Ma (Matheis, 1987).

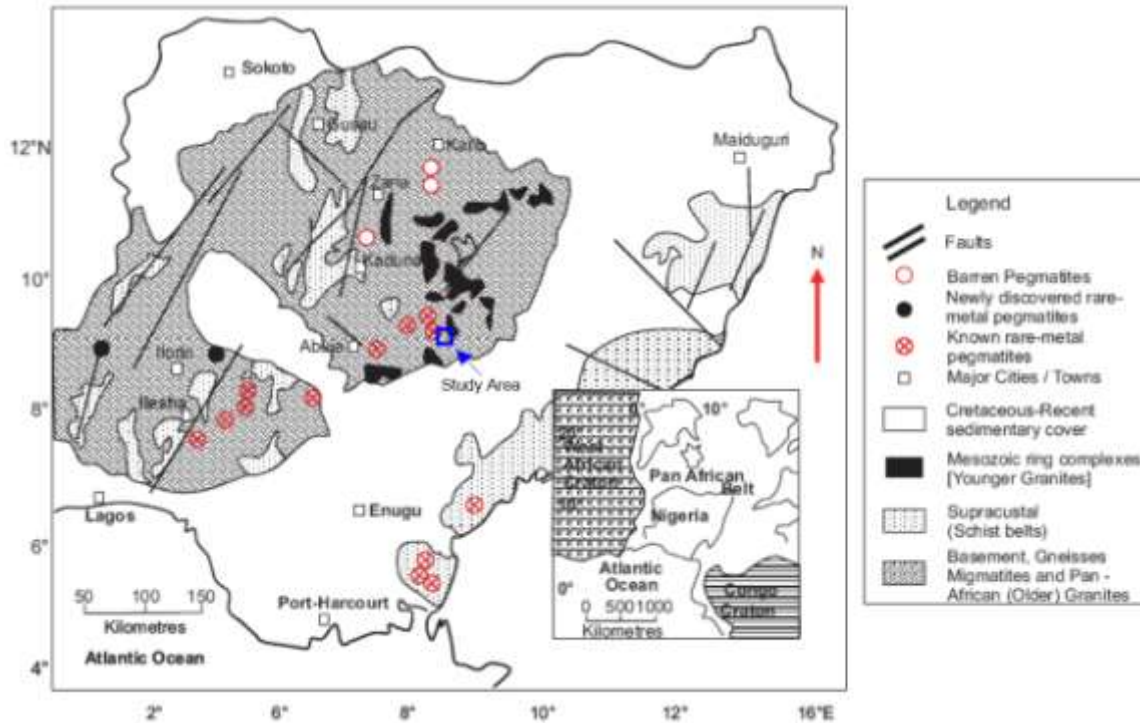


Fig. 6: Geological map of Nigeria indicating the locations of barren and rare-metal pegmatites (after Garba, 2003).

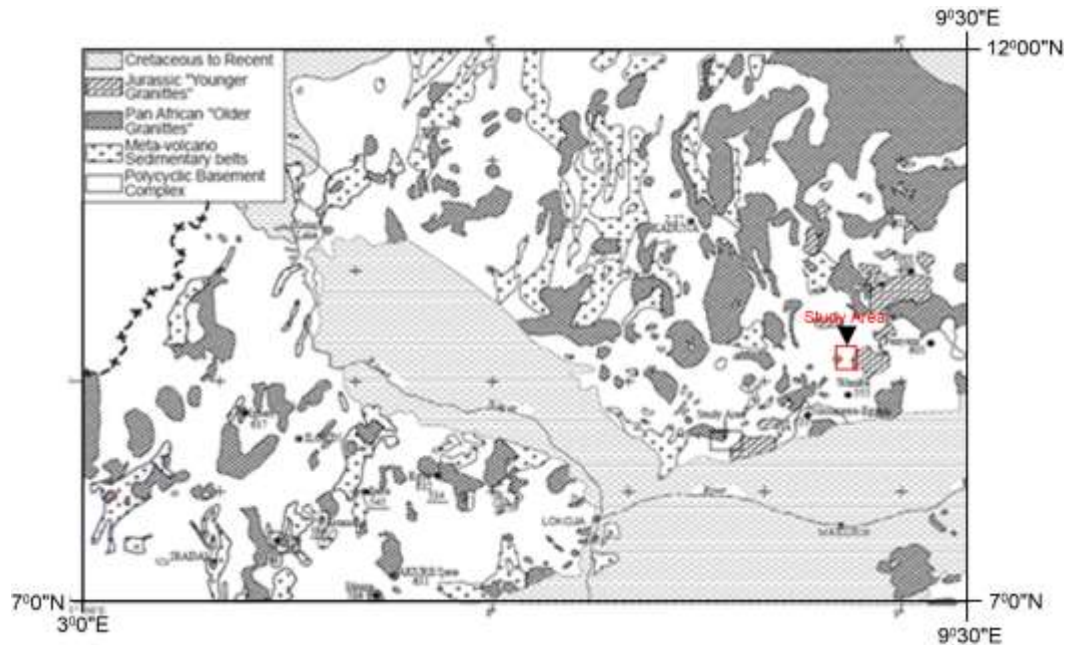


Fig. 7: Geological Sketch map of central and south-west Nigeria showing the location of the Wamba pegmatite field (study area) and the distribution of Pan-African Older Granites and pegmatites (underlined). Geochronological data sources are van Breemen *et. al.* (1977), Rahaman *et. al.* (1983), Matheis and Caen-Vachette (1983), Tubosun *et. al.* (1984),

### 2.5.2 Barren and Rare Metal Pegmatites

Moller and Morteani (1987), Černý (1989), Kuster (1990), Garba (2003) have contributed to a better understanding of southwestern and northern Nigeria pegmatite bodies distinguishing between the barren and rare metal bearing pegmatites and documenting that the pegmatites are not confined only to the earlier proposed 400 km long NE-SW trending belt stretching from Wamba area (near Jos plateau) to Ilesha area. Rare metal granitic pegmatites are products of extreme differentiation of large reservoir of granitic magma. The proportion of rare metals in such pegmatites is an indication of the level of fractionation achieved in the final stages of granitic differentiation (Černý, 1991).

Barren pegmatites are found associated with all the major lithologies of the basement, i.e. gneiss, migmatites, schists and granitoids. The morphology and major mineral composition (quartz–feldspar–mica) are mostly not different from those of the rare-metal types (Garba, 2003). The discrimination between the mineralized and barren pegmatites will depend very

much on the chemistry of the added pneumatolytic and/or hydrothermal fluids (Adedoyin et al., 2006). It has also been very much observed that the degree of albitisation and fractionation of the pegmatites plays significant role in the discrimination between barren and rare metal pegmatite (Oyebamiji 2014, Matheis, 1987; Akintola et al., 2012 (a), Kuster, 1990; Oyebamiji et al., 2018; Jacobson and Webb, 1946). Garba (2003) observed as common characteristics of rare metal pegmatites; sharp contacts with their host rocks, wall rock alteration (of mostly tourmalinisation) and their close proximity to major and subsidiary fault structures. Since rare metal pegmatites are related to the Nigerian major fault lineament systems, the albitisation and rare-metal mineralisation may have been due to late stage fluids available at the close of the Pan-African metamorphic cycle (Ekwueme and Matheis, 1995) or due to sodium rich hydrothermal solution from the mantle along ancient lineament (Wright, 1970). Okunlola (2005) defined the metallogeny of the rare metal pegmatites in Nigeria and outlined 7 broad fields, namely:

- I. Kabba-Isanlu
- II. Ijero-Aramoko
- III. Keffi-Nasarawa
- IV. Lema-Share
- V. Oke-Ogun
- VI. Ibadan-Oshogbo
- VII. Kushaka-Birnin Gwarri

These pegmatites show appreciable degree of mineralisation and are distributed with marked concentration in a broad zone extending NE from Ago-Iwoye area, towards the Younger Granite province (Akoh and Ogunleye, 2014). Late-stage albite and sericite are also commonly observed in rare metal pegmatites (Garba, 2003).

### 2.5.3 Structural and Geochemical characterisation of Nigerian pegmatites

The rare metal pegmatites occur in a distinct belt that extends SW–NE from Ife to Jos, and appears to cut across the boundary between the eastern and western Nigerian terranes, although the individual pegmatite intrusions are oriented north–south (Kinnaird, 1984; Matheis and Caen-Vachette, 1983; Woakes et al., 1987). Individual pegmatites vary in length from 10m to over 2 km, and can be up to 200m wide (Adetunji and Ocan, 2010). A direct genetic link between the rare-metal bearing pegmatites and proximal granite occurrences was never observed.

Mineralisation is not restricted to particular lithologies but only dependent on the geochemical characteristics of the host rock (Adedoyin et al., 2006). The pegmatitic belt and the orientation of the units within it appear to be related to rotational stresses created by the Benue Trough. From a more global perspective, this trend is probably the northern extension of the Brazilian pegmatite belt, which runs from Rio Grande del Sul to Rio Grande del Norte (Akintola and Adekeye, 2008). It is suggested that reactivation of old tectonic lineaments during the Pan-African orogeny provided excess heat and fluid to concentrate rare-metal pegmatites by partial melting with selective leaching from the country rocks, i.e. their lithological framework (Garba, 2003). This suggestion is supported by (Černý et al., 2012). The role of conjugate faults and shear belts proposed by Garba (2003) in accommodating the magmatic fluid is also considered important in terms of linear and sub-parallel orientation of the pegmatites. The rare metal pegmatites sometimes show significant pinch and swell structures associated with semi ductile deformation and mineralisation is well developed in the swells (Adedoyin et al., 2006).

The different pegmatite fields in Nigeria show distinctly different geochemical signatures which are related to their spatial geological framework (Matheis, 1987; Kuster, 1990).

Nigerian pegmatites show a marked difference in trace element and rare-earth element concentration and fractionation patterns between the rare-metal and barren pegmatites, of great significance is the distinct enrichment of Rb, Cs and in many, Ga, Nb, Ta, Sn, Li and Be in the rare-metal pegmatites relative to the barren types and the Pan-African granitoids (Garba, 2003). Pegmatites of the amphibolite complex such as the Egbe pegmatites display anomalous concentration of easily detectible pathfinders Li, Rb, F and K/Rb which correlate significantly with the whole rock tin content (Mathei, 1987; Kuster, 1990). The origin of the pegmatites also exerts a significant control on the geochemistry of the pegmatite. The barren pegmatites can be distinguished according to their origin (i.e. metamorphic and granitic) by the higher K/Ba ratios of the latter. The high K/Ba and Rb/Sr but low K/Rb ratios of the rare-metal pegmatites attest to their granitic origin (Garba, 2003).

#### **2.5.4 Evolution of pegmatites from a granitic melt**

The most accepted model for the formation of pegmatite is its derivation from granitic magmas, via igneous differentiation processes. Granitic magmas refine their compositions by crystal fractionation and by the separation of residual liquids from their crystalline products (Cerný et al., 2012). The incongruent partitioning of alkalis between the melt and an upwardly buoyant vapor phase generated the chemical and textural segregation that are the hallmark of granitic pegmatites (London, 2005). The slow rate of cooling of pegmatite zone will favour the growth of large crystals, but it is evident that the large crystals characteristic of pegmatites cannot be accounted for entirely by slow rate of cooling. Certainly a much slower rate existed in the central regions of parent rock during its formation, but extremely large crystals are not found there (Cerný et al., 1985). Evidence from mineral compositions and thermal models indicates that crystallisation within pegmatites commences at ~450 °C,

which is ~200–250 °C below the liquidus temperature at which crystallisation should commence (London and Kontak, 2012).

The rising melts containing H<sub>2</sub>O reaches H<sub>2</sub>O saturation (with perhaps some wall-rock dehydration also) and expel a fluid phase as it rises and expel even more as it crystallizes. Increase in H<sub>2</sub>O saturation can dramatically reduce the melting point of silicate systems at elevated pressures. When crystal growth commences, incompatible components H<sub>2</sub>O, OH<sup>-</sup>, CO<sub>2</sub>, HCO<sub>3</sub><sup>-</sup>, CO<sub>3</sub><sup>2-</sup>, SO<sub>4</sub><sup>2-</sup>, PO<sub>4</sub><sup>3-</sup>, H<sub>3</sub>BO<sub>3</sub>, F and Cl as well as the elements Li, Na, K, Rb, Cs and Be are rejected at the growing crystal interface of quartz and feldspar, and they concentrate along the margins of the growing crystal front where they act as fluxes (Cerný et al., 2012). Because of its increasingly flux-rich composition, the boundary layer liquid will acquire a low solidus temperature and enhanced silicate–H<sub>2</sub>O miscibility thus reducing the viscosity of the system (London, 2005). Volatile species, such as B, F, and P, can individually and collectively, lower the granite solidus temperature to below 500 °C and increase the range of temperatures over which magmatic crystallisation occurs (London, 1996).

Poor nucleation and very high diffusivity in the H<sub>2</sub>O-rich phase, permits chemical species to migrate readily and add to rapidly growing minerals, leading to large grain sizes in pegmatites (Winter, 2014). The petrologically important trace elements found in granite–pegmatite systems display variable degrees of incompatibility as functions of the pressure, temperature, and mineral phases in the system. Depending on their compatibility in the rock-forming minerals of granites, the relative and absolute abundances of the initial suite of trace elements may be modified by the process of fractional crystallisation or via contamination by assimilation of material from external reservoirs (Cerný et al., 2012).

## **2.6 Undeformed Acid and Basic Dykes**

The undeformed acid and basic dykes are late to post-tectonic Pan African. They cross-cut the Migmatite-Gneiss Complex, the Schist Belts and the Older Granites. The undeformed acid and basic dykes include:

a. Felsic dykes that are associated with Pan African granitoids on the terrain such as the muscovite, tourmaline and beryl bearing pegmatites, microgranites, aplites and syenite dykes (Dada, 2006)

b. Basic dykes that are generally regarded as the youngest units in the Nigerian basement such as dolerite and the less common basaltic, felsite and lamprophyric dykes. The age of the felsite dykes has been put at between 580 and 535 Ma from Rb-Sr studies on whole rocks (Matheis and Caen-Vachette, 1983; Dada, 2006), while the basic dykes have a much lower suggested age of ca. 500 Ma (Grant, 1970). The structural and geochronological importances of this suite of rocks, which have been put to immense chronological use elsewhere (Dada, 2006) are often overlooked in Nigeria. When they cross-cut basement, they could be used to infer relative age of metamorphic structures and rock suites and could also suggest the existence of older basement windows in the Nigerian schist belts, apart from the immense guide they provide in sampling for isotope geochemistry, analysis and interpretation (Dada, 2006).

## **2.7 Younger Granites**

The Mesozoic Younger Granite ring-complexes of Nigeria form part of a wider province of alkaline anorogenic magmatism. They occur in a zone 200 km wide and 1,600 km long extending from northern Niger to south central Nigeria (Obaje, 2009). In Nigeria and Niger, over 80 anorogenic centers representing the eroded roots of volcanoes form an extensive

chain of syenite-granite ring complexes (Bowden and Turner 1974). The post-collisional granites in Nigeria are associated with rare metal (tin–tantalum) granitic pegmatites, some of which have been artisanally mined (Adetunji and Ocan, 2010; Garba, 2003; Kinnaird, 1984; Kuster, 1990; Matheis and Caen-Vachette, 1983; Okunlola, 2005; Woakes et al., 1987). The Younger Granites ring-complexes of Nigeria are over 45% subalkaline types of granite, which are mineralized with rich deposits of cassiterite, columbite, sphalerite, wolframite and galena, consequent to fluid interaction in the cupolas. The peralkali granites, in addition to more common rock-forming minerals, contain in accessory amounts the rare minerals astrophyllite and pyrochlore, along with cryolite, zircon, topaz, thorite and occasional thomsonolite (Jacobson and Macleod, 1977).

The most striking petrographic feature of the whole province is the overwhelmingly acid nature of the rocks and the similarity of the rock types found in all areas. Over 95% of the rocks can be classified as rhyolites, quartz-syenites or granites, with basic rocks forming the remaining 5% (Obaje, 2009). Often several cycles of intrusion occur within the one complex and the large size of many of the complexes is due to the overlapping and superposition of separate intrusive cycles. Aeromagnetic anomalies suggest that a series of buried NE–SW lineaments of incipient rifts controlled the disposition of the individual complexes (Ajakaiye, 1986). Age determinations have shown that the Older Granites are probably early Paleozoic in age (Ferre *et al.*, 1998), whereas the Younger Granites are entirely Mesozoic (Van Breeman and Bowden 1973, Jacobson *et al.*, 1963,).

The province decreases in age from Ordovician in northern Niger to late Jurassic in central Nigeria (Karche and Vachette, 1976, Karche, 1978). Fifteen of the complexes have been isotopically dated and a perceptible trend in the north from  $213 \pm 7$  Ma (Dutse),  $186 \pm 15$  Ma (Zaranda) and  $183 \pm 7$  Ma (Ningi-Burra) to those in the south at  $151 \pm 4$  Ma (Pankshin),  $145 \pm 4$  Ma (Mada), and  $141 \pm 2$  Ma (Afu) is discernable. This progressive change in age, and the

fact that similar alkali granite ring complexes in southern Niger and further north in Air are Carboniferous, Devonian and Ordovician in age has prompted authors (Bowden *et al.*, 1976) to advocate a sequential age trend covering some 500 Ma over a distance of more than 2,000 km. Rahaman *et al.*, (1984) and Bowden and Kinnaird (1984) have provided further isotopic evidence of this age progression.

## **CHAPTER THREE**

### **MATERIALS AND METHODS**

#### **3.1 Introduction**

Desktop study, literature review, geological field mapping, satellite image interpretation, field mapping, laboratory analysis of collected samples, data analysis and interpretation, were carried out sequentially to study the host rocks and pegmatites in the area.

#### **3.2 Desk Study**

The desk study involved an intensive search and review of published and unpublished materials relevant to the research and the study area. These include journals, articles, geological maps, conference proceedings, unpublished reports, theses and dissertations.

#### **3.3 Field Method**

Field work was carried out in two phases. Firstly, a reconnaissance survey of the area was done to assess the accessibility of the study area and for logistical planning of the field mapping. The second phase of the field work involved geological field mapping on a scale of 1:50,000 as the base map. Geological features were identified and representative fresh samples were collected for petrographic studies. The instruments and materials used for the field mapping include: Global positioning system receiver (Garmin eTrex-10), compass with clinometer, digital camera, hand lens, geological hammer, measuring tape, sample bags, permanent marker, masking tapes, pencils and field notebook. Fifteen (15) fresh rock samples were collected, consisting of 7 pegmatites (including 4 muscovite extracts) and 8 host rocks. The samples were collected in the sample bags and they were well-labelled using

a permanent marker. The coordinates and elevations of sampling locations were recorded by a global positioning system (Garmin eTrex-10) and noted in the field notebook. Where necessary, strike and dip were measured for the host rock with the aid of compass clinometer and recorded in the field notebook. Thereafter, the observed outcrops were described and identified in order to determine their textural and structural characteristics, as well as their mode of occurrence. Textural characteristics of the rocks were elucidated using magnifying hand lens. Photographs of the outcrops were also taken using a digital camera.

### **3.4 LABORATORY ANALYSES**

Laboratory work carried out during this study is divided into petrographic and geochemical analysis.

#### **3.4.1 Petrographic Methods**

Fresh samples were selected from the different rock types and thin sections were prepared in the thin section laboratory of the Geology and Mining Department in the University of Jos. The rock samples were cut into small pieces (rectangular shape) using Struers cutting machine (secotom-10) and ground smooth (frosted) in order to obtain a flat smooth surface without the traces of cutting

- I. The flat, smooth samples were mounted on a 26 mm by 46 mm glass microscope slide using Struers specifix resin mixed with Struers specifix-40 curing agent in the ratio 5:2 by weight (the mounted sample was left for 24 hours).
- I. After the sample had been stuck to the microscope slide, it was trimmed using Struers machine (Accutom-50) until its thickness was about 30  $\mu\text{m}$ . The thickness of the section was measured with a digital micrometer.
- II. The samples were carefully cleaned and vertically stored in thin section boxes.

Three slides were prepared per sample and examined under the petrological microscope to identify the constituent minerals at a magnification of 10X/0.25mm. The properties of these minerals as seen in polarized light, crystal form and mutual interference between crystals were clearly stated.

### **3.4.2 Sample Preparation for Geochemical Analysis**

Geochemical analysis commenced with the pulverisation of the Fifteen (15) selected samples (11 whole rocks and 4 muscovite) for geochemical analysis were pulverized to minus 200 mesh size at the Activation laboratory, Ontario Canada. The pulverisation of the samples was undertaken with the aid of Retsch Planetary Ball Mill 400. Rock chips were loaded into the planetary ball mill and a time interval of 15 minutes was allowed for complete pulverisation to <200 mesh size. After pulverisation of each sample, the equipment was cleaned using acetone. Pulverisation was later followed by weighing 15 grams of each sample using an electronic weighing balance. Samples were then sealed, labeled. The samples were analysed for major, trace and rare earth elements using the 4 lithos package inductively-coupled plasma mass spectrometry (ICP-MS).

### **3.4.3 Analytical Technique**

The major elements were analysed by inductively couple plasma atomic emission spectrometry following a lithium borate fusion and dilute acid digestion while trace and REE were analysed by inductively-coupled plasma emission spectrometry (ICP-ES) following a multi-acid digestion method. Details of the analytical procedures adopted has been discussed in the work of (Maja *et al.*, 2011). As a means of dissolving the mineral constituents, the analytical procedure involved addition of 5 ml each of perchloric acid ( $\text{HClO}_4$ ), trioxonitrate

(V)  $\text{HNO}_3$  and 15 ml Hydrofluoric acid (HF) to 0.5 g of sample. The solution was stirred properly and allowed to evaporate to dryness after it was warmed at a low temperature for some hours. Four (4) ml of hydrochloric acid (HCl) was then added to the cooled solution and warmed to dissolve the salts. The solution was cooled; and then diluted to 50 ml with distilled water. The solution was then introduced into the ICP torch as aqueous - aerosol. The emitted light by the ions in the ICP was converted to an electrical signal by a photo multiplier in the spectrometer, the intensity of the electrical signal produced by emitted light from the ions were compared to a standard (a previously measured intensity of a known concentration of the elements) and the concentrations were then computed. Analytical precisions vary from 0.1% to 0.04% for major elements.

Data obtained was processed using the following softwares: Microsoft Excel, Geochemical data toolkit (GCD Kit 3.0 ) and Surfer 12.

## **CHAPTER FOUR**

### **RESULTS**

#### **4.1 Field Geology and Petrology**

Systematic geological field mapping of the study area on the scale of 1:50,000 revealed that it is underlain by Precambrian Basement Complex rocks and Younger Granites. The Basement Complex rocks include amphibolite, migmatite gneiss, banded gneiss, granite gneiss and albitised granite, while the Younger Granite rock is alkali granite. Petrographic studies were conducted under plane polarized light (PPL) and cross polarized light (XPL) on the prepared thin sections of rock samples and discussed below. The geological map produced is presented as Fig 8.

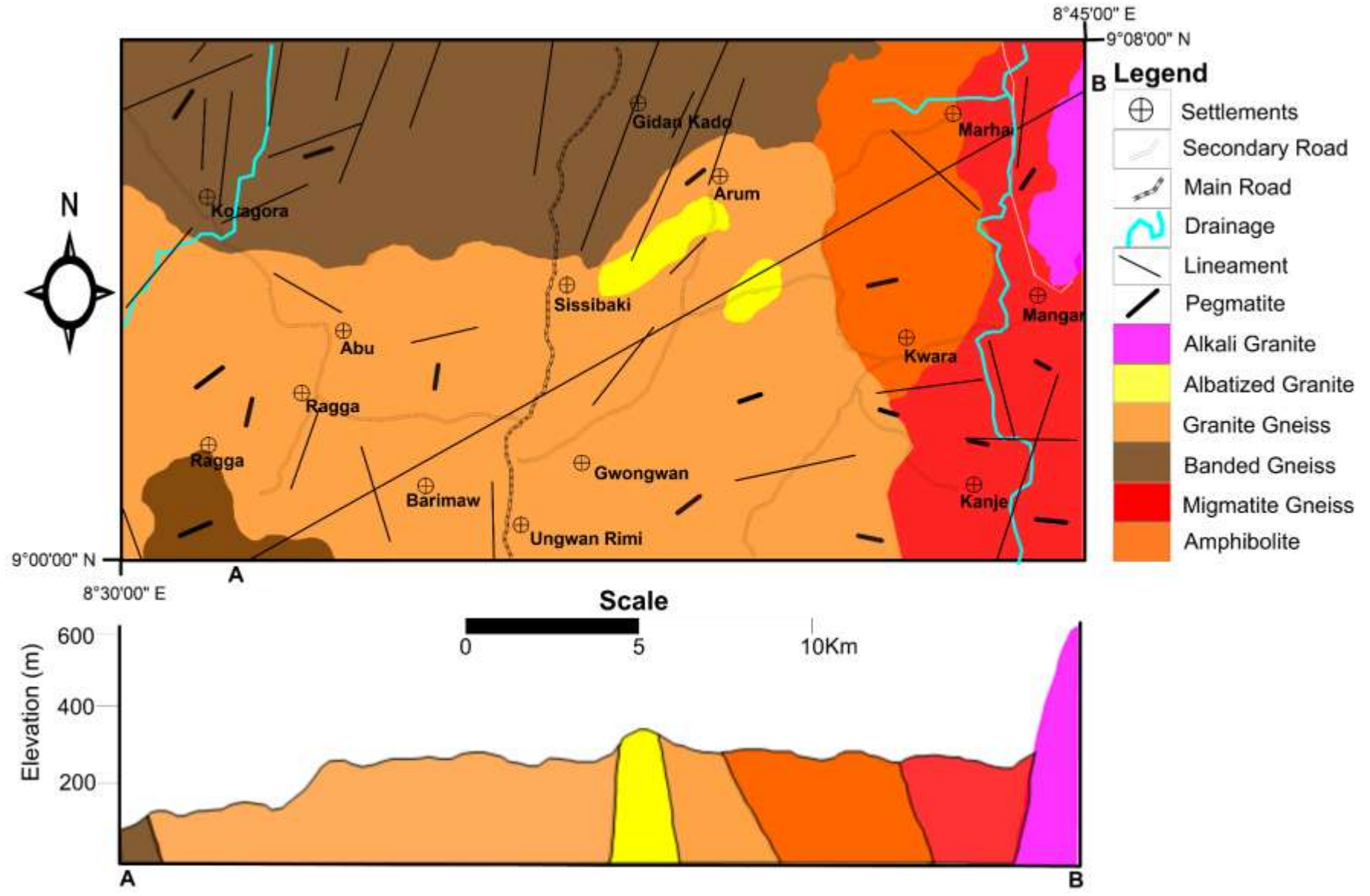


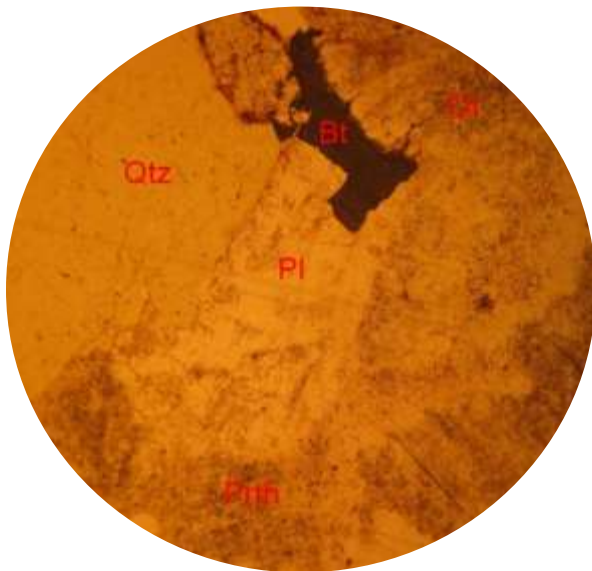
Fig 8: Geological map of the study area

### 4.1.1 Alkali Granite

The rock occupies less than 10% of the study area and is found around Mangar in the north eastern edge of the study area. It is a part of the Pankshin anorogenic granite ring complex which has been dated to have an age of about  $151 \pm 4$  Ma (Obaje, 2009). The rock occurs as massive batholiths and steep hills. It is generally pinkish colour and intrude the other rock units discordantly. The rocks do not show evidence of significant deformation like the other rocks in the study area. In hand specimen (Plate 1), the rock appears pinkish and coarse grained. The rock is rich in alkali feldspars, with a modal mineralogy comprising of 30% quartz, 14% plagioclase, 15% perthite, 35% orthoclase, 5% biotite and <1% zircon and opaque minerals (visual estimate). Thin section study of the rock reveals that the mineral grains are generally coarse and anhedral in shape. The alkali feldspars have been slightly altered to sericite. The minerals have a random orientation. Quartz occurs as polycrystalline mineral and displays undulose extinction. It is colourless, lacks cleavage and non pleochroic, and exhibits first order interference colour of grey-white, with low birefringence. Orthoclase is also colourless and non pleochroic like quartz, with very low relief distinguished from quartz by cloudy patches on individual crystals in plain polarized light which indicate weathering of the crystal along cleavage planes. Plagioclase is colourless, non pleochroic, low relief, and interference colour (grey-white), birefringence is low, with parallel extinction. Biotite is brown in colour, pleochroic from deep brown to greenish brown, with two sets of perfect cleavage, moderate relief, exhibits third order interference colour of grey-brown- red-blue-green, birefringence is strong, extinction is inclined. The Photomicrograph of the alkali granite under Cross Polarized Light (XPL) and Plane Polarized Light (PPL) is presented in Plate 2 (a and b) below.

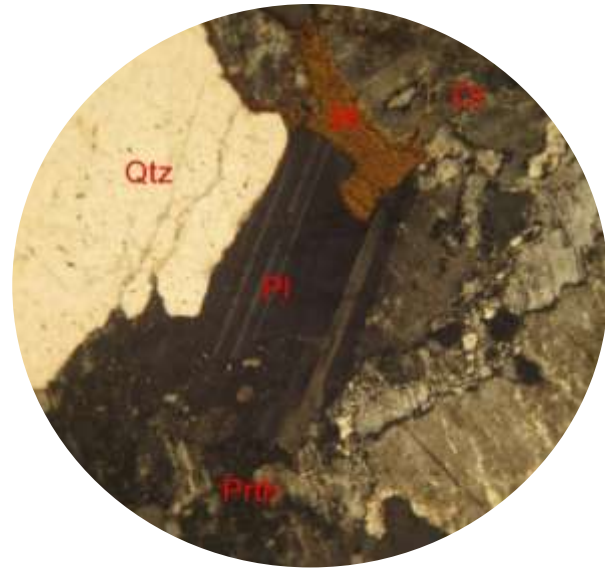


Plate 1: Hand specimen of the alkali granite in the study area (Latitude 9°06'05"N and Longitude 8°44'30"E)



a

PPL



b

XPL

Plate 2: Photomicrograph of alkali granite under (a) Cross Polarized Light (XPL) and (b) Plane Polarized Light (PPL) Biotite (Bt), Perthite (Prth), Orthoclase (Or), Plagioclase (Pl) and Quartz (Qtz). Mag.0.25mmX10.

### 4.1.2 Albitised Granite

The albitised granite covers about 5% of the study area. Albitisation is a common process during which hydrothermal fluids convert plagioclase and/or K-feldspar into nearly pure albite; however, its specific mechanism in granitoids is not well understood (Kaur et al., 2012). In parts, of the study area the rocks appear to be deformed and occurs as scattered outcrops particularly around Arum. The rock is medium grained (Plate 3), micaceous and whitish in hand specimen. The albitised granite is observed to have evidences of deformation and confined to the prevailing NE-SW trending lineaments in the study area suggesting that the albitizing fluids possibly originated during reactivation of the lineament during the Pan-African event. Similar suggestions has been made by Garba (2003), concerning the formation of rare metal pegmatites. Kuster (1990) generally classifies the granites in the study area as late tectonic granite, suggesting the role of residual hydrothermal fluids in their formation.

Petrographic studies reveal that the rock is composed of 40% quartz, 30% Plagioclase (albite), 25% muscovite and 5% biotite and opaque minerals (visual estimate). The albitised granite is characterised by the almost complete absence of microcline and is essentially a quartz-albite-muscovite assemblage (90-95% by volume) with only a minor mafic phase, biotite. The most prominent feature of this rock is occurrence of broad albite twins which is considered to have formed by the replacement of K-feldspar by albite (Smith, 1974, Slaby, 1992). It has extinction angle of about  $30-35^{\circ}$ . The remnant of the K-feldspars (plagioclase) show continuation of their twin lamellae with the newly formed albite. The muscovites form subhedral laths and have sharp termination. It shows no reaction-relation with other minerals and strong birefringence features which are believed to be indicative of its primary magmatic

origin. A second fine grained, moderately sericitized type of muscovite is observed and are considered products of sodic metasomatism (Kuster, 1990).

It is colourless, showing moderate relief and perfect cleavage in PPL (Plate 4a). Under cross polarized light (XPL) (Plate 4b), the quartz exhibit undulose extinction, no twinning but shows grey to white interference colour. Under plane polarized light (PPL), the quartz is large, colourless with anhedral shape, non-pleochroic, no cleavage, no inclusions, not fractured nor altered.

Under cross polarised light, the albite mineral is subhedral and display broad lamella albite twins with grey and white lines interference colour. Under plane polarized light, it is non-pleochroic, has a weak birefringence and low relief.



Plate 3: Field photograph of albitised granite (Latitude 9°04'10"N and Longitude 8°47'43"E)

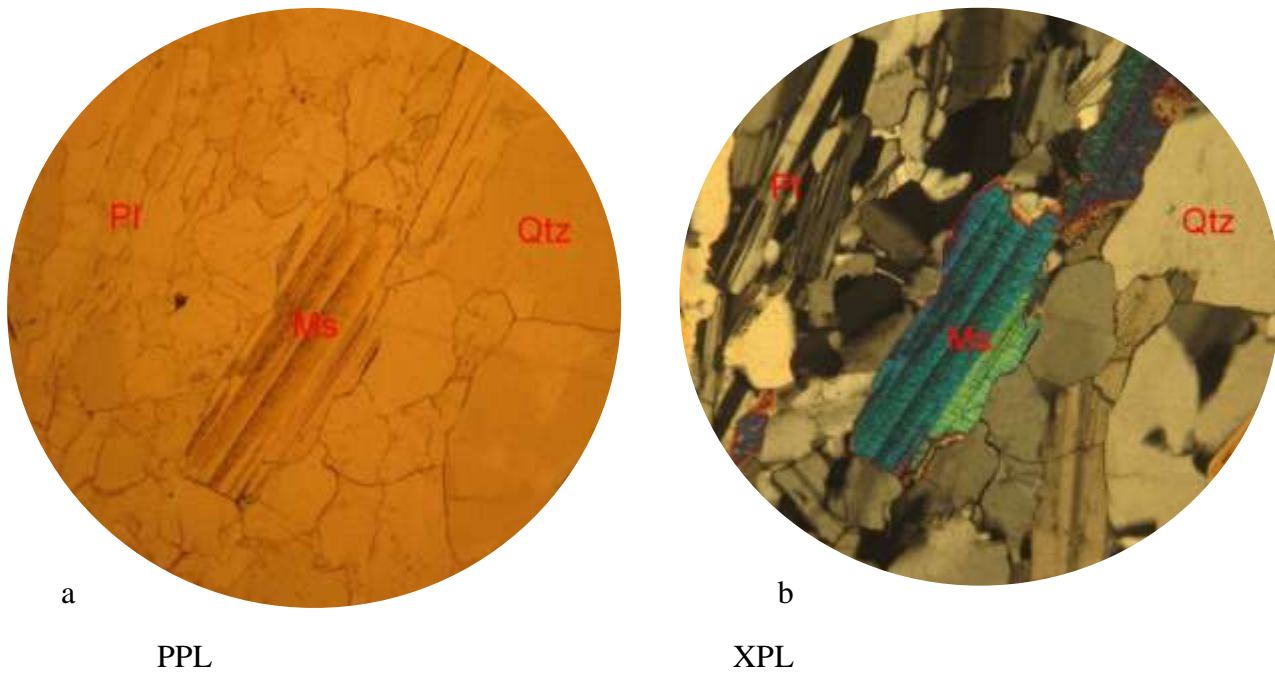


Plate 4: Photomicrograph of Albitised granite under (a) (XPL) and (b) (PPL) composed of Plagioclase (Pl), Quartz (Qtz) and muscovite (Ms). Mag. 0.25mmX10.

#### 4.1.3 Granite Gneiss

The granite gneiss in the study area is medium grained and dominantly granitic in composition. It is the most dominant rock unit in the study area. A variety of coloured minerals ranging from grey to brown and pink are visible in a hand specimen of the rock. There is a slight foliation of the felsic and mafic minerals. The granite gneiss in the study area has been exposed to weathering conditions and shows evidences of deformation. The granite gneiss outcrop is well expose around Sissibaki, Ragga, Gwongwong, Ungwan Rimi, Barimaw and Abu.

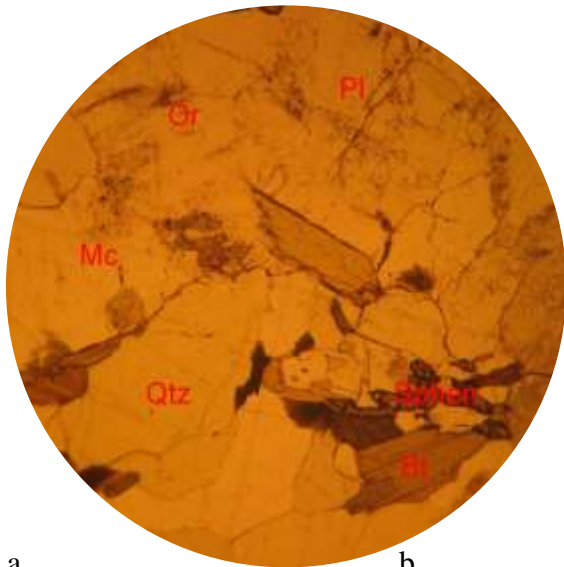
Petrographic studies conducted on the thin section (granite gneiss) shows that the gneiss consists of quartz 35%, biotite 23%, plagioclase 25%, orthoclase 13, and Spene 2%. The rock also displayed varieties of structural elements such as folds, fractures, folded quartz-veins and foliations (Plate 5). Thin section studies reveal that the mineral grains are subhedral to anhedral in shape. There is a weak alignment of minerals in a common plane. The

melanosome (mafic part) consist of biotite and sphene while the leucosome (felsic part) consist of plagioclase, quartz and orthoclase. Under plane polarized light (PPL) (Plate 6 a), the quartz is colourless with anhedral shape, non-pleochroic, no inclusions, not fractured nor altered and shows no cleavage. The feldspar and quartz grains are medium grained while the biotites are fine grained. Biotite also occurs as xenomorphic crystals with high relief, the crystals are brown in colour. Plagioclase shows one directional cleavage across twinning surfaces in some grains and weak cleavage in others and has inclusion of quartz grains.

Under cross polarized light (XPL) (Plate 6 b), the quartz exhibits undulose extinction, no twinning but shows grey to white interference colour. The plagioclase feldspar display polysynthetic twinning, grey and white interference colour. The biotite shows parallel/straight extinction and shows no twinning. The microcline can be easily distinguished with its cross-hatched twinning and grey to white interference colour. The opaque minerals were dark in colour under both PPL and XPL.



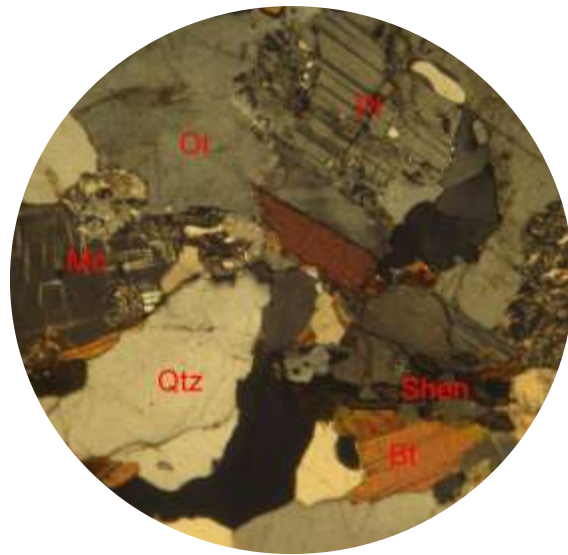
Plate 5: Field photograph of a granite gneiss outcrop (Latitude 9°03'23"N and Longitude 8°33'43"E)



a

b

XPL



PPL

Plate 6: Photomicrograph of granite gneiss under (a) PPL and (b) XPL composed of Biotite (Bt), Microcline (Mc), Orthoclase (Or), Plagioclase (Pl), Quartz (Qtz) and Sphene (Shen).

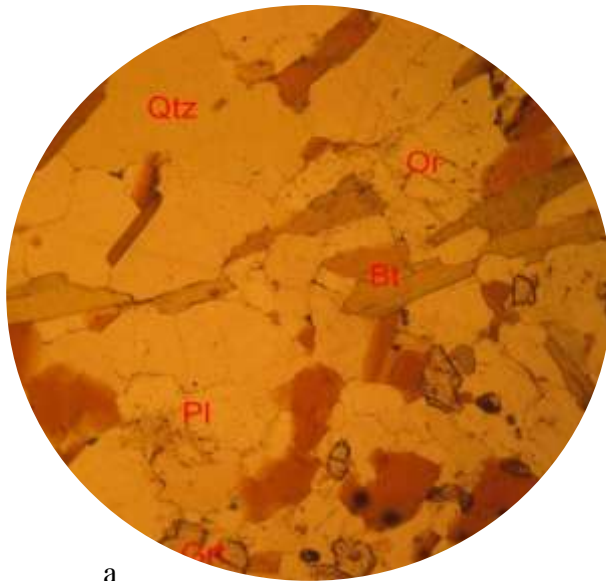
#### 4.1.4 Banded gneiss

The banded gneiss in the study area is medium to coarse grained rock with alternating felsic and mafic bands (Plate 7). In hand specimen, the rock consists of quartz, feldspar and biotite. There are quartz veins running concordantly to the foliation surface and some cross cutting. The rocks constitute a major rock unit of the study area making up about 30% of the rocks in the study area. The rock are found around Kotagora area and in some parts of Ragga. The rock is made up of felsic and mafic bands; the felsic bands consists of quartz and feldspars while the mafic bands which are made up of predominantly pf biotite. The rock is observed to host quartzo-feldspathic veins trending along with the foliation in the NE-SW direction (Fig. 9). The rocks contain pinch and swell structures (Plate 20) typical of rocks that have deformed by a mixture of semi-brittle to ductile flow (Garner et al., 2015).

Photomicrographs obtained from the thin section studies of the rock (Plate 8) reveal that the banded gneiss exhibit variable mineral grains closely packed with preferred orientation, quartz, biotite and feldspars form the bulk of the mineral composition. The rock is composed of quartz (39%), biotite (30%), plagioclase (13%), orthoclase (15%) and garnet (2%) (visual estimates). Quartz occurs as cloudy anhedral grains, with wavy extinction and a low birefringence. The crystals of biotite are subhedral, brown in colour and of high relief.

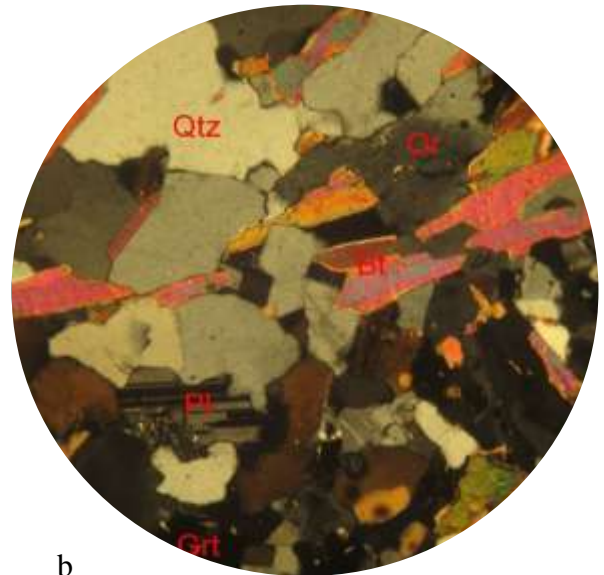


Plate 7: Field photograph of banded gneiss with quartz and quartzo-feldspathic veins (Latitude 9°05'05"N and Longitude 8°31'36"E).



a

PPL



b

XPL

Plate 8: Photomicrograph of banded gneiss under PPL (a) and XPL (b) composed of biotite (Bi), garnet (Grt), orthoclase (Or), plagioclase feldspar (Pl), and quartz (Qtz).

#### 4.1.5 Migmatite Gneiss

Migmatite gneiss is a banded, granular metamorphic rock that contains light and dark coloured bands with evidence for partial melting. Migmatite gneiss appear to represent the most extreme case of metamorphism. The migmatite gneiss in the study area are medium grained. The rocks are located in the eastern part of the study area around Kanje and parts of Marhai. The rocks show characteristic ptygmatitic folding (Plate 9) which is an evidence of plastic deformation. Other structures observed in the rock are folds, veins, and joints. Often pre-migmatisation structures in form of schollens are developed in which streaked portion of the host rock (paleosome) is enclosed in melted material (neosome) (Plate 10). These features are indicative of melt-residuum separation at low degrees of partial melting and consequently low melt fraction, characteristic of metatexite migmatite (Milord et al., 2001).

Petrographical studies of the thin section (Plate 11 a and b) reveals that the felsic bands consist of quartz and plagioclase while the mafic bands consist of mainly of biotite. Under plane polarized light (PPL), Quartz is colourless with no pleochroism, and twinning, no cleavage, no inclusions, not fractured nor altered, and sometimes have straight boundaries with other mineral grains. It has a low relief in xpl. Orthoclase appears colourless to cloudy with low relief. It is grey in cross polarized light and exhibits no twinning whatsoever. Biotite is brownish in colour and has prismatic, subhedral to anhedral habit with two sets of cleavage. It shows no twinning and occurs in patches with moderate to high relief. The plagioclase feldspar shows one directional cleavage across twinning surfaces in some grains and weak cleavage in others and has inclusion of quartz grains. Under cross polarized light (XPL), the quartz shows

low relief exhibits undulose extinction, no twinning and shows grey to white interference colour. Plagioclase is grey in cross polarized light and display polysynthetic twinning.

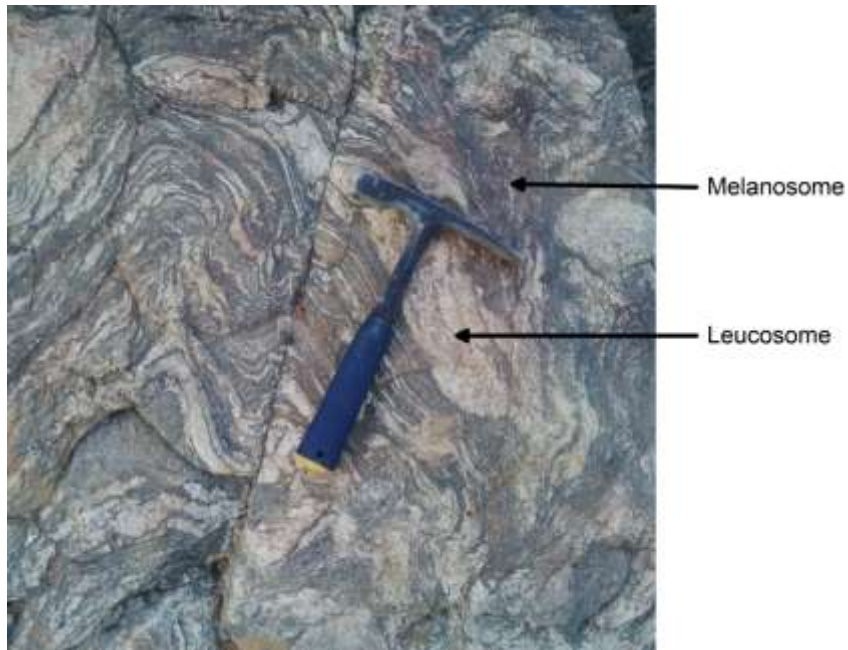
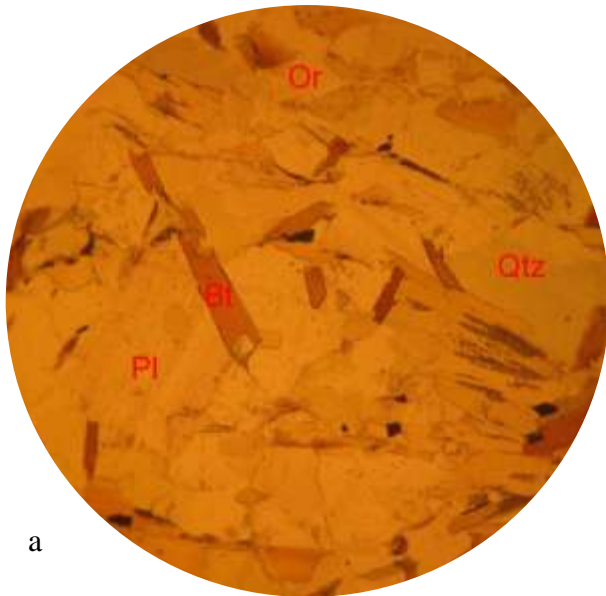


Plate 9: Field Photograph migmatite gneiss with pygmatitic folding (Latitude 9°00'28"N and Longitude 8°42'30"E)

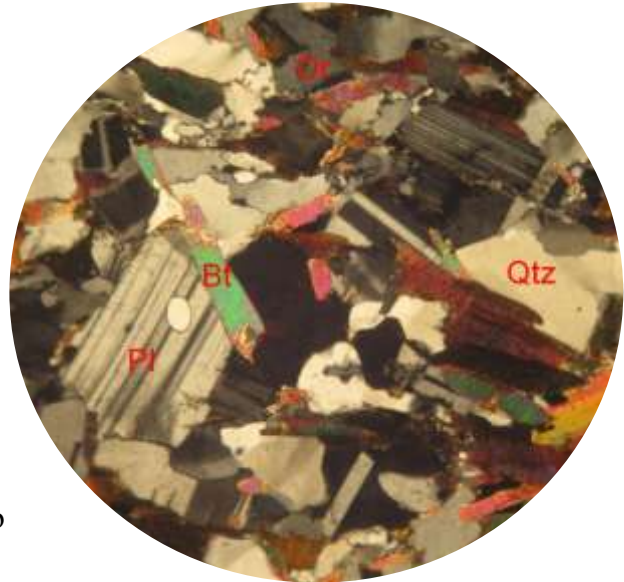


Plate 10: Field Photograph of Migmatite with pre-migmatisation structures (Latitude 9°06'42"N and Longitude 8°43'52"E)



a

XPL



b

PPL

Plate 11: Migmatite gneiss under (a) (XPL) and (b) (PPL) composed of biotite (Bi), orthoclase (Or), plagioclase feldspar (Pl), and quartz (Qtz).

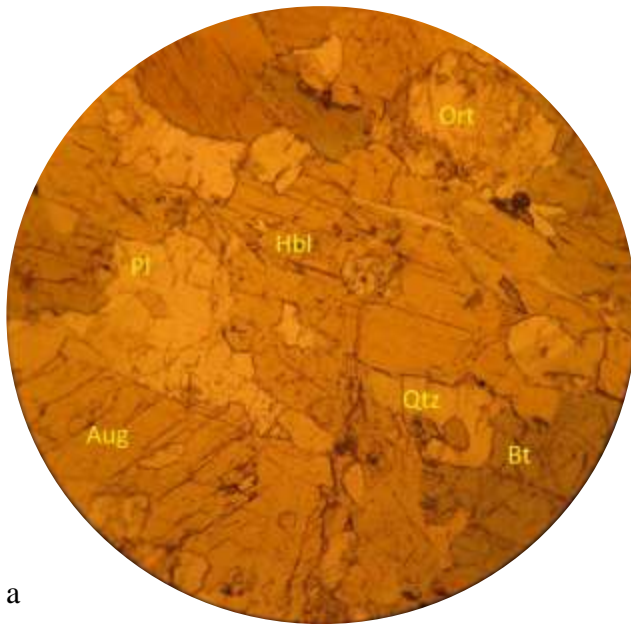
#### 4.1.6 Amphibolite

Amphibolite is a metamorphic rock consisting mainly of amphibole and plagioclase, little or no quartz. In the study area the amphibolites are found around Marhai and Kwarra. The rock is an ultramafic rock consisting of about 80% augite, hornblende and biotite with only 7% quartz, 6% plagioclase and 8% orthoclase. The rock contains a hornblende-plagioclase mineral assemblage characteristic of amphibolite facie metamorphism which is marked by medium pressure and temperature (Winter, 2014). The amphibolites are fine to medium grained and are found in the North eastern part of the study area. The rocks occur in uplifted regions and are highly fractured and scattered outcrops. The rocks are brecciated and occur as fragments produced by fracturing during faulting or other crustal deformation processes. The rocks appear to be spatially related to the migmatite gneisses and banded gneisses. The rock has a dark colour and fine to medium grained texture in hand specimen (Plate 12).

Thin section study of the amphibolite shows it is composed of augite, hornblende, orthoclase, plagioclase and quartz. The crystals are generally highly fractured and fine to medium grained. Augite crystals occurs largely as subhedral poikiloblastic crystals characterized by the inclusion of quartz and two of sets of cleavages intersecting at nearly  $120^\circ$ . The augite crystals show undulose extinction indicating that their crystals grew before a deformation event. Hornblende shows pleochroic colours ranging from yellow to brown and show one set of cleavage. Hornblende has high relief in PPL. The quartz crystal shows low relief and undulose extinction. The quartz polycrystalline with irregular grain boundaries formed in response to grain boundary migration recrystallisation. Orthoclase appears colourless to cloudy with low relief. It is grey in cross polarized light with oblique extinction and exhibits no twinning whatsoever. The plagioclase is colourless with low relief and anhedral to subhedral crystals with inclusion of quartz. It is grey in cross polarized light and display polysynthetic twinning and oblique extinction twinning. In plane polarized light biotite is brown in colour.

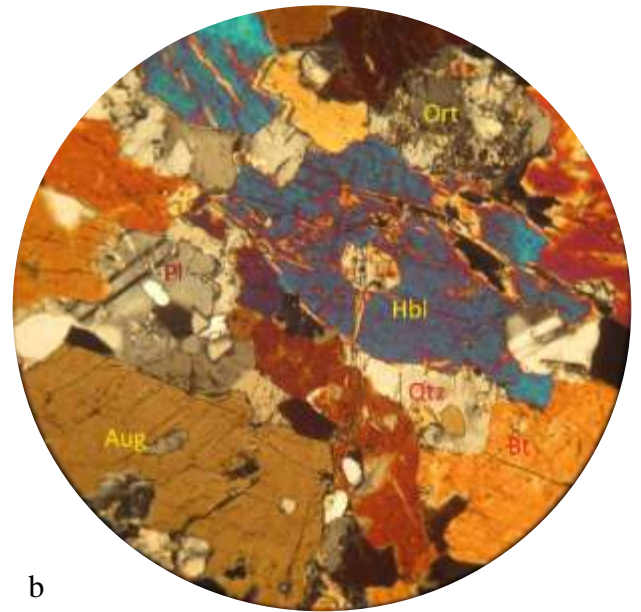


Plate 12: Hand Specimen of amphibolite rock in the study area (Latitude 9°07'17"N and Longitude 8°41'50"E).



a

PPL



b

XPL

Plate 13: Photomicrograph of Sheared amphibolite under (a) (XPL) and (b) (PPL) composed of augite (Aug), biotite (Bi), hornblende (Hbl), orthoclase (Or), plagioclase feldspar (Pl), and quartz (Qtz).

#### 4.1.7 Pegmatite

Most of the pegmatites in the study area occur as near vertical dykes and intrude into the older lithology of granite gneiss, banded gneiss, amphibolites and migmatite gneiss. The pegmatites are sparsely distributed occurring as veins (Plate 14) in the migmatite and granite gneisses and as dikes/boulders (Plate 15) in the banded gneisses and amphibolites. Some of the pegmatites are fractured and weathered. The size of the pegmatite veins varies from about 10 – 110cm in length and 2-10 cm in width. A few relatively small-sized pegmatites intercept bigger pegmatite bodies. Some occur as stumps of partially exposed pegmatites. There is generally a sharp contact between the pegmatite and the country rock, and in some cases, contact phenomena are restricted to a narrow zone of tourmalinisation (Plate 14b). The major strike directions of the pegmatites are NE-SW, NNE-SSW and NW-SE with a few in the N-S and EW. There are two observable types of pegmatites in the study area namely: quartz-feldspar-pegmatite and the quartz-muscovite-pegmatites. The quartz-feldspar-pegmatite occur predominantly trending NW-SE and are mostly found occurring in the migmatite gneisses while the quartz-muscovite-pegmatites predominantly trend NE-SW and are populated in the banded gneisses and granite gneisses. The bulk of the pegmatites in the study area are of the quartz-feldspar type, it is usually less deformed than the quartz-muscovite type. The quartz-muscovite-pegmatite are concentrated around the south western portion of the study area in the Abu and Kotangora area. There is a clear distinction in the two types of pegmatites observed. The quartz-feldspar-pegmatites are predominantly muscovite deficient while the quartz-muscovite-pegmatites are muscovite rich.

The quartz-muscovite-pegmatites are highly deformed and occurs as large dikes. The rocks are sometimes seen as scattered boulders in uplifted regions (Plate 16b). Their deformed

nature may be connected to shearing as the rocks are located in areas of denser lineaments (Fig. 14) which represents a region with a higher degree of rock fracturing. quartz-muscovite-pegmatites are mostly hosted in banded gneiss rocks which show notable pinch and swell structures associated with semi brittle failure in conjunction with subsequent material softening.



a.

b.

Plate 14: a. Field Photograph of quartz-feldspar-pegmatite intrusion into migmatite gneiss. (Latitude 9°00'20"N and Longitude 8°42'16"E)

b. Field photograph showing a narrow zone of tourmalinisation around the contact between quartz-feldspar-pegmatite and the host rock. (Latitude 9°00'30"N and Longitude 8°44'27"E)



a b  
 Plate 15: Quartz-muscovite-pegmatites boulders (b) Whitish quartz-muscovite-pegmatites intrusion in granite gneiss (Latitude 9°02'45"N and Longitude 8°34'38"E)



a b  
 Plate 16:(a)Highly deformed quartz-muscovite-pegmatites trending NE (9°02'16"N and Longitude 8°35'36"E). (b) Deformed nature of quartz-muscovite-pegmatites in uplifted region (9°02'48"N and Longitude 8°31'10"E).

#### 4.1.8 Dolerite

Dolerite constitutes a minor geological unit in the study area, occurring in sizes too small to be mapped. The dolerites intrude some of the banded gneiss, granite gneiss and migmatite gneiss in the study area. The dolerites mostly occur as dykes (plate 17) and occasionally as sills. The dolerites vary size, shape and orientation. When considering the minerals within the rocks, the dolerites are noted by their differences in colours. The proportion of the dolerites to the host rock is seen to vary in the study area. The migmatite gneisses are noted to have more of dolerite than the other rock types.



a



b

Plate 17: (a) Field photograph of dolerite dykes intrusion into granite gneiss (9°01'18"N and Longitude 8°36'53"E). (b) Field photograph of dolerite dike intrusion into Migmatite gneiss (9°06'56"N and Longitude 8°44'39"E)

## **4.2 Structural Geology and Lineament Analysis**

### **4.2.1 Introduction**

Relics of tectonic activities is noticeable in structures encountered in the area. The structural features observed in the study area include; foliation, fractures, veins, lineation, joints folds and minor faults. The predominant structures trend N-S to NE-SW and this conforms to Pan-African structural pattern. Shear fractures observed on the granites are either filled by late pegmatitic veins or display evidence of free aperture.

### **4.2.2 Foliation**

Foliation is a parallel orientation of platy minerals or mineral banding in rocks as seen in the banded gneisses (Plate 18). The predominant strike direction of foliation in the banded gneiss of the study area is NE-SW direction (Fig. 9) which is defined by parallel orientation of trends in the general N-S direction of the meta-sedimentary group of the Basement Complex of Nigeria (Jatau et al., 2012). The foliation in the banded gneiss have strikes ranging from  $22^{\circ}$  to  $54^{\circ}$ .



Plate 18: Photograph of foliation structure in the banded gneiss of the study area (Latitude  $9^{\circ}05'35''\text{N}$  and Longitude  $8^{\circ}31'42''\text{E}$ ).

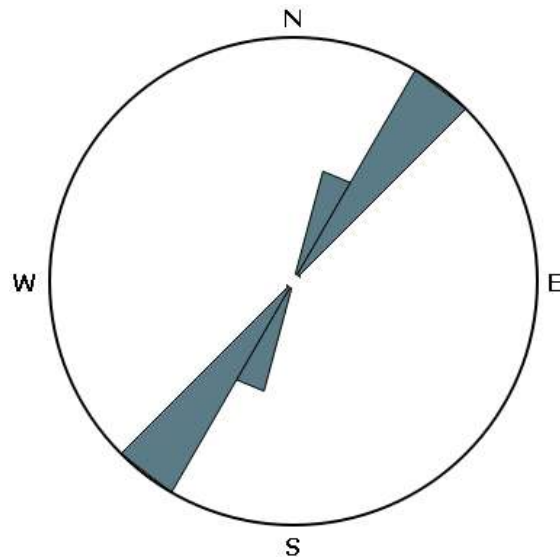


Fig9: Rose diagram of foliation in the banded gneiss of the study area.

Lineation and foliation also occur in most of the gneisses encountered. They probably developed as a result of tectonic differentiation. The preferred orientation of the foliation is NW-SE trending which is indicating imprint of the Pan-African orogeny (Ball, 1980).

### 4.2.3 Joints

The major trend of joints in the Banded gneiss is NNE-SSW (Fig. 10). Joints are formed as a result of tensional strain on an outcrop and they generally occur as sets, with each set consisting of sub-parallel joints to each other. Variable dip angles and direction characterize the strike joints of the granites and gneisses. The amphibolites and the biotite granite in the study area have the highest concentration of joints in the study area.



Plate 19:Field photograph of joints in the granite gneiss of the study area (Latitude 9°02'09"N and Longitude 8°38'34"E).

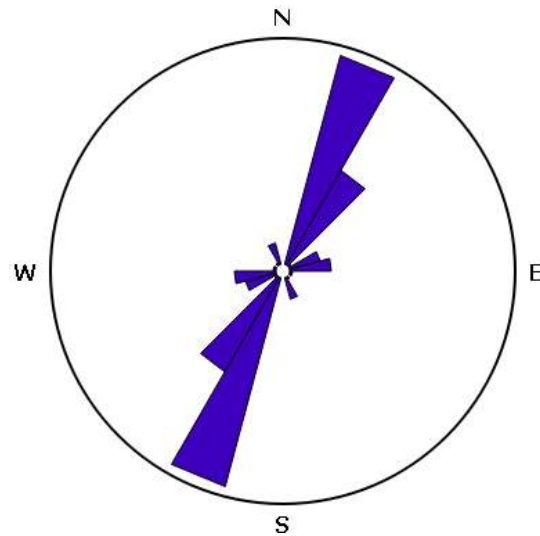


Fig. 10: Rose diagram of joints in the rocks of the study area.

#### 4.2.4 Veins

Veins are distinct sheet-like body of crystallized minerals within a rock, and are formed when mineral constituents carried by an aqueous solution within the rock mass are deposited through precipitation. Generally, veins are believed to have resulted from growth of crystals on the walls of planar fractures in rocks, with the crystal growth occurring normal to the walls of the cavity, and the crystal protruding into/filling up the open space (voids). Veins are very essential to mineral deposits because they are the source of mineralisation either in or proximal to the veins. Both quartz and pegmatitic veins are found in the rocks of the studied area. The veins are irregular. The veins also occur as sheet-like or tabular body of one or more minerals deposited in opened fissures/fractures (cracks), as pegmatitic veins (Plate 20a) or as quartzo-feldspathic veins (Plate 20b). Some of them run parallel to the general structural NE-SW trend, while others crosscut especially the quartz veins. It can be inferred that they formed at a later age. The pegmatite veins in the study area vary in sizes generally ranging from as small as 1.5cm to 30cm. It predominantly trends in the NE-SW orientation (Fig. 11).



a



b

Plate 20: (a) Field photograph of pegmatite veins that intruded the migmatite gneiss of the study area (Latitude  $9^{\circ}01'15''\text{N}$  and Longitude  $8^{\circ}41'30''\text{E}$ ). (b) Field photograph of quartzo-feldspathic veins in the banded gneiss within the study area (Latitude  $9^{\circ}05'05''\text{N}$  and Longitude  $8^{\circ}31'12''\text{E}$ ).

Quartz or quartzo-feldspathic veins have a dominant trend of NE-SW (Fig. 12) and are formed as a result of recrystallisation of silicate grains in the rock crevices or joints that are being filled up with hydrothermal fluid, which is mainly quartz and feldspar and later solidifying (Jatau et al., 2012). Some of these veins may be discordant to foliation planes. In the study area, this structure is mostly associated with the gneiss.

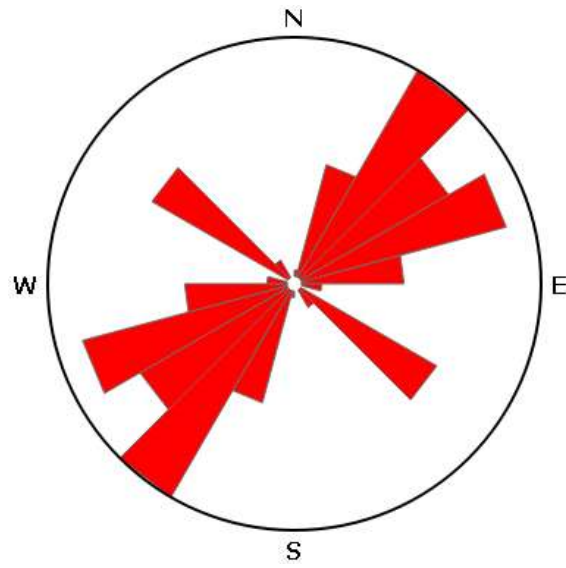


Fig. 11: Rose diagram of pegmatite veins in the study area showing the NE-SW dominant trend.

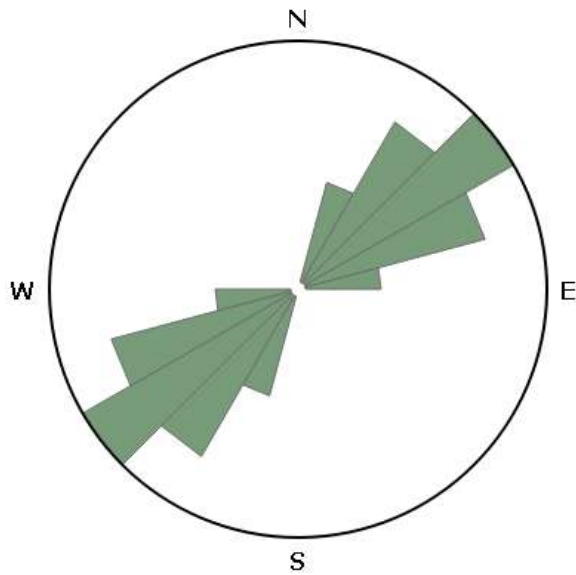


Fig. 12: Rose diagram of quartzo-feldspathic veins showing the NE-SW dominant trend in the banded gneiss of the study area.

#### 4.2.5 Folds

Different types of folds were seen in the study area. The folds were seen in the study area and are mostly associated with the banded gneisses and migmatite gneisses. The folds are asymmetrical folds (Plate 21a), ptygmatitic folds (Plate 21b) and recumbent folds. The recumbent fold has near horizontal or horizontal axial plane; some of them are results of highly ductile deformation with valid axial planes (Pollard and Fletcher, 2005).



a.

b.

Plate 21: (a) Asymmetrical folding observed on the banded gneiss (Latitude  $9^{\circ}05'05''\text{N}$  and Longitude  $8^{\circ}31'36''\text{E}$ )(b) Ptygmatitic folding seen on the migmatite gneiss (Latitude  $9^{\circ}00'25''\text{N}$  and Longitude  $8^{\circ}43'30''\text{E}$ )

Asymmetrical folds were seen on the banded gneisses and usually contain a folded quartzofeldspathic material embedded in it and forming a lineation of quartz minerals. Asymmetrical folds are of unequal limbs and the axial planes are not equidistant from the limbs. The observed ptygmatitic folds occur on the migmatitic gneisses and are due to ductile

deformation during to partial melting of crustal rocks. Ptygmatic folding is typically associated with migmatitic rocks.

#### 4.2.6 Pinch and Swell

Pinch and swell structures form when a more competent layer undergoes layer parallel extension in a weaker matrix, and can range in size from microscopic to outcrop to regional scales (Goldstein, 1988). Pinch and swell structures may be initiated by brittle failure of the more competent layer in conjunction with subsequent material softening. Pinch and swell structures were observed occurring on the banded gneiss rocks (Plate 22). The banded gneiss rock shows well developed felsic and mafic layers with the different layers exhibit different structures. Some layers form well defined pinch and swell chains, while others display only minor undulation of the mafic to felsic edge. Very narrow to wider neck thicknesses as well as short to long swell separations develop in different layers.



Plate 22: Pinch and swell structures in the biotite gniesses (Latitude 9°05'12"N and Longitude 8°31'26"E).

#### 4.2.7 Fault

When stress is applied on a rock, the competent rocks tend to fold as a result of strain while the incompetent rocks become fractured. Most of the fractures observed in the study area range from about 2 mm to 10 cm. High fracture density were observed in the gneisses. Minor strike slip faults occur in the study area. In some cases, NE-SW trending fractures displace NNE-SSW trending veins with strike slip of about 17 - 20 cm (Plate 23). Also the N-S and E-W trending veins are either truncated or crosscut by NE-SW trending faults. There are both sinistral and dextral fault types. Similar oriented strike slip faults are common in the whole Pan-African belt of west Africa and are interpreted to represent the last compressional phase that occurred after about 530 Ma related to the Pan-African tectogenesis (Ball, 1980).



Plate 23: Field photograph of dextral fault along a quartz veins in the banded gneiss (Latitude 9°05'35"N and Longitude 8°30'06"E).

### 4.3 Lineament analysis

O'leary et al 1976, defined lineaments as mappable linear features which differs distinctly from the pattern of adjacent features and presumably reflect subsurface phenomena. Lineament usually follows regional geology (e.g., intrusive bodies or large faults' strikes) and is thus useful in mapping structural trends. The structural lineaments in the area were thus mainly faults and fractures.

The structural lineaments were extracted from landsat ETM<sup>+</sup> image of the study area. Landsat band7 was downloaded from Global Land Cover Facility Website ([glcf.umd.edu/data/landsat/](http://glcf.umd.edu/data/landsat/)). It was then enhanced using ENVI v4.5 software to make the lineaments more visible. Individual lineaments were traced out using Global Mapper v15 software before exporting to ArcGIS and Rockware softwares for statistical and orientation analysis. A total of 31 lineaments were extracted from the study area. The minimum length derived from these lineaments was 822.50m, maximum length was 6275.15m. The non-geological lineaments such as paths, roads, power cables and field boundaries in the study area were eliminated using the topographical map (Yassaghi, 2006).

The mapped structural lineaments were analyzed using lineament density (LD) and lineament frequency (LF) parameters (Solomon and Ghebreab, 2006). The results of the analysis are presented as structural lineament map (Fig. 13) lineament density map (Fig. 14) and rose diagram (Fig. 15).

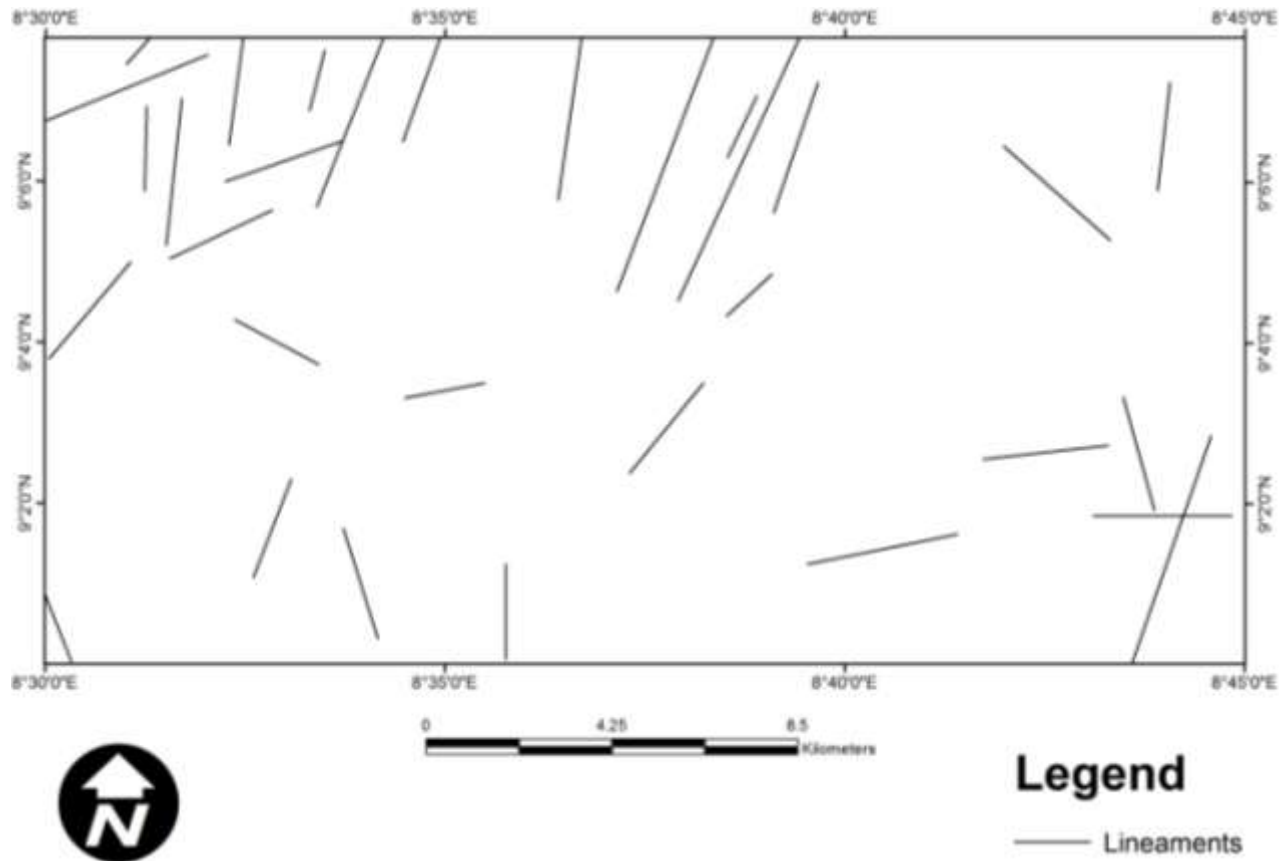


Fig. 13: Structural lineament map of the study area

The qualitative study of the geological map, structural lineament map and Lineament density map of the study area showed that structural lineaments were more concentrated in the migmatites, banded gneisses and amphibolites (Pre-Cambrian basement rocks) than on the Jurassic Younger Granites. This was due to the effect of several tectonic deformations that accompanied the different orogenic events that have occurred throughout the Nigerian polycyclic basements.

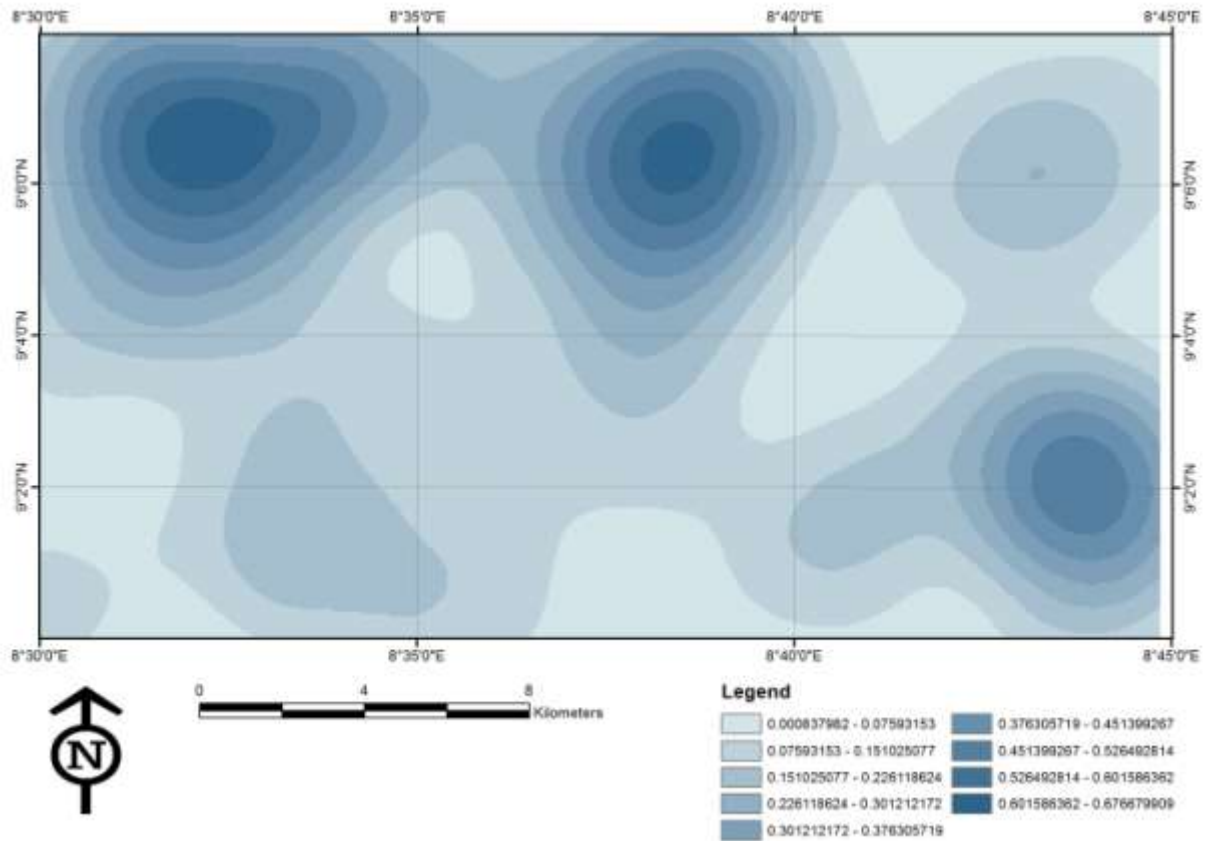


Fig. 14: Lineament density map of the study area (the denser lineaments are indicative of the intensity of rock fracturing)

The orientation of structural lineaments on rocks can be correlated to past tectonic events that have affected them. The orientation of the structural lineaments on the structural lineament map was measured and plotted on a rose diagram using Georose software. The rose diagram of the lineament trends in the study area (Fig. 15) revealed that well developed principal structural trends are N-S, NE-SW, and NNE-SSW with minor ENE-WSW and NNW-SSE trends. This finding is in agreement with previous works suggesting that Nigeria has a complex network of fractures and lineaments with dominant trend directions of NE-SW, NW-SE, and N-S directions. (Ananaba et al., 1987; Chukwu-Ike., 1977, Obiora 2009). These

trends also agree with more recent works carried out in parts of the basement complex adjoining the Benue Trough by Olasehinde et al., (1990) and Anudu et al., (2012). Many of the lineaments coincided with drainage lines indicating that drainage in the study area may be structurally controlled (Samaila et al., 2011). According to Obiora (2009), NNE-SSW and N-S trends are Pan-African, while E-W and NNW-SSE trends are pre-Pan-African. Hence the NE-SW, N-S and NNE-SSW trends in the study area may probably have been Pan-African, whereas the NNW-SSE and E-W trends may have been relicts of pre-Pan- African events and hence less pronounced.

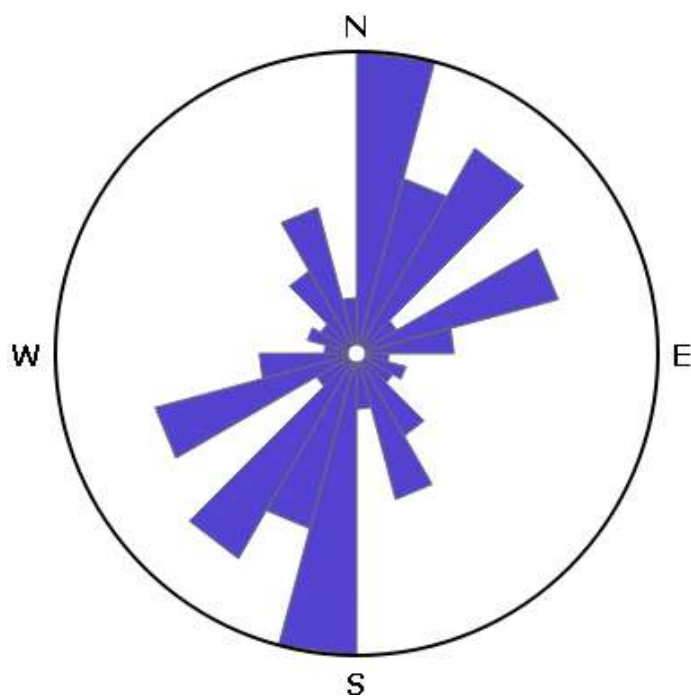


Fig. 15: Rose diagram of structural lineament trends of the study area

## **4.4 GEOCHEMISTRY**

### **4.4.1 Introduction**

A total of 11 whole rock samples and 4 muscovite extracts from the quartz-muscovite-pegmatite were analysed for major and trace elements including rare earth element (REE). The whole rock samples include one representative sample each of the amphibolite, migmatite gneiss, banded gneiss, granite gneiss, two samples each of alkali granite and albitized granite with three samples of quartz-feldspar-pegmatite. The major elements were analysed by inductively couple plasma atomic emission spectrometry following a lithium borate fusion and dilute acid digestion while trace and REE were analysed by inductively couple plasma mass spectrometry following a multi-acid digestion method. Oxides of the major elements concentration provided basis for a comprehensive rock classification while trace elements including the rare-earth elements (REE) composition were used for the determination of the petrogenetic and mineralisation processes as well as the associated tectonic environment.

### **4.4.2 Major Element Geochemistry**

The major oxides composition of the rocks in the study area is presented in Table 1 while Table 2 shows the CIWP Norm values for the granitic rocks of the study area. The Harker's plot for albitized granite, pegmatites and alkali granites are shown in Fig. 16.

Table 1: Major oxide compositions of the rocks in the study area.

Petrology	Amphibolite	Migmatite Gneiss	Banded Gneiss	Granite Gneiss	Albitised Granite		Alkali Granite		Quartz Feldspar Pegmatite			Muscovite (Quartz Muscovite Pegmatite)			
Sample (wt%)	S10	S3	S9	S7	S4	S12	S2	S6	S1	S5	S8	S13	S14	S15	S16
SiO <sub>2</sub>	50.43	70.25	67.79	69.76	74.02	73.7	73.88	74.48	74.3	73.9	73.5	60.91	67.7	61.6	54.3
Al <sub>2</sub> O <sub>3</sub>	13.69	14.23	14.96	15.30	15.24	15.21	12.06	12.36	13.5	14.4	13.1	23.70	19.9	24.5	28.2
Fe <sub>2</sub> O <sub>3</sub> (T)	10.65	6.53	5.20	3.41	0.76	0.89	2.48	2.96	0.69	0.84	0.68	2.26	1.51	1.32	3.13
MnO	0.18	0.02	0.06	0.05	0.05	0.05	0.04	0.04	0.01	0.03	0.01	0.09	0.10	0.05	0.05
MgO	7.57	1.08	1.14	0.71	0.02	0.02	0.08	0.06	0.04	0.03	0.04	0.08	0.15	0.17	0.55
CaO	12.35	1.62	3.24	1.93	0.11	0.14	0.61	0.64	0.28	0.28	0.98	0.34	0.11	0.11	0.08
Na <sub>2</sub> O	0.93	3.13	4.12	3.84	5.07	5.05	3.45	3.36	3.70	3.66	3.30	1.86	1.66	1.22	0.99
K <sub>2</sub> O	0.44	2.21	2.19	4.02	3.78	3.64	5.10	5.38	5.80	5.74	4.63	6.99	5.54	6.72	8.31
TiO <sub>2</sub>	0.938	0.200	0.925	0.517	0.002	0.04	0.162	0.159	0.03	0.03	0.02	0.016	0.08	0.09	0.057
P <sub>2</sub> O <sub>5</sub>	0.12	0.08	0.24	0.17	0.38	0.35	0.03	0.03	0.62	0.61	0.06	0.46	0.19	0.16	0.06
Total	97.29	99.35	99.86	99.7	99.43	99.09	97.89	99.46	98.9	99.5	96.3	96.7	96.9	95.4	95.7

Table 2: CIWP Norm for the granitic rocks of the study area

Normative Minerals	Albitised Granite		Alkali Granite		Quartz-Feldspar-Pegmatites			Quartz-Muscovites-Pegmatites			
	S4	S12	S2	S6	S1	S5	S8	S13	S14	S15	S16
Q	29.438	29.72	31.27	30.87	30.02	29.97	34.15	21.45	35.47	27.37	13.60
C	2.813	3.102	0.000	0.000	1.59	2.406	1.73	13.07	10.46	14.76	17.64
Or	22.33	21.51	30.13	31.79	34.261	33.92	27.36	41.30	32.74	39.71	49.11
Ab	42.875	42.73	29.19	28.43	31.280	30.97	27.92	15.73	14.04	10.32	8.377
An	0.000	0.000	2.357	2.753	0.00	0.000	4.47	0.000	0.000	0.000	0.005
Di	0.000	0.000	0.418	0.201	0.00	0.000	0.00	0.000	0.000	0.000	0.000
Hy	1.388	1.599	3.881	4.748	1.24	1.517	1.20	4.082	3.032	2.666	6.548
IL	0.004	0.008	0.308	0.302	0.006	0.006	0.03	0.030	0.034	0.036	0.108
Ap	0.198	0.252	0.071	0.071	0.509	0.504	0.14	0.612	0.198	0.198	0.142
Sum	99.054	98.93	97.64	99.17	98.91	99.29	97.02	96.29	95.99	95.07	95.54

### Silica SiO<sub>2</sub>

The SiO<sub>2</sub> concentration in the host rocks ranges from 50.43 to 74.48 wt%. The alkali granites have the highest SiO<sub>2</sub> concentration with an average of 74.18 wt%., followed by the albitised granite with a SiO<sub>2</sub> concentration of 73.89 wt%. The high content of SiO<sub>2</sub> in the granites is an indication of their acidic nature and enrichment in common rock forming minerals such as quartz and feldspar. The migmatite gneiss has the highest SiO<sub>2</sub> concentration amongst the metamorphic rocks in the study area with a value of 71.97. the other metamorphic rocks Granite gneiss, banded gneiss and amphibolite have SiO<sub>2</sub> concentrations of 69.76wt%, 67.79wt% and 50.43wt% respectively.

### Aluminum Oxide Al<sub>2</sub>O<sub>3</sub>

The Al<sub>2</sub>O<sub>3</sub> concentration in the host rocks ranges from 11.06wt% – 15.35wt% with albitised granites having the highest average concentration of 15.29 and the alkali granite with the lowest average concentration of 11.56. The metamorphic rocks consisting of migmatite

gneiss, banded gneiss, granite gneiss and amphibolite in the area have similar  $\text{Al}_2\text{O}_3$  concentration of 14.89, 14.96, 15.3 and 13.69 respectively. On the Harker's diagram, the rocks form a somewhat vertical linear trend with the younger granites plotting on the lower end of the trend.

#### Iron (ii) Oxide $\text{Fe}_2\text{O}_3$

The  $\text{Fe}_2\text{O}_3$  concentration in the host rocks ranges from 0.76wt% – 10.25wt%. The albitised granites have the lowest  $\text{Fe}_2\text{O}_3$  concentration which is indicative of its acidic and felsic nature. The amphibolite has the highest  $\text{Fe}_2\text{O}_3$  content of 10.25 wt% which reflects its mafic and ferromagnesian rich composition. The banded gneiss has a relatively high  $\text{Fe}_2\text{O}_3$  composition of 5.2wt% which may be due to its biotite rich nature. The alkali granite has an average  $\text{Fe}_2\text{O}_3$  concentration of 2.72 while the migmatite gneiss and granite gneiss have a concentration of 1.52 and 3.41 respectively. On the Harker's diagram the rocks form a negative correlation with  $\text{SiO}_2$ , the  $\text{Fe}_2\text{O}_3$  concentration dropping steadily as  $\text{SiO}_2$  content increases from amphibolite to albitised granite. The alkali granite plot slightly off the trend.

#### Magnesium Oxide (MgO)

The rocks rich in felsic phases such as the alkali granite and the albitised granite have the lowest MgO concentrations of 0.07wt% and 0.02wt% respectively. The higher MgO concentration of the amphibolite 7.57wt% reflects the modal mineralogy of the rocks which contains a higher proportion of mafic minerals. The migmatite gneiss, banded gneiss and granite gneiss have MgO concentrations of 0.7wt%, 1.14wt% and 0.71 wt% respectively. The rocks form a somewhat negative correlation with  $\text{SiO}_2$  with the metamorphic rocks showing a

weak correlation and the felsic rich rocks (abitized granite and alkali granite) forming a cluster in the lower portion of the trend.

#### Manganese Oxide (MnO)

The rocks generally have a low MnO concentration with a range of 0.02wt% – 0.18wt%. The migmatite gneiss has the lowest value while the amphibolite has the highest concentration of 0.18wt%.

#### Calcium Oxide (CaO)

The CaO content in the rocks ranges from 0.11 wt%– 12.35wt%. the albitised granite has the lowest average CaO content of 0.12wt% while the amphibolite has the highest of 12.35wt%. The banded gneiss has a relatively high concentration of 3.24wt% while the migmatite and the granite gneiss have concentrations of 2.96wt% and 1.93wt% respectively. The SiO<sub>2</sub> concentration seems not to exert any significant control on the CaO concentration.

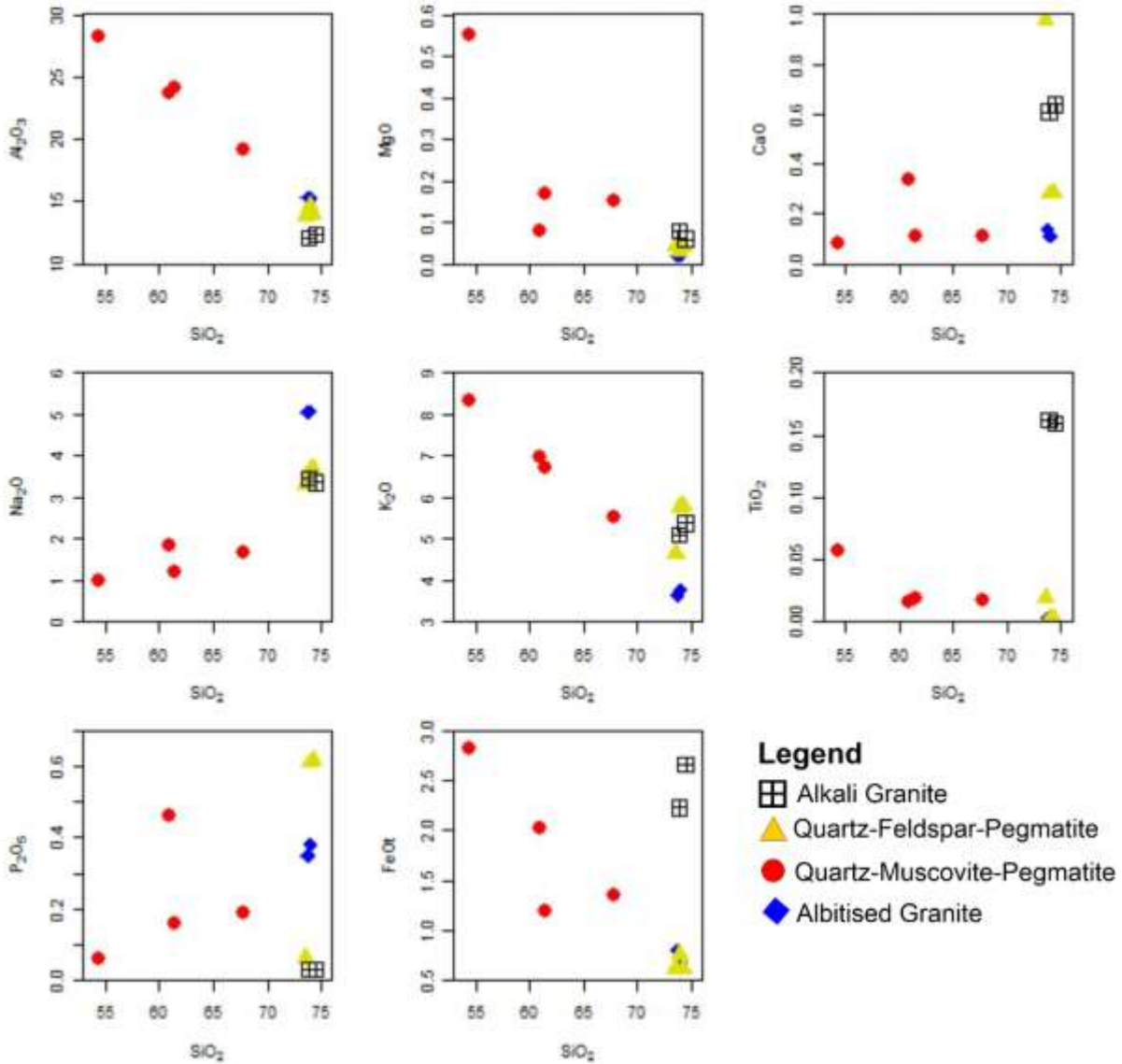


Fig. 16: Harker plot of  $\text{Al}_2\text{O}_3$ ,  $\text{CaO}$ ,  $\text{K}_2\text{O}$  and  $\text{Na}_2\text{O}$  against silica ( $\text{SiO}_2$ ) for the granite suites in the study area. S2 and S6 (Alkali Granite), S4 and S12 (Albitized Granite), S2 and S6 (Alkali Granite), S4 and S12 (Albitized Granite).

#### 4.4.3 Major Oxides Geochemistry in the Pegmatites

The muscovite extract samples have an average  $\text{SiO}_2$  concentration of 61.12wt% ranging from 54.35wt% – 67.77wt%. The whole rock pegmatites have an average  $\text{SiO}_2$  concentration of 73.9wt% ranging from 73.56wt% – 74.29wt%. The muscovite samples have the highest values of  $\text{Al}_2\text{O}_3$ ,  $\text{MgO}$ ,  $\text{K}_2\text{O}$  and  $\text{MnO}$  with mean concentrations of 23.80 wt%, 0.23 wt%,

6.89 wt% and 0.07 wt%. The muscovite extract also have a high value of  $\text{Fe}_2\text{O}_3$  and  $\text{P}_2\text{O}_5$  with mean values of 2.05 wt% and 0.21 wt% respectively. It is however marked with relatively low values of  $\text{SiO}_2$  and  $\text{CaO}$  with mean values of 61.12 wt% and 0.16 wt% respectively. The high  $\text{Al}_2\text{O}_3$  values of muscovite samples attests to its peraluminous nature consistent with rare metal pegmatites. The rocks show a negative correlation with  $\text{Al}_2\text{O}_3$  on the Harker's diagram (Fig. 16). The quartz-feldspar-pegmatite are  $\text{SiO}_2$  rich with an average value of 73.92 wt%. It has the highest value of  $\text{P}_2\text{O}_5$  with a mean value of 0.42 wt%. It also has relatively high values of  $\text{Al}_2\text{O}_3$ ,  $\text{CaO}$  and  $\text{Na}_2\text{O}$  with mean values of 14.13 wt%, 0.51 wt% and 3.55 wt%. The quartz-muscovite-pegmatites are observed to have a negative correlation on the Plot of  $\text{K}_2\text{O}$  vs,  $\text{SiO}_2$ , and a positive correlation of  $\text{Na}_2\text{O}$  vs  $\text{SiO}_2$  (Fig. 16). The pegmatites show a negative correlation with  $\text{Fe}_2\text{O}_3$  on the Harker's diagram. They also show a positive correlation with  $\text{P}_2\text{O}_5$ , indicating the increase of  $\text{P}_2\text{O}_5$  with increasing  $\text{SiO}_2$  during magmatic differentiation. Phosphorous is an incompatible element and concentrates in the residual melt where they act as fluxes and enhance growth of large crystals as observed in the pegmatites (London, 2008).

On the Shand index plot (Fig. 17) the albitised granite and the pegmatites plot in the peraluminous ( $\text{ASI} > 1.0$ ) field with an aluminium saturated index (ASI) ranging from 0.99 wt% to 2.64 wt% and modified alkali-lime index ranging from 3.07 wt% to 9.22 wt%. The albitised granites and the muscovites showing the strongest peraluminous values of (ASI 1.26 and 2.40 respectively). The alkali granite has a mean ASI value of 0.98 and plot in a metaluminous field close to the border of the peralkaline field.

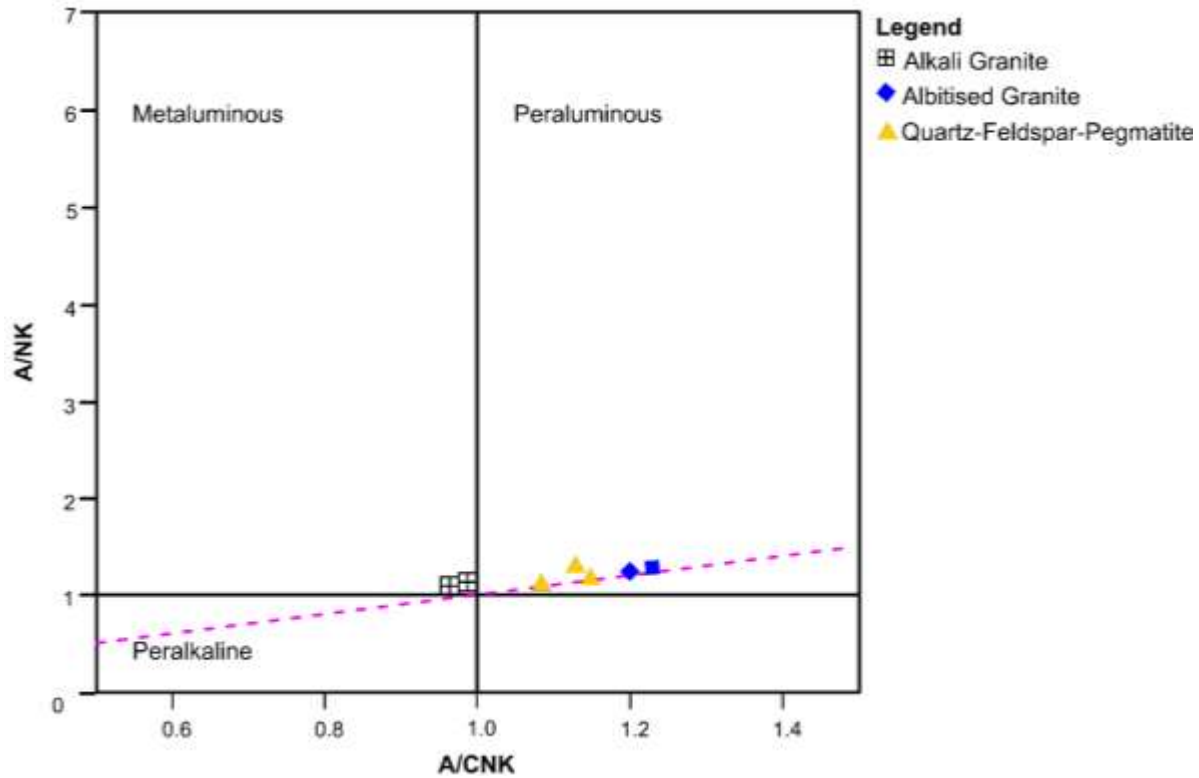


Fig. 17: A/CNK – A/NK plot for the granitoids in the study area after Shand (1943)

A plot of  $\text{Fe (total)}/(\text{Fe (total)}+\text{MgO})$  versus  $\text{SiO}_2$  (Fig. 18) and  $\text{Na}_2\text{O}+\text{K}_2\text{O}-\text{CaO}$  versus  $\text{SiO}_2$  (Fig. 19) after Frost *et al.* (2001) shows the pegmatites, alkali granites and albitized granite have strong iron enrichment. Ferroan (Fe-enriched) are interpreted to be closely associated with conditions of limited availability of  $\text{H}_2\text{O}$  and low oxygen fugacity during partial melting of their source rocks (Frost *et al.*, 2001). The  $\text{Na}_2\text{O} + \text{K}_2\text{O}$  versus  $\text{SiO}_2$  diagram after Frost *et al.* (2001) (Fig. 18) categorised the granitic rocks into the alkali, alkali-calcic, calcic-alkali and calcic series. All the granites fall in the alkali-calcic field so also the pegmatites with the exception of one quartz-feldspar-pegmatite sample (S8) that falls in the calcic-alkali field

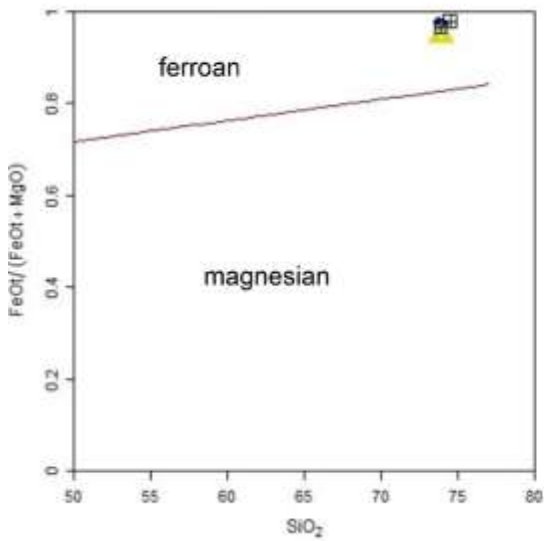


Fig. 18

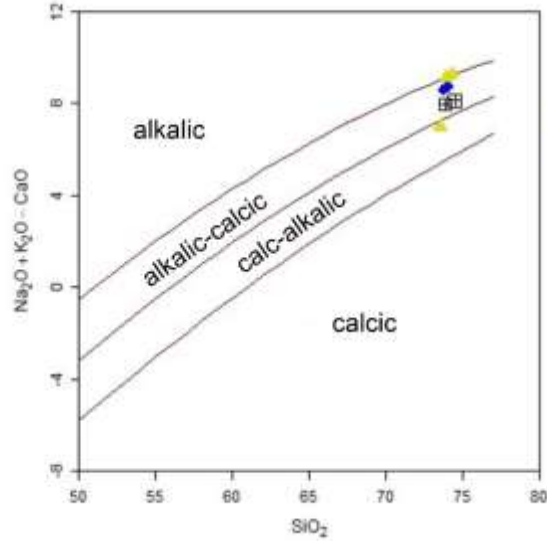


Fig. 19

Fig. 18: Fe (total)/(Fe (total)+MgO) versus SiO<sub>2</sub> after Frost et al 2001.

Fig. 19: Na<sub>2</sub>O + K<sub>2</sub>O - CaO versus SiO<sub>2</sub> after Frost et al 2001.

On the SiO<sub>2</sub> vs. Na<sub>2</sub>O+K<sub>2</sub>O diagram of Middlemost,(1985) (Fig. 20), the quartz-feldspar-pegmatite, alkali granites and albitised granite samples also plot in the granite field, indicative of the bulk granite geochemistry of these rocks.

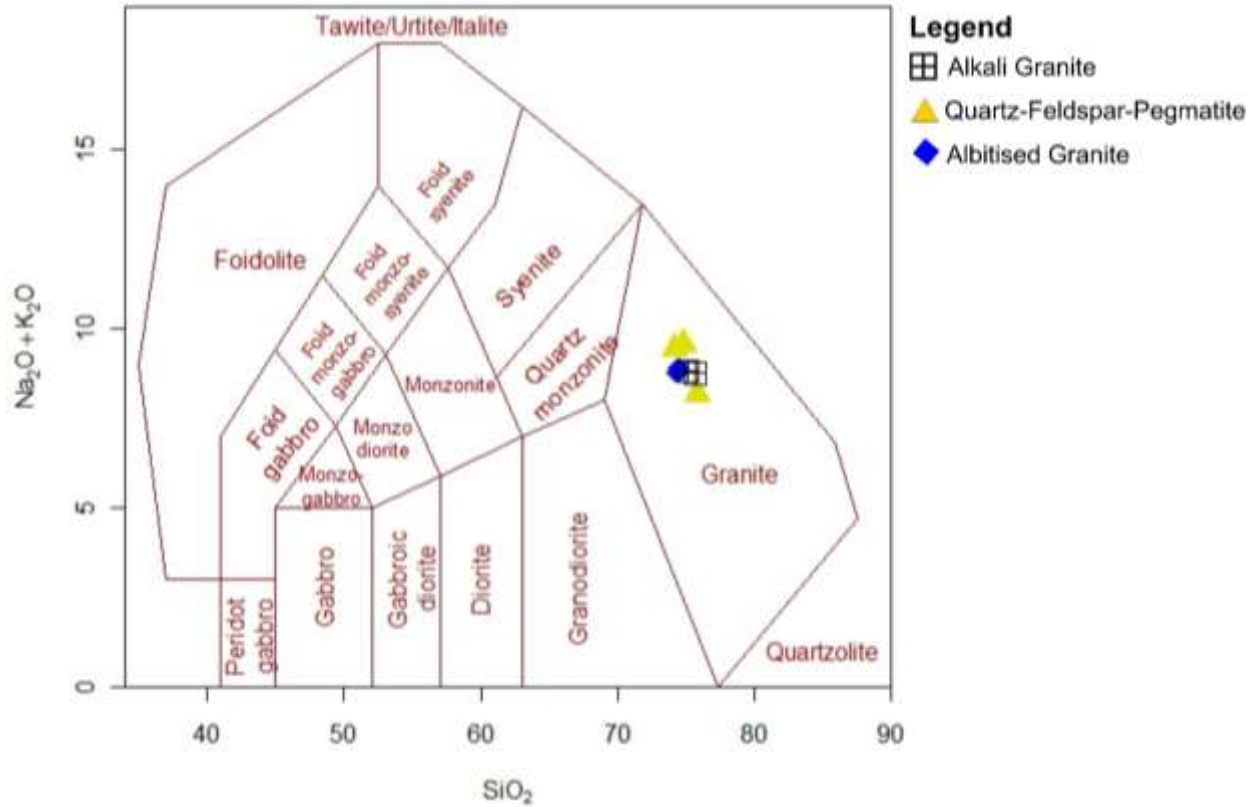


Fig. 20:  $\text{Na}_2\text{O}+\text{K}_2\text{O}$  vs.  $\text{SiO}_2$  for the granitoids diagram of Middlemost,(1985). S2 and S6 (Alkali Granite), S4 and S12 (Albitized Granite), S1,S5 and S8 (Quartz-Feldspar-Pegmatite).

The Ternary plot after O'Connor, (1965) (Fig. 21), the major element changes are illustrated in the normative Ab-Or-An diagram. The rocks are delineated by their variable contents of albite as compared with the other feldspar components. The pegmatites, albitised granite and alkali granite all plot within the granite field, with the albitized granite plotting much closer to the Ab corner due to its albite rich nature.

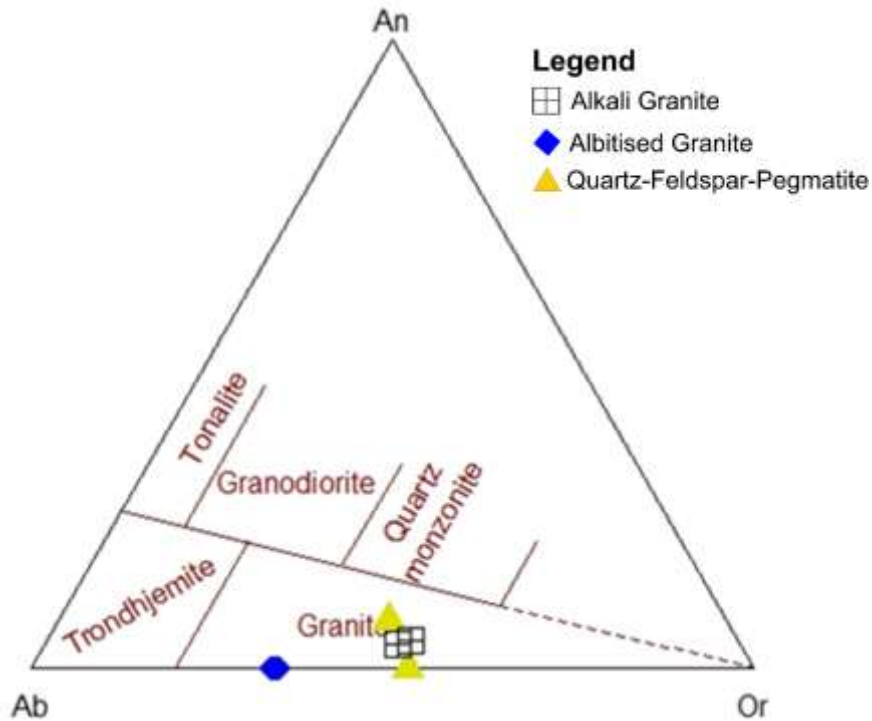


Fig. 21: Ternary normative Ab-Or-An diagram after O'Connor, 1965.

The granites were plotted on the A/CNK versus SiO<sub>2</sub> discrimination diagram after (after Chappel and White, 1974) (Fig. 22). The albitised granite, quartz-feldspar-pegmatite and quartz-muscovite-pegmatite all plotted within the S-type granite while the alkali granite plotted within the I-type field. S-type granitoids are products of the partial melting of already peraluminous sedimentary source rocks imprinted by weathering at the Earth's surface (Winter, 2014) while the I-type are interpreted as those derived from recycled, dehydrated continental crust (Collins *et al* 1982) and those derived directly from melting of subducted oceanic crust or overlying mantle (White, 2005; Whalen *et al.*, 1987).

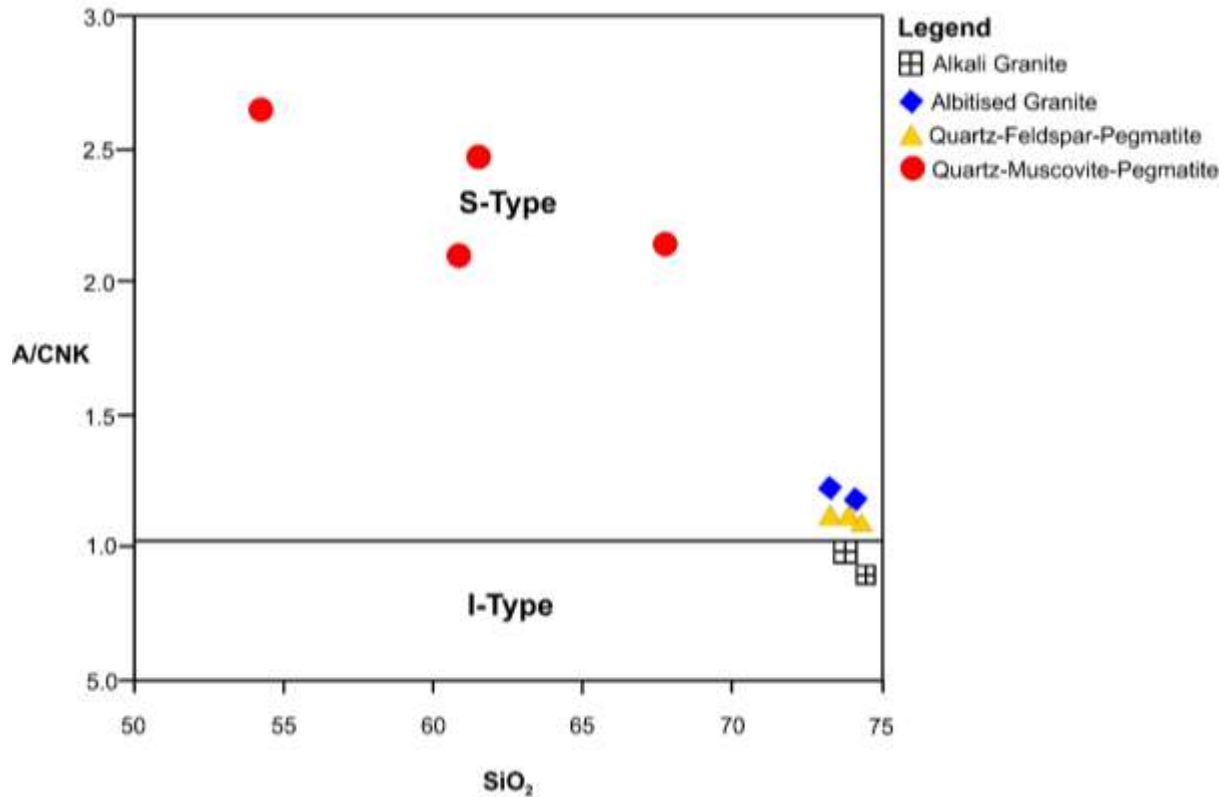


Fig. 22: A/CNK vs SiO<sub>2</sub> plot of rocks from the study area after (Chappel and White, 1974)

#### 4.4.4 Trace Element Geochemistry

The trace element contents of granitic melts changes substantially as crystallisation proceed and can be used as indicators of magmatic fractionation and chemical evolution of pegmatites (London, 2008). The trace elements composition and some important ratios are presented in Table (Table 3) while Table 4 shows the concentration of rare earth elements in the samples. The average abundances and ranges of some trace elements, rare earth elements and selected ratios from upper continental crust values from Taylor and McLennan (1985) are presented in Table 5.

Table 3: Concentration of some selected trace elements and some important elemental ratios in the rocks of the study area

Petrology	Amphibolite	Migmatite	Banded Gneiss	Granite Gneiss	Albatized Granite		Alkali Granite		Quartz-Feldspar-Pegmatite			Quartz-Muscovite-Pegmatite			
Elements (ppm)	S10	S3	S9	S7	S4	S12	S2	S6	S1	S5	S8	S13	S14	S15	S16
Be	1	2	3	6	351	315	8	13	5	4	2	21	43	55	19
Ba	45	836	844	741	7	3	351	379	72	48	924	19	73	58	14
Sr	145	477	451	323	11	4	44	50	65	48	317	60	40	55	12
Y	21	17	10	14	3	2	94	99	2	1	2	2	2	3	1
Zr	65	185	250	134	29	22	280	292	35	23	117	12	21	18	4
Co	70	59	56	58	69	56	47	53	66	56	29	60	119	114	66
Zn	100	106	110	80	163	140	80	91	< 30	< 30	< 30	120	130	100	240
Ga	14	17	23	26	47	36	25	29	30	22	16	127	97	100	179
Rb	13	54	85	152	465	822	214	231	542	511	83	3213	2946	3482	3957
Nb	4	8	12	14	30	22	28	34	7	5	3	187	116	164	194
Tl	0.2	0.2	0.5	1.1	4.2	1.0	1	2	0.9	2.5	0.7	8.4	5.6	11.7	6.6
Sn	1	1	3	7	81	66	7	11	25	20	3	328	189	585	798
Cs	0.7	1.6	3.2	15.1	57	49.9	7.6	12.4	10.8	14.9	1.3	67.9	54.7	133	62
Hf	1.6	1.4	5.8	3.2	1.97	2.1	7.6	6.5	4.1	1.8	3.7	1.2	1.5	2.1	0.3
Ta	0.5	1.1	1.4	1.7	5.3	4.2	4.2	6.3	7.56	21.7	11.3	70.5	65.5	91.1	77.2
W	142	132	298	345	412	378	298	310	285	352	187	405	745	802	429
Pb	10	18	15	32	18	10	28	35	58	27	52	20	12	7	8
Bi	0.4	< 0.4	< 0.4	1.1	2.3	1.8	< 0.4	< 0.4	< 0.4	< 0.4	< 0.4	2.3	3.1	< 0.4	< 0.4
Th	1.2	1.3	12.4	7.7	0.8	0.4	26.4	31	0.6	0.3	0.4	0.7	1	0.1	1
U	0.3	0.4	1.6	2.7	7.4	6.2	6.4	7.6	18	23.4	1.9	15.2	8	2.6	0.4
K/Rb	280.97	405.85	213.89	219.55	67.48	36.76	197.84	182.56	88.80	93.25	463.08	18.06	15.61	16.02	17.43
Nb/Ta	8.00	7.27	8.57	8.24	7.92	5.24	6.67	5.40	12.50	2.94	10.00	9.59	10.09	3.99	22.38
Rb/Sr	0.09	0.11	0.19	0.47	42.27	205.50	4.86	4.62	8.34	10.65	0.26	53.55	73.65	63.31	329.75
Na/K	1.89	1.60	1.68	0.85	1.20	1.24	0.60	0.59	0.57	0.57	0.64	0.24	0.27	0.16	0.11
K/Ba	81.17	26.22	21.54	45.04	4482.82	10072	120.62	111.27	668.43	992.72	41.60	3054.08	630.01	961.83	4927.54

Table 4: Concentration of rare earth elements in the rocks of the study area

Petrology	Amphibolite	Migmatite	Banded Gneiss	Granite Gneiss	Albitised granite		Alkali Granite		Quartz-Feldspar-Pegmatite			Quartz-Muscovite-Pegmatite			
Sample	S10	S3	S9	S7	S4	S12	S2	S6	S1	S5	S8	S13	S14	S15	S16
La	6.2	11.9	40.7	20.3	0.8	0.5	79.6	92.4	5.1	0.6	4.6	0.4	0.5	1.4	0.6
Ce	13.3	22.4	85.2	41	1.3	1	149	180	7.1	0.6	6.7	0.8	0.9	1.4	0.9
Pr	1.84	2.5	8.96	4.61	0.21	0.1	16.8	24	1.1	0.1	0.81	0.1	0.13	0.21	0.17
Nd	8.9	11.7	34	17.5	0.45	0.3	59.9	81.2	3.2	0.3	2.8	0.4	0.4	0.6	0.5
Sm	2.4	3.1	6.6	3.7	0.23	0.1	13.4	19	0.8	0.14	0.5	0.3	0.4	0.6	0.5
Eu	0.99	1.12	1.57	1.05	0.38	0.34	1.13	1.69	0.97	0.75	0.93	0.05	0.06	0.08	0.07
Gd	3.5	3.4	4.7	3.2	0.35	0.1	14.5	16	0.7	0.1	0.5	0.3	0.4	0.7	0.5
Tb	0.7	0.6	0.6	0.5	0.45	0.2	2.6	3.3	0.5	0.3	0.4	0.2	0.3	0.4	0.3
Dy	3.9	3.7	2.6	2.7	0.25	0.1	15.5	18.9	0.4	0.1	0.3	0.1	0.4	0.5	0.2
Ho	0.8	0.7	0.4	0.5	0.6	0.3	3.1	4.2	0.5	0.2	0.3	0.2	0.3	0.5	0.4
Er	2.6	1.9	0.8	1.3	0.4	0.3	9.1	11.1	0.35	0.2	0.2	0.1	0.2	0.5	0.3
Tm	0.37	0.24	0.11	0.17	0.32	0.35	1.29	1.72	0.4	0.23	0.17	0.07	0.08	0.1	0.09
Yb	2.4	1.6	0.7	1.1	0.4	0.2	8.1	9.9	1.7	1.3	1.1	0.2	0.3	0.5	0.4
Lu	0.36	0.21	0.09	0.15	0.2	0.11	1.09	1.4	0.17	0.14	0.12	0.05	0.07	0.1	0.08
Ratios															
Eu/Eu*	1.05	1.06	0.87	0.94	4.12	10.45	0.25	0.3	3.98	19.49	5.72	0.51	0.42	0.38	0.43
LaN/YbN	1.72	4.96	38.76	12.30	1.33	1.67	6.55	6.22	2.00	0.31	2.79	1.33	1.11	1.87	1.00
∑REE	48.26	65.07	187.03	97.78	6.34	4.00	375.11		22.99	5.06	19.43	3.27	4.44	7.59	5.01

Table 5: Average abundances and ranges of some trace elements, rare earth elements and selected ratios from upper continental crust values from Taylor and McLennan (1985)

Element (ppm)	Average upper continental crust	Albitised Granite		Quartz-Feldspar-Pegmatite		Quartz-Muscovite-Pegmatite	
	(ppm)	Mean	Range	Mean	Range	Mean	Range
Rb	112	643.5	465-822	378.68	83-542	3399	2946-3957
Ba	425	5	3-7	348	72-924	41	14-73
U	2.7	6.8	6.2-7.4	14.4	1.9-23.4	6.55	0.4-15.2
Cs	3.7	53.45	49.9-57	9	1.3-14.9	79.4	54.7-133
Be	3	333	315-351	3.6	2-5	34.5	19-55
Nb	25	26	22-30	5	3-7	165.3	116-194
Ta	2.2	4.75	4.2-5.3	13.5	7.56-21.7	76.1	65.5-91.1
Sn	5.5	73.5	66-81	16	3-25	475	189-798
Ga	17	41.5	36-47	23	16-30	136.4	97-179
W	1.5	395	378-412	274	187-352	595.3	405-802
La	30	0.65	0.5-0.8	3.3	0.6-4.8	0.7	0.4-1.4
Ce	60	1.15	1-1.3	4.7	0.6-6.9	1	0.8-1.4
Pr	8.2	0.155	0.1-0.21	0.7	0.1-1.1	0.15	0.1-0.21
Nd	28	0.36	0.3-4.5	2.03	0.3-3	0.47	0.4-0.6
Sm	6.0	0.165	0.1-0.23	0.5	0.14-0.8	0.17	0.1-0.2
Eu	1.2	0.36	0.34-0.38	0.9	0.75-0.97	0.49	0.11-0.97
Gd	5.4	0.225	0.1-3.5	0.4	0.1-0.7	0.17	0.1-0.3
Tb	0.9	0.325	0.2-0.45	0.4	0.3-0.45	0.4	0.3-0.6
Dy	3.0	0.175	0.1-2.5	0.3	0.1-0.4	0.22	0.1-0.4
Ho	1.2	0.45	0.3-0.6	0.3	0.2-0.5	0.3	0.2-0.4
Er	2.8	0.35	0.2-0.35	0.3	0.3-0.4	0.6	0.1-0.8
Tm	0.48	0.335	0.32-0.35	0.3	0.17-0.4	0.27	0.23-0.31
Yb	3	0.3	0.2-0.4	1.3	1.1-1.5	0.25	0.22-0.34
Lu	0.5	0.155	0.11-0.2	0.2	0.12-0.34	0.16	0.11-0.19
K/Cs	7630	578.04	550-605	12406.8	4456-29566	1170.2	419.4-1729.6
K/Rb	252	52.12	36.7-67.4	215.04	88.8-463.1	16.78	18.06
Nb/Ta	11.4	6.58	5.2-7.9	8.4	2.9-12.5	11.51	3.9-22.3

Spider diagrams for all the rocks samples normalized to average crust after McDonough and Sun (1995) are shown in Fig. 23

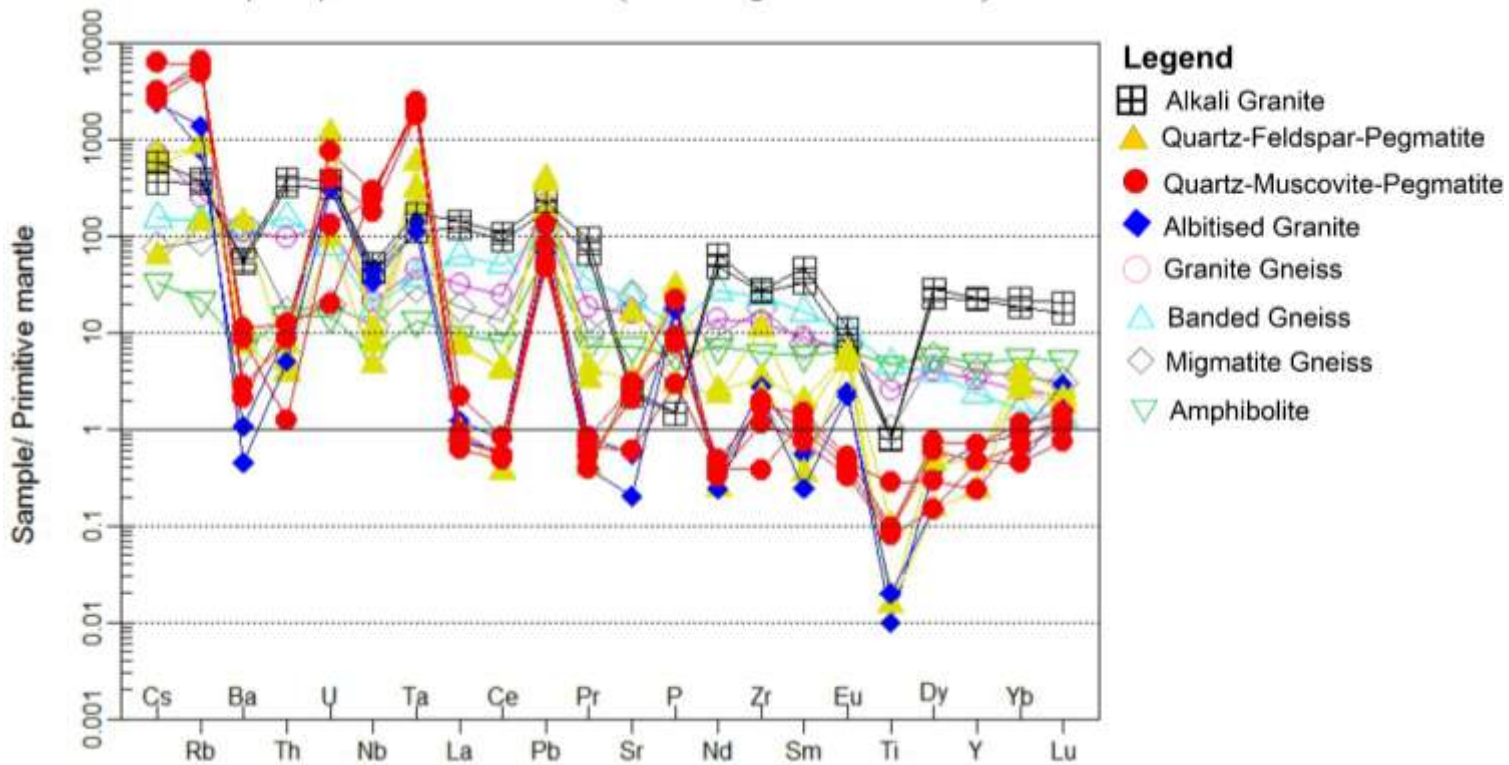


Fig. 23: Spider diagrams for all the rocks samples normalized to average crust after McDonough and Sun (1995).

The normalized abundance patterns permit characterisation of the rocks. The migmatite gneiss, banded gneiss, amphibolite and granite display similar pattern. They are all characterized by negative anomalies of some incompatible elements, namely; Nb, Ce, Zr, Ti; and positive anomalies for Pd, Ta, Sr, Dy. The banded gneiss has a slight positive anomaly for Th while the other metamorphic rocks all show a negative anomaly for Th. The amphibolite shows a slight negative Zr anomaly. The albitised granite shows a prominent negative anomaly for Ba, Ce, Sr, Nd and Ti and a marked positive anomaly for U, Ta, Pb and Zr. The alkali granite is characterized by negative anomaly for Sr, Nb, Ce, Zr, Ti and Ba with positive anomaly for Pb and the radioactive elements Th and U. Trace element patterns for all pegmatites samples are generally characterised by positive anomalies for Rb, Ta, Pb, Zr and U, and relative depletion in Ba, Nb, Ce and Ti. The quartz-feldspar-pegmatite generally

are more HREE enriched than the mica samples. The muscovite sample has the lowest K/Rb ratio (mean value of 16.78) as well as Ce (mean 1 ppm) among the other samples. It also has notably low Ba (mean 41 ppm) and Sr (42 ppm) below the crustal abundances of 425 and 375 respectively (Taylor, 1964). The manifest depletion in Ba and Sr is probably due to K and Na feldspar or plagioclase fractionation respectively (Akoh et al., 2015). The quartz-muscovite-pegmatites are relatively enriched in Ga (mean 126 ppm), Rb (mean 3399 ppm), W (mean 595 ppm), Ta (mean 22 ppm), Sn (mean 475 ppm), Cs (mean 79.4 ppm), and Nb (mean 165 ppm) well above the crustal abundances of Ga 15 ppm, Rb 90 ppm, W 1.5 ppm, Ta 2 ppm, Sn 2 ppm, Cs 3 ppm, and Nb 20 ppm (Taylor, 1964). The relative concentration of Nb and Ta are influenced by volatiles which are associated with the late stage magma and hence the quartz-muscovite-pegmatite represent the more evolved facies (Akoh et al., 2014). The spatially associated quartz-feldspar-pegmatites have enhanced concentrations of Ba 348 ppm, Rb 378 ppm, Zr 58.33 ppm low Nb/Ta ratios of 8.48.

#### 4.4.5 Rare Earth Element (REE) Geochemistry

All the REE values were normalized to values given by Nakamura (1974) and then plotted on a spidergraph (Fig. 22, 23 and 24). The alkali granites have the highest sum of REE ( $\sum$ REE) with an average of 419.96 (Fig 26). The albitised granites have the lowest sum of REEs with an average value of 5.17, the low value of the sum of REEs for the albitised granite may be due to the effect of element mobility during hydrothermal alteration. The sum REEs for the other rock types are 65.07, 48.26, 97.78 and 187.03 for migmatite gneiss, amphibolite, granite gneiss and banded gneiss respectively (Table 6).

The degree of negative Eu anomaly varies widely in the rocks 0.25 – 10.45. Eu anomaly denoted by  $Eu/Eu^*$  derived by dividing the chondrite normalized value of Eu concentration by half the sum of the normalized concentration of Sm and Gd (Terekhov and Shcherbakova, 2006).

The REE pattern of the alkali granite is subparallel, LREE enriched ( $LaN/YbN$  value of 6.38) and are characterized by nearly flat HREE profile. The alkali granite show a weak negative Europium anomaly ( $Eu/Eu^* = 0.4$ ) indicating that it was produced from melts that was once in equilibrium with a plagioclase rich phase during partial melting or fractional crystallisation, where the plagioclase was either retained in the residual solid or removed as phenocrysts during the earlier stages of crystallisation (Winter, 2014).

The banded gneiss and the granite gneiss show similar REE patterns (Fig. 24) with  $\sum$ REE values of 187.03 and 97.78 respectively. These rocks have weak Eu anomalies ( $Eu/Eu^*$  0.87 and 0.94 respectively). The weak negative Eu anomaly can be attributed to the formation of the rock from a protolith that is plagioclase deficient (Hugh, 1993). The migmatite gneiss and amphibolite both have a subparallel REE pattern with LREE enrichment which may be indicative of the absence of accessory phases like garnet and zircon which accommodate the

HREEs. The migmatite show a relatively higher degree of fractionation of the LREEs relative to the HREEs compared to the amphibolite ( $\text{LaN/YbN} = 38.76$  and  $12.30$  respectively). This is indicated graphically by the notable downward trending slope from La – Lu on the REE spidergraph.

The albitized granite has nearly similar REE patterns as quartz-feldspar-pegmatite, but with lower total  $\sum\text{REE}$  ( $5.17$  and  $15.82$  respectively). On the REE diagram for albitized granite (Fig. 26) and pegmatites (Fig. 25) it is observed that neighboring elements are segmented into successive troughs and crest, giving it a jagged-edge pattern known as REE tetrad effect. The REE tetrad effect observed is the W-type, which begins with a downward convex from La alternating progressively with increasing atomic number to Lu (Fernando, 2015). Hydrothermal fluids may have caused the more mobile REEs to be leached relative to the less mobile ones hence producing the observed trend. The albitized granite and quartz-feldspar-pegmatite both have well pronounced positive Eu anomaly (mean  $\text{Eu/Eu}^* = 7.28$  and  $9.73$  respectively). This may be explained as the abundance of early fractionated plagioclase feldspars in the rock that were formed in a region of low oxygen fugacity (Milord et al., 2000; Winter 2014). The albitized granite and the quartz-feldspar-pegmatite have average  $\text{LaN/YbN}$  values of  $1.5$  and  $1.7$  respectively indicating a moderate fractionation of the LREEs relative to the HREEs.

The quartz-muscovite-pegmatite has a low mean  $\Sigma\text{REE}(5.07)$  and also displays a REE tetrad effect pattern similar to the ones observed in the albitized granite and quartz-feldspar-pegmatite, but with a well pronounced negative Eu anomaly ( $\text{Eu}/\text{Eu}^* 0.44$ ). The rocks have a slight to moderate fractionation of the LREEs relative to the HREEs with a  $\text{LaN}/\text{YbN}$  value ranging from 1.00 to 1.8

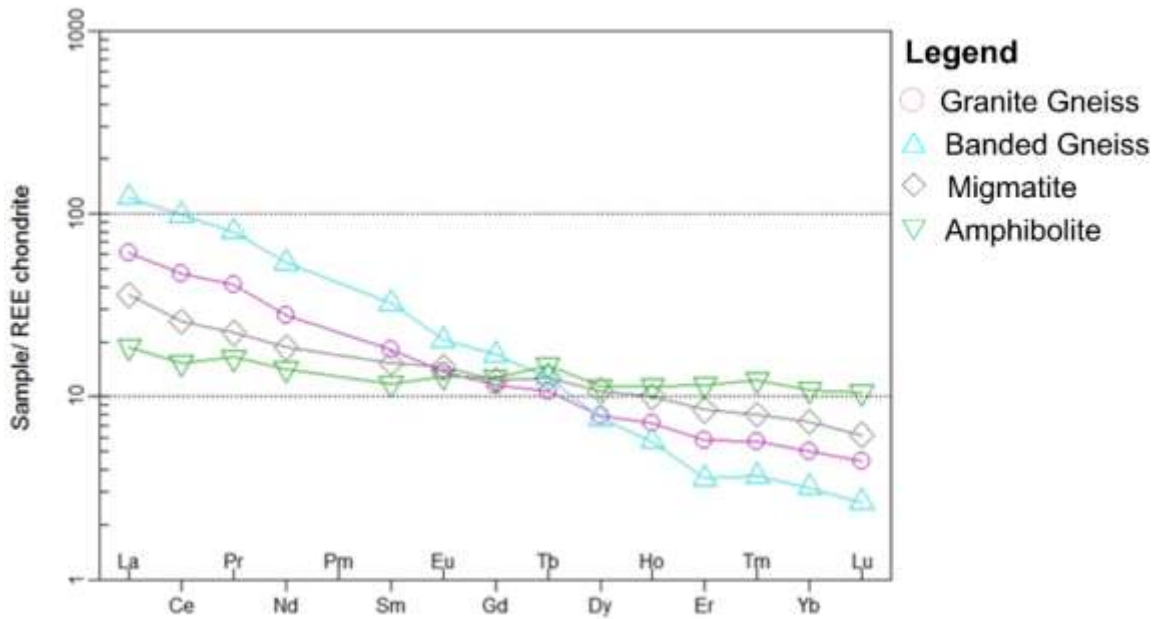


Fig. 24: Chondrite normalized plot (After Nakamura, 1974) rare elements (REE) pattern for the metamorphic rocks from the study area.

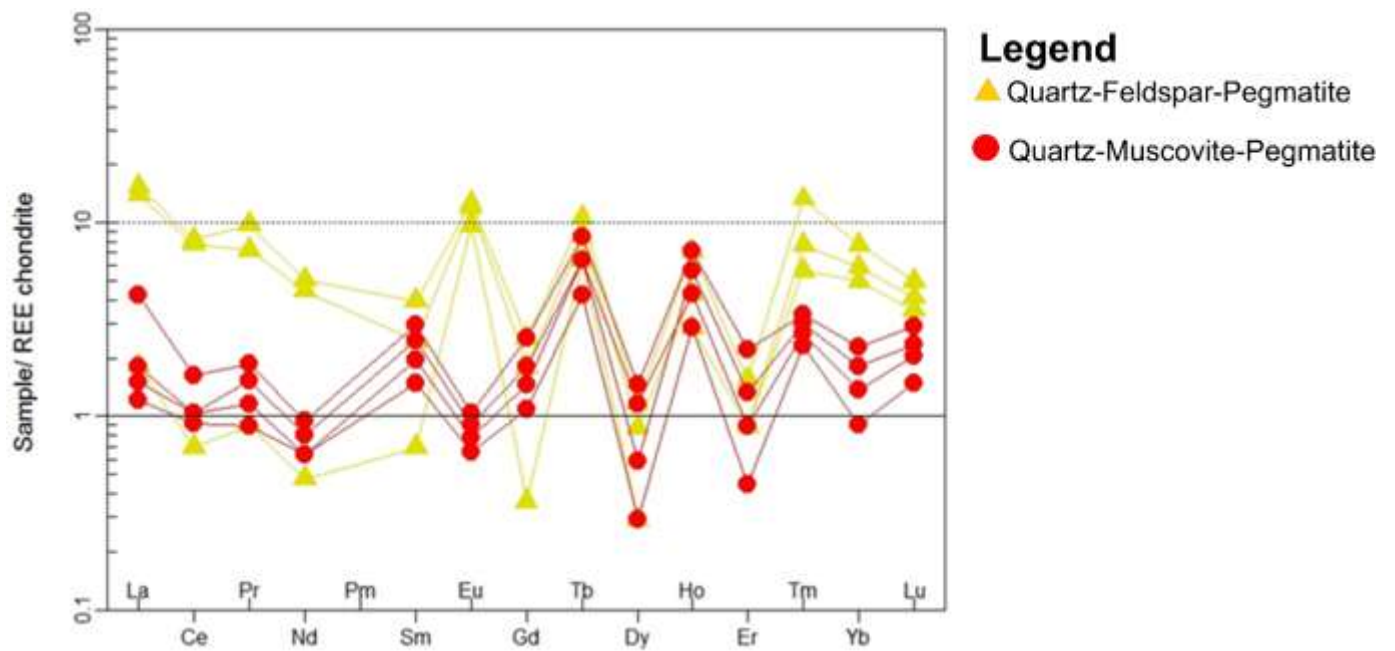


Fig. 25: Chondrite normalized plot (After Nakamura, 1974) rare elements (REE) pattern for the Pegmatites in the study area.

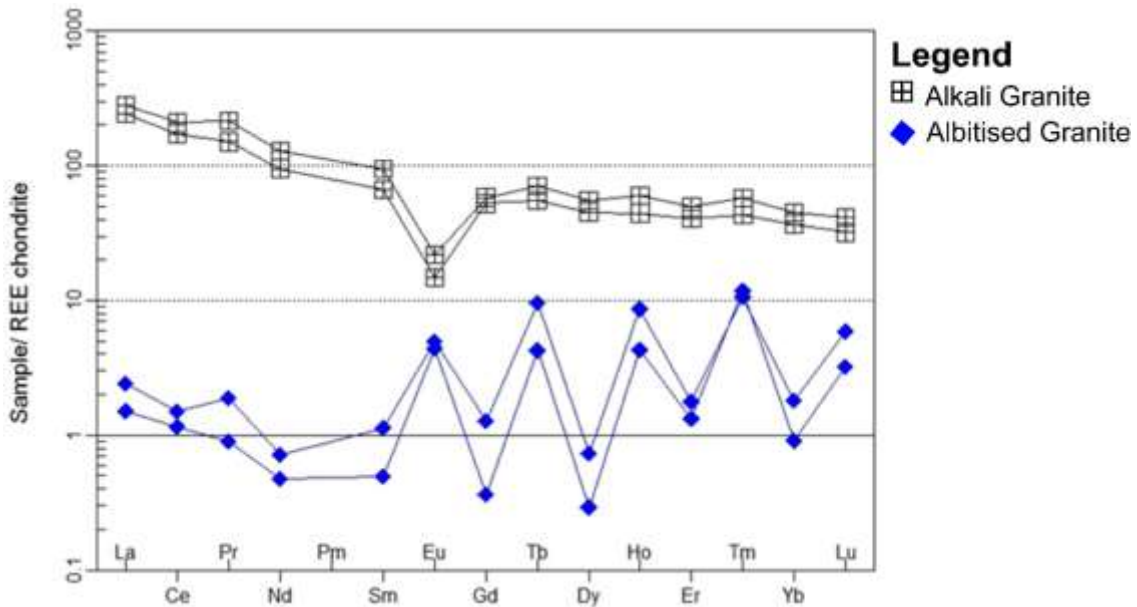


Fig. 26: Chondrite normalized plot (After Nakamura, 1974) rare elements (REE) pattern for the granites from the study area.

The alkali granite, albitised granites and pegmatites all plot in the field of strongly differentiated granites in the ternary plot of Rb-Ba-Sr plot of El Bouseily and El Sokkary (1975) (Fig. 27). The albitised granite and quartz-muscovite-pegmatite manifest their highly evolved nature by plotting close to the peak in the field of strongly differentiated granites

while the alkali granite plots close to the normal granite boundary much closer to the Ba corner.

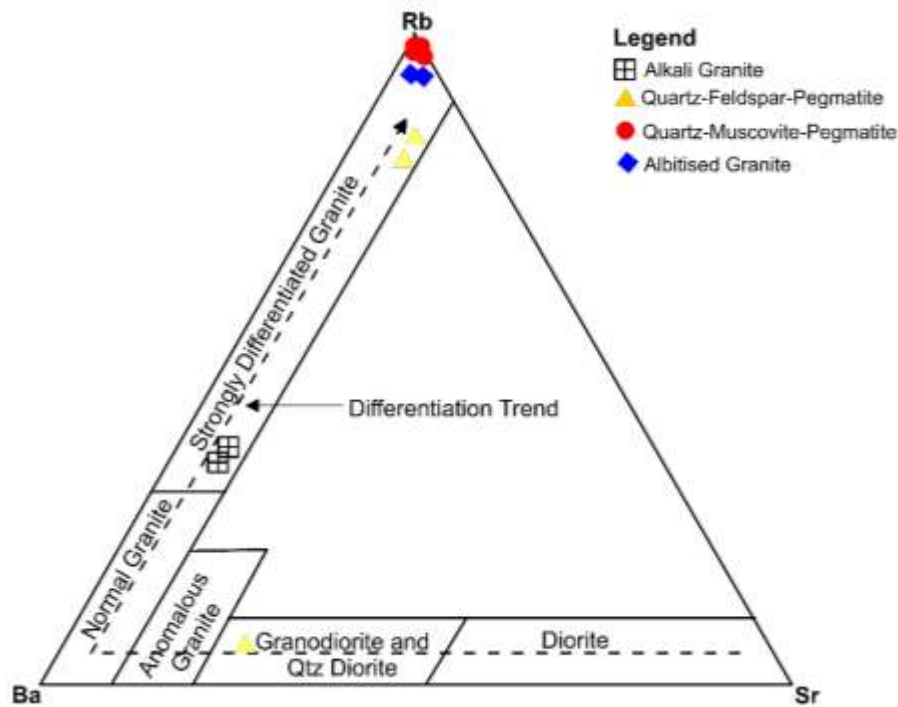


Fig. 27: Plot of Rb-Ba-Sr after El Bouseily and El Sokkary (1975) for granitic rocks

The plot of Rb vs Na/K (Fig. 29) after Kaur et al., (2012) shows the progressive depletion of Rb with the advancing albitisation. The plot reveal that the quartz-feldspar-pegmatite and the albitized granite have undergone the strongest degree of albitisation and show the lowest Rb concentrations respectively. The albitized granite, quartz-feldspar-pegmatites and quartz-muscovite-pegmatites all plot in the zone of albitisation in the modified triangular discriminating plot of Ti-Sn-(Nb+Ta) after Kuster (1990) (Fig. 28).

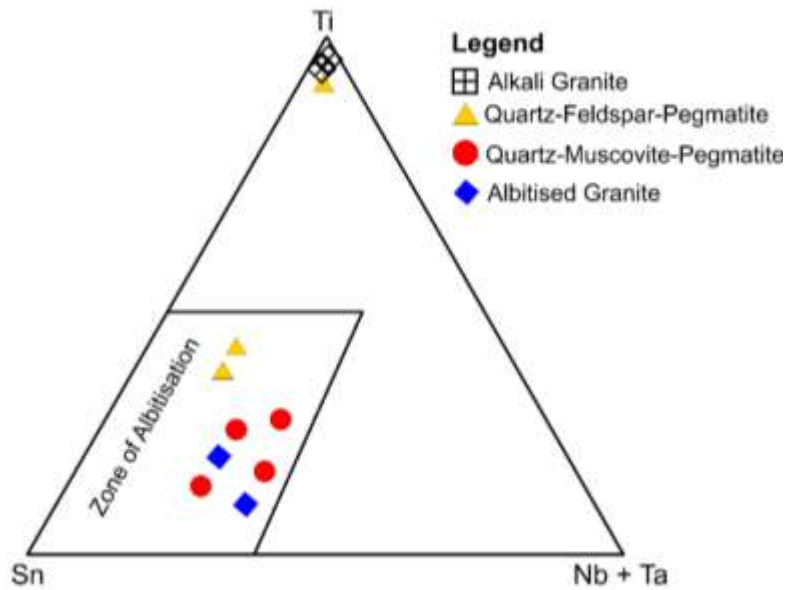


Fig. 28: Modified Triangular Ti-Sn-(Nb+Ta) Plot for albitized granite and pegmatites in the study area (after Kuster, 1990).

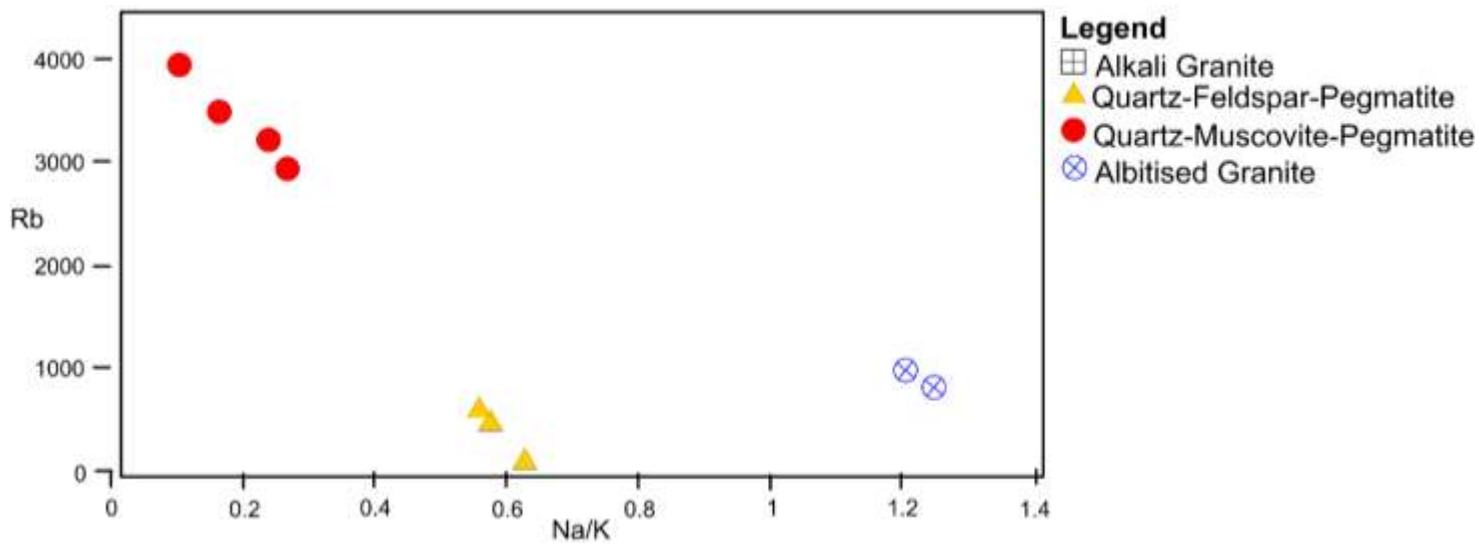


Fig. 29: Plot of Rb vs Na/K after Kaur et al., (2012) showing the progressive depletion of Rb with the advancing albitisation of K-feldspar.

### Mineral Potential Diagrams

Plots of Ta versus Cs (Fig. 30), Ta versus K/Cs (Fig. 31) and Ta versus Ga (Fig. 32), were used to discriminate mineralized pegmatites from the non-mineralized pegmatites based on the Beus (1966) and Gordiyenko (1971) lines of mineralisation. Based on these plots,

the quartz-feldspar-pegmatite plot entirely below the Beus (1966) and Gordiyenko (1971) lines of mineralisation while the quartz-muscovite-pegmatite plot predominately plot above the Beus (1966) line of mineralisation but below the Gordiyenko (1971) lines of mineralisation. Plots of K/Rb versus Cs (after Černý and Burt, 1984) (Fig. 33) and K/Rb versus Cs (after Trueman and Černý 1982) (Fig. 34) were also used to determine the mineralisation potential in pegmatites. From the plots it was observed that quartz-feldspar-pegmatite plot within the barren field while the muscovite extracts plot in the field of rare metal pegmatites, akin to Be and Li enrichment.

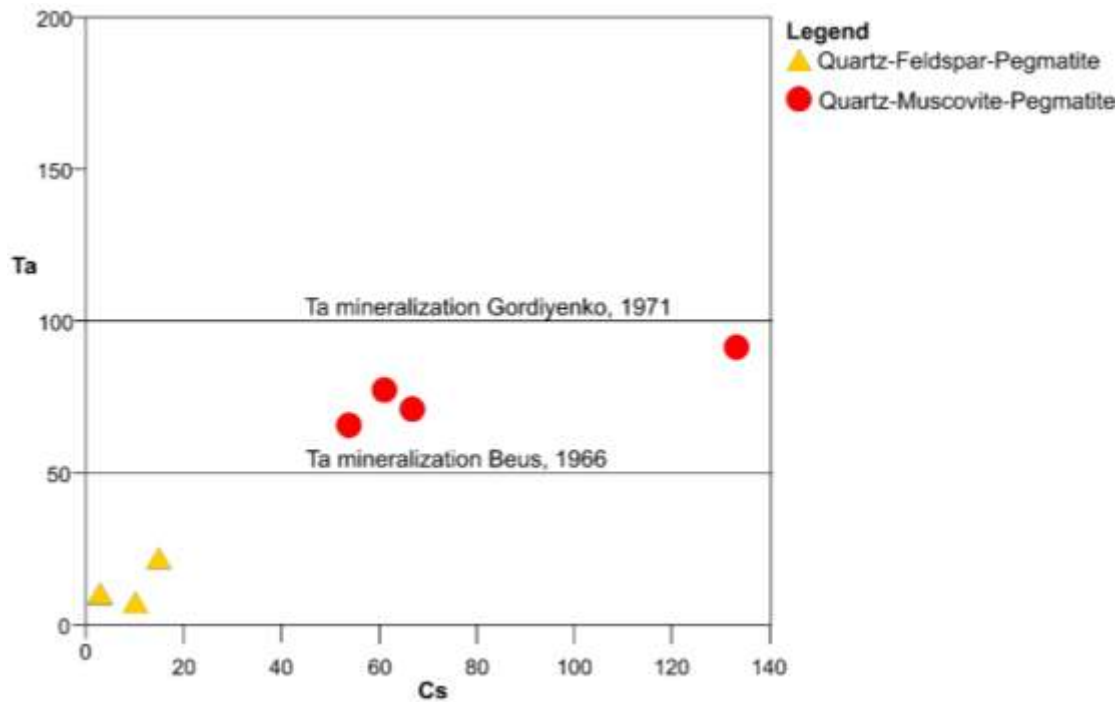


Fig. 30: Plot of Ta Versus Cs for The Muscovites of the pegmatites in the Kwarra area.

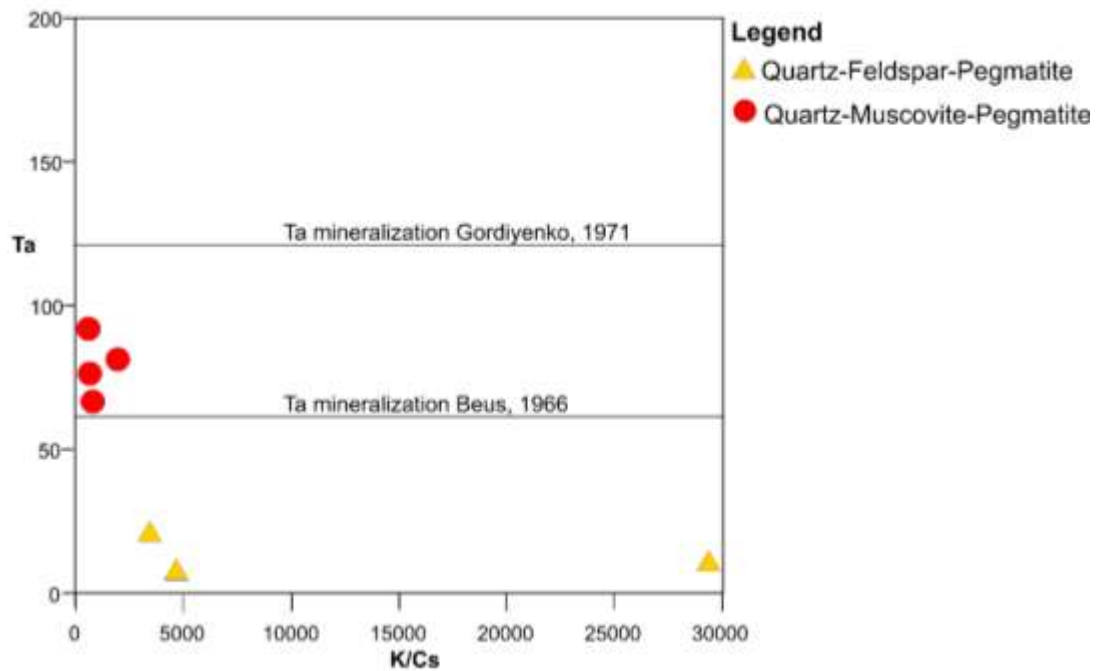


Fig. 31: Plot of Ta Versus K/Cs For The Muscovites of Pegmatites in the study area. (After Beus 1968), Gordiyenko (1971).

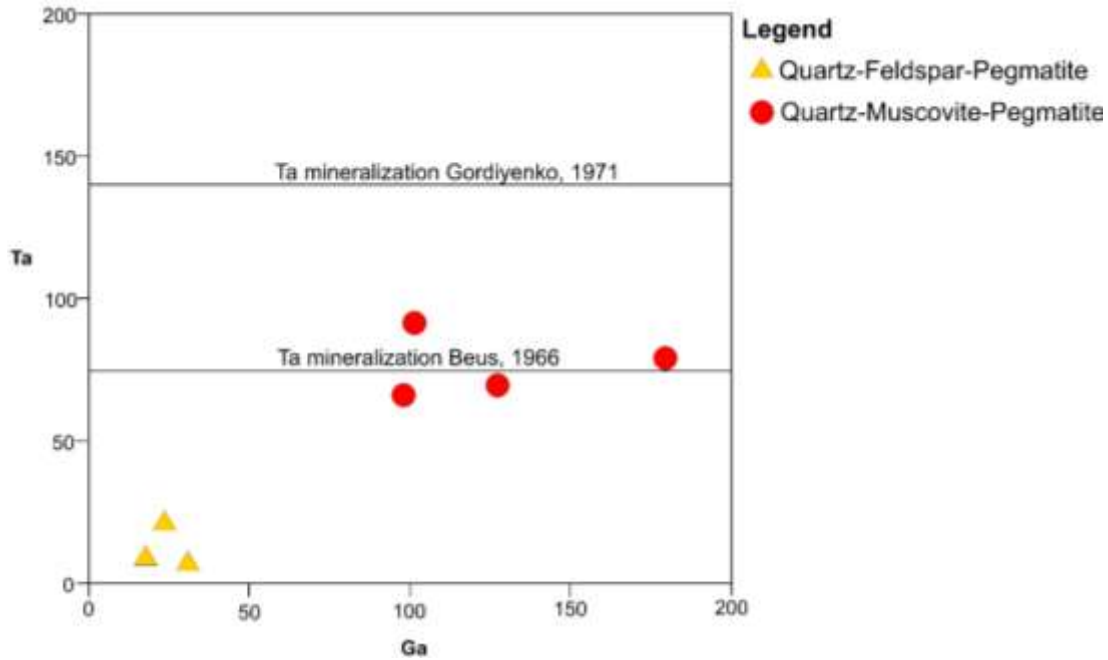


Fig. 32: Plot of Ta versus Ga for the pegmatites in the study area (After Černý and Burt, 1984).

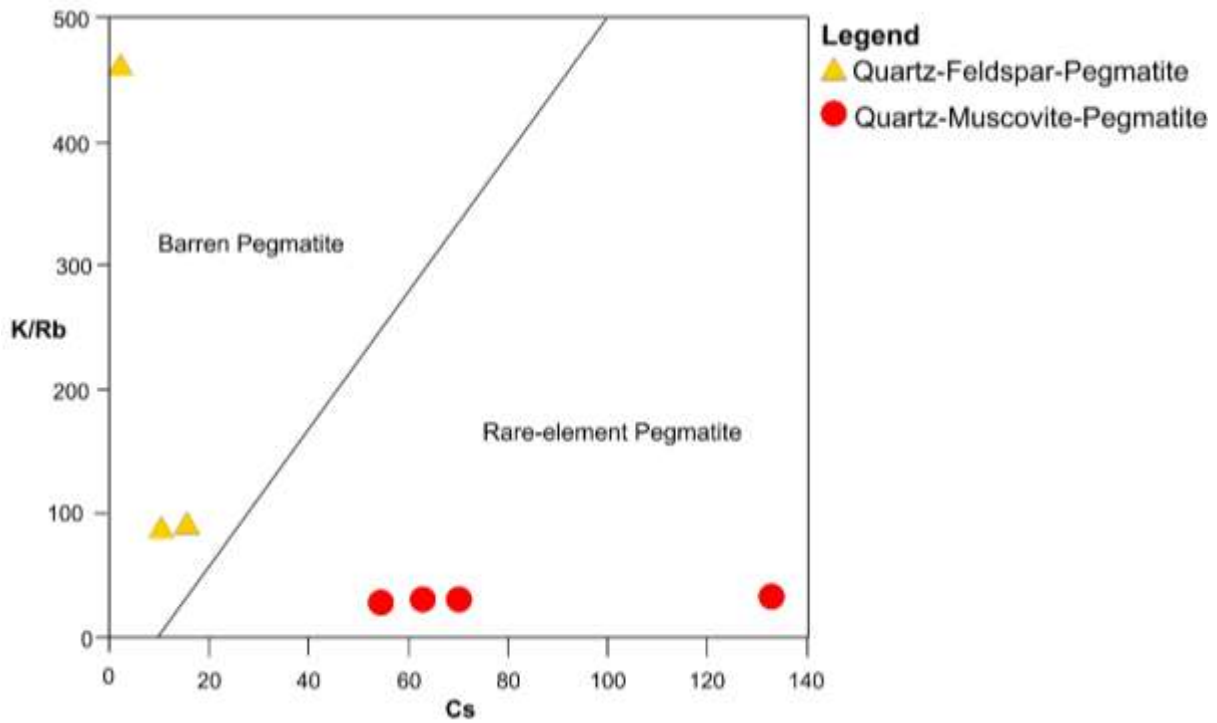


Fig. 33: Plot of K/Rb versus Cs for the pegmatites (after Černý and Burt, 1984).

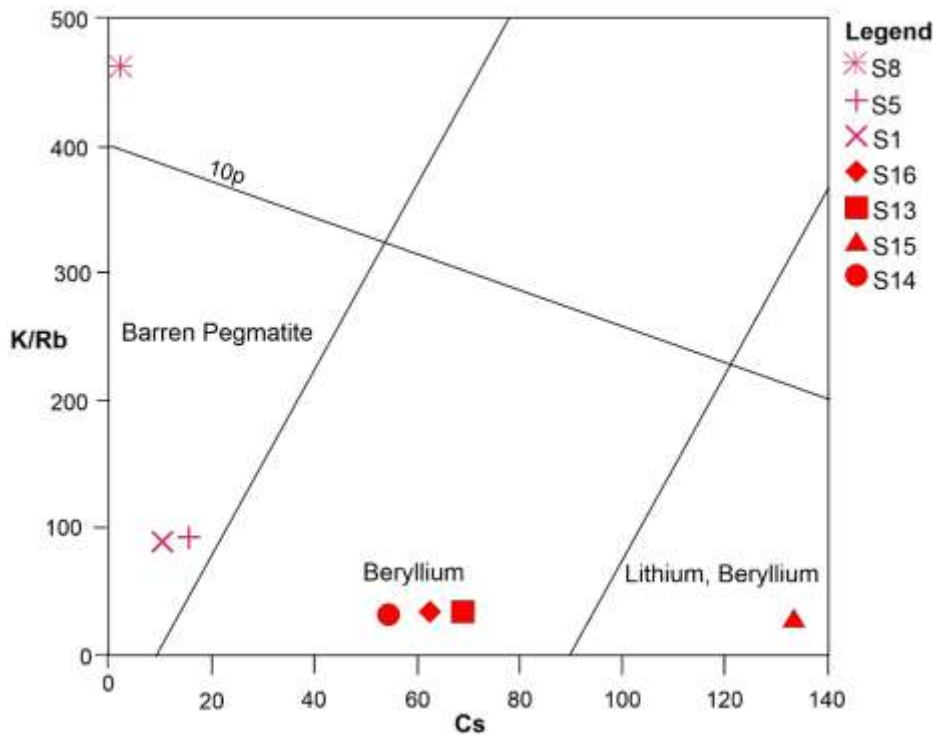


Fig. 34: Classification of the pegmatites using the plots of K/Rb versus Cs (after Trueman and Černý 1982).

The mineralisation potential of the granites in the study area is evaluated using a plot of Nb/Ta versus Zr/Hf after Ballouard et al., (2016) as shown in Fig. 35. The albitized granite plot off the field of rare-metal granites and Sn-W-U related granites while alkali granite with Nb/Ta values ranging between 5 to 16 plot specifically in the barren granite field. None of the granites in the area can therefore be classified as a fertile granite that can be parental to rare metal pegmatites.

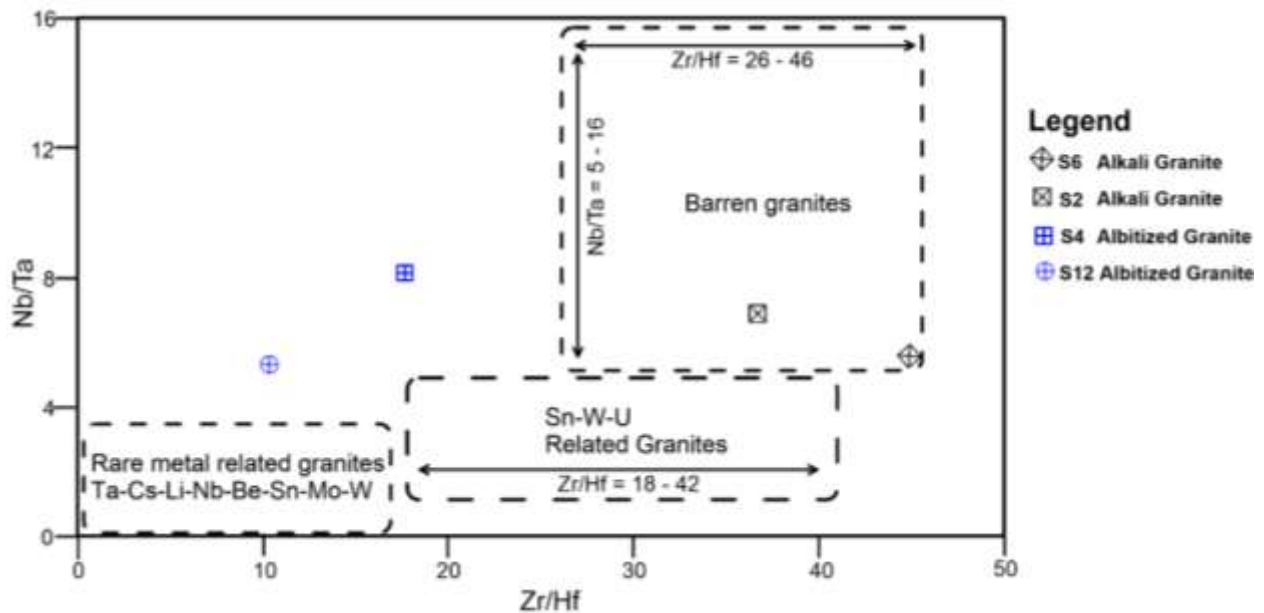


Fig. 35: Nb/Ta versus Zr/Hf diagram differentiating the barren granites and granites hosting ore deposits (after Ballouard et al., 2016).

#### 4.4.5 Tectonic Discrimination Diagram

In the Rb vs. Y+Nb tectonic discrimination diagram after Pearce *et al.* (1984) (Fig. 36), the pegmatites and albitized granite sample plotted in the syn collisional granite field associated with orogenic events. The Alkali granite plot within in the within-plate field consistent with A-type granites.

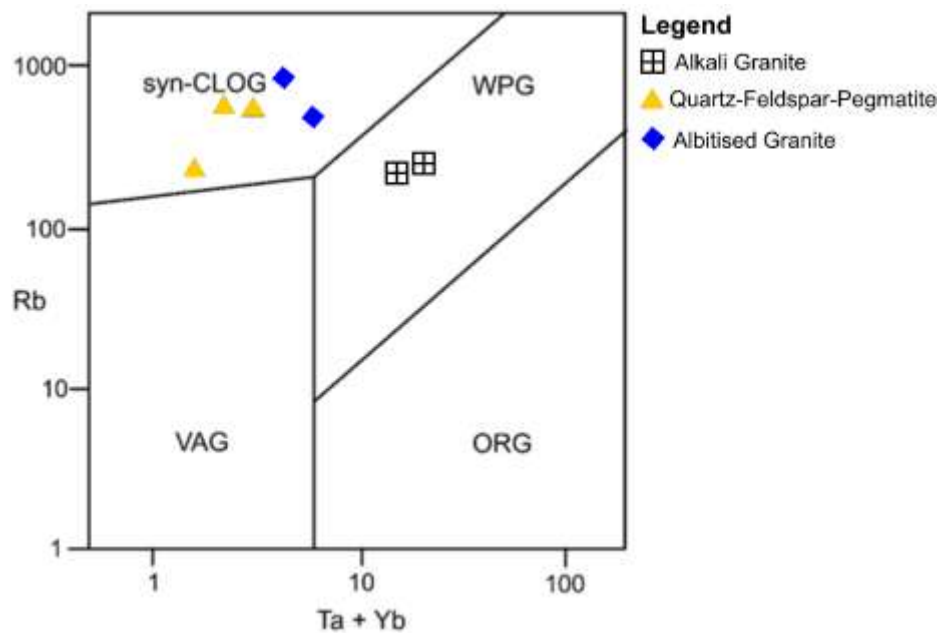


Fig. 36: Rb vs. Y+Nb tectonic discrimination diagram after Pearce *et al.* (1984)

Based on the plot of  $FeO_t / MgO$  vs.  $Zr+Nb+Ce+Y$  (Fig. 37) after Whalen *et al.* (1987) for distinguishing between A-type granites and other granitoids (M-, I- and S-type), the alkali granite plot in the A-type granite field.

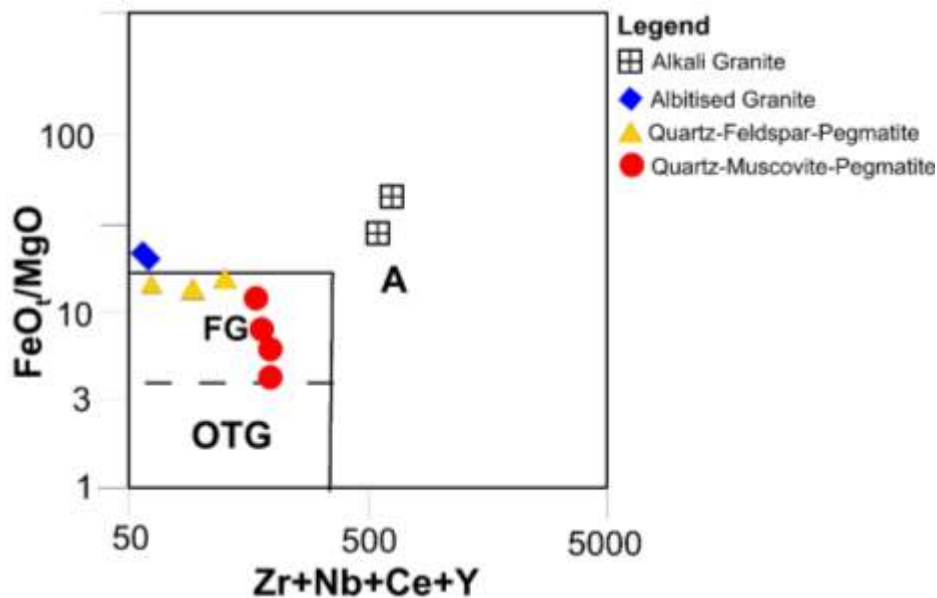


Fig. 37: Plot of  $FeO_t / MgO$  vs.  $Zr+Nb+Ce+Y$  for discriminating A-type granites after Whalen *et al.*, (1987)

The alkali granites in the study area fall both under the within-plate granite field of Pearce et al., (1984) (Fig. 36) and A-type granite field of the Ga/Al vs. Zn plots after Whalen et al., (1987) and therefore qualify for a plot of Nb-Y-Ce (Fig. 38) for A1, A2 granite discrimination after Eby (1992). The discrimination plot reveals the A2 nature of the granite, which are considered to be a subtype of the I-type and indicate crustal source that is not metasedimentary. The A2 group of magmas represent magmas derived from continental crust or underplated crust that has been through a cycle of collisional or island arc magmatism (Eby, 1992).

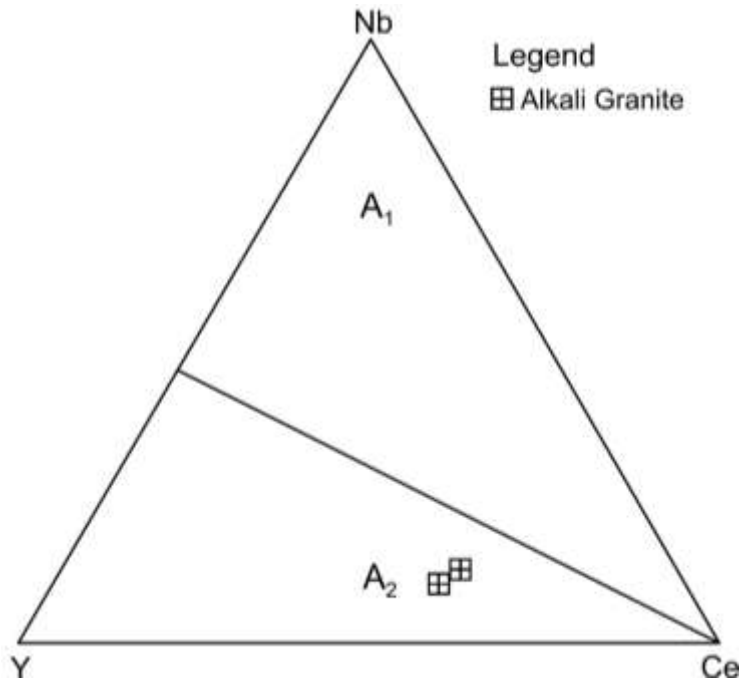


Fig. 38: Triangular plot of Nb-Y-Ce for distinguishing the alkali granites into A1 and A2 granite (After Eby, 1992)

## CHAPTER FIVE

### DISCUSSION

#### 5.1 Field Relationship

The alkali granites represent the youngest lithologic unit in the study area and intrude the older rocks discordantly to form high rising hills and steep outcrops. The Pan-African Older Granite rocks represented by the albitized granites and the pegmatites occur as both low lying plutons and sometimes occur in uplifted regions as scattered outcrops. The albitized granites intrude the much older granite gneiss host rock and are highly deformed. The rocks are brecciated and have a NE-SW trend. The pegmatites intrude granite gneiss, banded gneiss, amphibolite and migmatite gneiss. The pegmatites are sparsely distributed occurring as veins (Plate 14a) in the migmatite and granite gneiss and as dikes/boulders (Plate 15) in the banded gneisses and amphibolites. Some of the pegmatites are fractured and weathered. The granite gneiss, banded gneiss, amphibolite and migmatite gneiss constitute the polycyclic migmatite gneiss complex rocks in the study area. They show different varying degrees of deformation with the migmatite gneiss showing the most ductile form of deformation while the amphibolite deforms in a more brittle manner. The amphibolite has a spatial relationship with the granite gneiss, banded gneiss and migmatite gneiss. The banded gneiss and migmatite gneiss usually occur as flat lying, pavement outcrops while the amphibolite occur in uplifted area as scattered outcrops. In the Abu area, the granite gneiss occurs as lowlying outcrops sometimes showing signs of exfoliation.

## 5.2 Geochemistry and Structural Geology of the Polycyclic Basement Rocks

The pegmatites are emplaced in the polycyclic migmatite gneiss complex made up of migmatites, banded gneisses, granite gneiss and amphibolite. Obaje (2009), noted that Petrographic evidence indicates that the Pan-African reworking led to recrystallisation of many of the constituent minerals of the Migmatite – Gneiss Complex by partial melting with majority of the rock types displaying medium to upper amphibolite facies metamorphism. The end of the orogeny was marked by faulting and fracturing (Gandu et al., 1986; Olayinka, 1992) that gave rise to a regional shearing and tectonometamorphic evolution of the terrain. The type of deformation varies considerably between the rock types, and according to particular pressure, temperature and strain rate. The variation between rock types is also due to the fact that the constituent minerals of each rock type have different mechanical properties. At low pressure-temperature (P-T) conditions of high crustal levels, rocks behave in a largely brittle manner, involving fracturing on all scales (cataclasis) as observed in the amphibolites. In contrast, at high temperatures and low strain rates in the upper amphibolite facies, and higher grades of metamorphism, rearrangement of grains by diffusive transfer of atoms (diffusional creep) can be a significant process facilitating ductile deformation (Andy, 1998) as expressed by the ptygmatic folding (Plate 19b) in the migmatite. Somewhere between the two end-member situations of brittle and ductile deformation there is a macroscopic 'brittle-ductile' transition, where rocks display features of both brittle and ductile or semi brittle conditions (Murrell, 1990), this type of deformation is clearly displayed by the pinch and swell structures developed in the banded gneiss. At higher temperatures, both quartz and feldspar experience ductile deformation. Other minerals such as hornblende also experience brittle deformation at low metamorphic grades, but behave in a ductile manner at

high metamorphic grades. This gives rise to strain partitioning, with some areas experiencing only low strain while others become highly strained. This partitioning occurs from the macro scale right down to the micro scale, with significant strain variations developing pinch and swell structures (Andy, 1998).

The amphibolite has the lowest SiO<sub>2</sub> content among the rocks in the study area. It also has the lowest K<sub>2</sub>O and Na<sub>2</sub>O values of 0.93 and 0.44 wt% respectively. The ferromagnesian nature of the amphibolite is revealed by its high Fe<sub>2</sub>O<sub>3</sub> (10.65 wt%), MgO (7.57 wt%) and CaO (12.35 wt%) values. The rock also contains the highest value of TiO<sub>2</sub> of 0.93 wt% reflective of the presence of mafic rich phases in the rock. The rock is HSFE depleted with low values for Zr, Y, Nb, Hf and Ta which can be interpreted as being formed from protoliths poor in garnet and other accessory phases like zircon, rutile and titanite. It also shows low values for the LILE such as Rb, Ba and Sr with values of 13, 145 and 45 ppm respectively. The rock is generally REE depleted ( $\Sigma$ REE= 48.26). The rock has a subparallel REE pattern indicating a slight enrichment of the LREEs over the HREEs (LaN/YbN = 1.72). There is a slight positive Eu and Tb anomalies.

Petrographic evidence reveal that the amphibolite is composed of hornblende, augite, orthoclase, plagioclase and quartz most of which are highly fractured. The hornblende and augite crystals occur largely as subhedral poikiloblastic crystals characterized by the inclusion of quartz and two sets of cleavage. The deformed nature of the rock can be clearly observed by the brecciated and scattered nature of the outcrop which is characteristic of rocks formed during faulting or other crustal deformation processes. The amphibolites coincide with major linearments in the study area attesting to their highly deformed nature.

The granite gneisses are the most common rock type in the mapped area. It has a SiO<sub>2</sub> value of 67.79 wt.%, relatively high Al<sub>2</sub>O<sub>3</sub>, Fe<sub>2</sub>O<sub>3</sub>, K<sub>2</sub>O and TiO<sub>2</sub> concentration of 15.3, 3.41, 4.02

and 0.517 wt.% respectively. Compared to the crustal abundance of the HSFE elements Ga, Nb, Zr and Y of 15, 20, 165 and 33ppm (Taylor, 1964) the granite gneiss is enriched in Ga 26ppm but depleted in Nb, Zr and Y having values of, 14, 134 and 14ppm respectively. The rock is depleted in Sr (323ppm) compared to the crustal abundance of 375 but slightly enriched in the other lithophile elements Ba and Rb compared to the crustal abundance of 425 and 90ppm respectively (Taylor, 1964). The REE pattern of the rock shows the fractionation of the LREEs relative to the HREEs ( $\text{LaN/YbN} = 12.3$ ). Hugh (1993), noted that the fractionation of the light REEs relative to the heavy REEs may be caused by the presence of olivine, orthopyroxene and clinopyroxene for the partition coefficient in order of magnitude from La – La in these minerals.

The banded gneisses are medium grained and display very strongly lineated, weakly to highly foliated gneissic structures and prominent pinch and swell structures. The banded gneiss mostly occurs as low lying and pavement outcrops and are characterized by well-developed mafic and felsic bands. Diffusive mass transfer and in situ partial melting contribute to the enhancement of any primary compositional banding, as well as producing additional segregation of felsic and mafic minerals (Andy, 1998) as observed in the banded gneiss. The felsic bands, which consists of quartz and feldspars and the dark bands which is made up of biotite. The prominent pinch and swell structures observed in the banded gneisses are indicative of semi brittle deformation (Garner et al., 2015). The banded gneiss and migmatite gneiss both have a similar geochemistry. They are fairly rich in  $\text{SiO}_2$  with values of 67.79 and 70.25 wt% respectively. They both have relatively high concentrations of  $\text{Al}_2\text{O}_3$  of 14.96 and 14.23 wt% respectively. The banded gneiss is relatively rich in CaO (3.24 wt%) and  $\text{Na}_2\text{O}$  (4.12 wt%) but poor in  $\text{K}_2\text{O}$  (2.19 wt%).

### 5.3 Geochemistry and Structural Geology of the Granites

#### 5.3.1 Alkali Granites

The alkali granite in the study area is part of the well-studied Nigerian Younger Granites. It is an extension of the Pankshin Younger Granite Ring Complex that extends from Pankshin area in the Jos Plateau to parts of Wamba, Nasarawa State north central Nigeria. The alkali granites represent the youngest lithologic unit in the study area and intrude the migmatite gneiss in the north eastern portion of the study area. The slightly lower AI for alkali granite indicate that it is less evolved than the pegmatites and albitized granite (Abdelfadil et al, 2016). The alkali granite plot consistently in the A-type granite field on the Ga/Al vs. Zn diagram of Whalen *et al.* (Fig. 37). The alkali granites plot on the I-type granite field on the A/CNK versus SiO<sub>2</sub> (Fig. 22) protolith discrimination diagram after (after Chappel and White, 1974). Whalen *et al.*, (1987) noted that highly fractionated felsic I-type granites can have Ga/Al ratios and some major and trace element values that overlap those of typical A-type granites. Hence, it is possible that the A-type characteristics of the studied rocks might be explained by extreme fractionation from calc-alkaline I-type magmas. It plot in the A2 subgroup (Fig. 37) for A-type granite which is interpreted to represent rocks that crystalized from magmas derived from continental crust or underplated crust that has been through a cycle of continent-continent collision or island arc magmatism (Eby, 1992). It also plot in the within plate granite field of the Rb vs. Y+Nb tectonic discrimination diagram of Pearce *et al.* (1984) (Fig. 36) characteristic of A-type granites (Winter, 2014). The alkali granite is rich in SiO<sub>2</sub> and have the highest mean SiO<sub>2</sub> value (74.18wt%) amongst the rocks in the study area. It also so have the highest mean value of Fe<sub>2</sub>O<sub>3</sub> (2.72 wt %) and CaO (0.64 wt %). It is enriched in the HFSE elements such as Ga, Zr, Hf, Nb and Y with mean values of 27 ppm, 286 ppm, 7.05 ppm, 31 ppm and 96.5 ppm respectively indicating that it was produced from

melts rich in accessory phases such as zircon, garnet and sphene (Hanson, 1978 and Hanson, 1980). The alkali granites have the highest mean Ba and Ce values of 365 ppm and 164.5 ppm. The alkali granites do not show signs of significant deformation both in megascopic and microscopic observations. It occurs as high rising plutons in a ridge-like manner extending much further beyond the study area from the north-eastern portion. In the Rb-Sr-Ba ternary diagram of El-Bouseily and El-Sokkary (1975) (Fig. 27), the alkali granites plot in the field of strongly differentiated granite close to the normal granite boundary and much closer to the Ba corner of the plot. The REE pattern of the alkali granite is subparallel, LREE enriched (LaN/YbN value of 6.38), prominent negative Eu anomaly (Mean  $Eu/Eu^* = 0.27$ ) and are characterized by nearly flat HREE profile consistent with REE patterns for A-type granite (Eby, 2011; El Hadek et al., 2016) .

### **5.3.2 Albitised Granite**

The albitised granite is severely depleted in Ba, Pb and Sr. Hofman (1972) noted that the transformation of K-feldspar and calcic plagioclase to albite causes severe depletion in Rb, Ba, Sr and Pb. The metasomatic process may have also led to the severe leaching of the REEs ( $\sum REE = 5.17$ ) as observed in these rocks. The REE depletion may be related to the transformation of accessory phases, such as monazite to apatite and thorite in albitised granitoid (Boulvais et al., 2007). The albitised granite have low K/Rb (36.7 – 67.4) and low Nb/Ta ratio (5.2 – 7.9) reflecting their highly evolved nature. The albitised granite are  $SiO_2$  rich with a mean value of 73.89 wt%. It has the highest  $Na_2O$  value of 5.06 wt% reflective of its albite rich nature. The rock contains a relatively low  $K_2O$  value (3.71 wt.%) but a high  $Na_2O$  concentration, indicating the extent of K replacement by Na (Kaur et al., 2012). It also has a high  $P_2O_5$  value of 0.35 – 0.38 wt%. The alkali granites have very low values of CaO (0.11 – 0.14 wt%),  $TiO_2$  (0.002 – 0.004 wt%) and  $Fe_2O_3$  (0.76 – 0.89 wt%) which can be

attributed to the effect of leaching during hydrothermal alteration (Denies and Mark, 2000). The most prominent feature of the albitized granite is the occurrence of broad albite lamellas which is considered to have formed by the complete replacement of K-feldspar by albite (Moody et al., 1985).

The albitized granite has a prominent positive Eu anomaly (Fig. 26) and a low Rb/Sr ratio which can be interpreted as an indication of the accumulation of early formed feldspar crystals rich in Eu (Milord et al., 2000). The REE plot for albitised granite shows an alternating enrichment and depletion of neighboring elements from Eu-Lu creating a REE tetrad pattern. The REE tetrad pattern which is the W-type is interpreted to represent an open system fluid-melt reaction in a magmatic-hydrothermal system during the final stages of crystallisation (Irber W., 1999; Zhao et al., 2002).

The rock is biotite poor and feldspar rich, hence the positive Eu anomaly may be indicative that it was derived from melts depleted in the other REEs and probably because the accessory phases containing them remained armored in the biotite and were not available to the melt (Milord et al., 2000). The albitized granite occur in an uplifted region as highly deformed and scattered outcrops. It contains several joints prominently running along the NE-SW direction. A thin zone of fine grained greenish possibly chlorite resulting from hydrothermal alteration exists along the joints. Thin section analysis reveals sericitization along the muscovite and feldspar grain boundaries indicative of hydrothermal alteration. The rock is whitish and fine grained in hand specimen. The albitized granite plot off the field of rare-metal granites and Sn-W-U related granites in the plot of Nb/Ta versus Zr/Hf (Fig. 35) after (Ballouard et al., 2016) and therefore seems very unlikely to be classified as a fertile granite that can be parental to rare metal pegmatites.

#### 5.4 Geochemistry and mineral potential of the pegmatites

The trace element composition of muscovite mica has been reported to be another useful indicator of the extent of fractionation in rare-metal pegmatites (Tischendorf et al., 2001; London, 2008). The concentrations of Rb, Cs, Mn, Ga, Tl, Sn and Ta in muscovite mica increase, whilst K/Rb, Ba/Rb, Rb/Sr, Na/Ta and Fe/Mn ratios show a concomitant decrease characteristic of highly fractionated pegmatites (Černý et al., 1985; Shaw et al., 2016). Muscovite samples in the study area are enriched in a number of trace elements including Rb (up to 3957 ppm), Be (up to 55 ppm), Sn (up to 798 ppm), Ga (up to 179 ppm), W (up to 802 ppm) and Nb (up to 194 ppm). Other trace element concentration in the muscovite include Cs (up to 133 ppm), Ta (up to 91.1 ppm) and Tl (up to 11.7 ppm) but is relatively depleted in Ba, Sr, REE, Th and U. These patterns of enrichment and depletion could indicate the presence of micro-inclusions within the muscovite crystals (Shaw et al., 2016). On the other hand, the quartz-feldspar-pegmatite sample is observed to be enriched in Ba, Th, Pb and but depleted in Be, Nb, Ce and Ti. The quartz-muscovite-pegmatite is richer in Be, Mn, Nb, Ta and W than the quartz-feldspar-pegmatite. These differences can be attributed to the presence of accessory minerals such as beryl and columbite in former.

The muscovite samples are rich in Al, K, Sn and Rb but low in Ca Ba and Sr. Rubidium contents in the muscovite samples range between 2946 and 3957ppm. Far lower concentrations are however observed in quartz-feldspar-pegmatites samples ranging between 83 and 542ppm. K/Rb ratios are generally lower in muscovite samples ranging between 15.61 and 18.06 compared to quartz-feldspar-pegmatite samples with K/Rb ratios between 88.79 and 463.08 (Table 3). The low K/Rb ratio of the muscovite samples expresses their more evolved nature (Černý, 1982). In the Rb-Sr-Ba ternary diagram of El-Bouseily and El-Sokkary (1975) (Fig. 27), the quartz-muscovite-pegmatite and albitized granites are clustered

close to the peak in the field of strongly differentiated granite. The alkali granites plot in the field of strongly differentiated granite close to the normal granite boundary and much closer to the Ba corner of the plot. Černý (1982) observed that the ratios, K/Rb, Ba/Rb, Rb/Sr and Na/Ta all tend to decrease to extremely low values with increasing pegmatite fractionation. Accordingly, the values recorded for the quartz-muscovite-pegmatite trace element ratios (K/Rb, Ba/Rb, Rb/Sr and Na/Ta), are low, indicating a high degree of fractionation of the pegmatites. The quartz-muscovite-pegmatites is observed to have a negative correlation on the Plot of  $K_2O$  vs,  $SiO_2$ , and a positive correlation of  $Na_2O$  vs  $SiO_2$  (Fig. 16), possibly indicating Na–K exchange, caused the influence of coexisting metasomatic fluid during the evolution of their magma.

Notably, REE patterns for rare-metal pegmatites exhibit strong negative Eu anomalies and enrichment in the MREE and HREE relative to the LREE. Such strong negative Eu anomalies might indicate fractionation of plagioclase, melting of a plagioclase-depleted source material, or melting of a plagioclase-rich material, in which the plagioclase did not melt (Zhao et al., 2002). On the other hand, the quartz-feldspar-pegmatite is marked by a prominent positive Eu anomaly (Fig. 25), which is indicative of the fractionation of Eu into feldspars during the early stages of fractional crystallisation possibly in the lower crust (Shaw et al., 2016). Rudnick and Gao(2003) noted that positive Eu anomaly as being characteristic of rocks sourced from the lower crust. Occurrence of a weak negative Ce anomaly accompanied by a significant negative Eu anomaly in the quartz-muscovite-pegmatite indicates the role of late stage or metasomatic fluids in the genesis of these rocks (Akintola et al., 2012b, Taylor et al., 1986). However, this is not the case with the quartz feldspar pegmatites which displays weak negative Ce signature and strong positive Eu anomaly on the REE trend (Fig. 25).

The pegmatites and albitized granite display a noticeable W-type REE tetrad effect pattern. The W-type tetrad effect is interpreted to indicate open system conditions during granite crystallization (Irber W., 1999). Zhao *et al.*, (2002) observed that pegmatites evolved dominantly from fluid/melt mechanism often show strong Eu depletion and REE tetrad effect in the melt and in the rock-forming and accessory minerals crystallizing from this melt as observed in both types of the Kwarra pegmatite. Similar REE tetrad effects have been reported for a number of highly evolved granitic rocks including leucogranites and pegmatite (Walker *et al.*, 1986; Zhao, 1988; Jolliff *et al.*, 1989; Yurimoto *et al.*, 1990; McLennan, 1994; Irber, 1999).

The overall chemical differences between quartz-muscovite-pegmatites and quartz-feldspar-pegmatites can be attributed to differences in original magma composition, which may be related to assimilation of crustal rocks during ascent of the magmas or to differences in derivation of both magmas (London 2008, Černý 1991).

The mineral potential for rare metals such as Rb, Cs, Be, Y, REE, Zr, Hf, Nb, Ta (Smirnov *et al.*, 1986) in the pegmatite of the area was assessed using geochemical criteria and representative diagrams for the whole rock pegmatites and mineral extracts. The Ta and Cs content of muscovite mica have also been used as an exploration tool to identify the potential for Ta–Nb mineralisation in pegmatites (Selway *et al.*, 2005). Selway *et al.*, (2005) noted that Pegmatites containing muscovite with a Ta concentration greater than 65 ppm and a Cs concentration above 500 ppm are highly likely to contain Ta–Nb mineralisation. However the muscovite samples has Ta concentrations ranging from 65.5 – 91.1 ppm and Cs concentration ranging from 37.4 – 133 ppm significantly less than 500 ppm and are thus not to be considered as a prolific source of Nb-Ta mineralisation. On the other hand, the quartz-feldspar-pegmatite has a Ta concentration ranging from 11.3 to 21.7 ppm and a Cs

concentration ranging from 1.3 -14.9 ppm. Considering Ta-Nb mineralisation potential trend of Ta versus Cs (Fig. 30), Ta versus K/Cs (Fig. 31) and Ta versus Ga (Fig. 32), in these plots, the quartz-feldspar-pegmatite consistently plot below the Beus (1966) and Gordiyenko (1971) lines of mineralisation while the quartz-muscovite-pegmatite plot predominately plot above the Beus (1966) line of mineralisation but below the Gordiyenko (1971) lines of mineralisation. Based on Ta-Nb mineralisation potential plots done for the pegmatites, the quartz-feldspar-pegmatite is interpreted as barren while that of the quartz-muscovite-pegmatite can be described as not well developed.

K/Rb versus Cs discrimination plot (Fig. 33) adapted from Černý and Burt (1984) was used to determine the mineralisation potential of the pegmatites. A discrimination line was used to separate the rare - metal class from the barren class. From this plot it was observed that the quartz-quartz-muscovite-pegmatite plot within the field of rare metal pegmatites, while the quartz-feldspar pegmatites plot within the field of barren pegmatite. A second plot used to further separate the pegmatites into Be-class and Be-Li class pegmatites after Trueman and Černý (1982) shows that the quartz-muscovite-pegmatite are of the Be-Li class (Fig. 34). There is a relatively high Sn concentration in the Kwarra pegmatite (up to 798 ppm) (Table 3), amounts high enough to be associated with a cassiterite mineralisation.

Although the analytical method used for measuring the values of the various trace element does not record the concentration of lithium, samples of quartz-muscovite-pegmatite fall in the field of lithium and beryllium enrichment in the plot of of K/Rb versus Cs (Fig. 34) of their muscovite after Trueman and Černý (1982) and thus can be considered as enriched in Li. The concentration of Cs and Ta (mean 63.9 and 22.3 ppm respectively) in the quartz-muscovite-pegmatite indicates that the Cs-Ta mineralogy is not well developed in the rock.

However, their concentrations significantly exceed the crustal abundance of 2 and 3 ppm respectively (Taylor, 1964).

Based on their chemistry and mineralogy, quartz-muscovite-pegmatite (rare-metal) are most akin to LCT-type (Lithium, Cerium and Tantalum) pegmatites, and thus likely to have an ultimate source in sedimentary rocks (Černý, 1991; Martin and De Vito, 2005; London, 2008; Černý et al., 2012). The plot of A/CNK vs SiO<sub>2</sub> after Chappel and White (1974) (Fig. 20) further supports the S-type source of the pegmatites. LCT pegmatites are more abundant and enriched in Be, B, F, P, Mn, Ga, Rb, Nb, Sn and Hf (Oyebamiji et al., 2018) consistent with the Sn, Ga, Rb, Nb and W enriched nature of the rock.

## **5.5 The Role of Hydrothermal Alteration on the Geochemistry and Mineralogy of the Granitoids**

In the modified triangular Ti-Sn-(Nb+Ta) discriminant plot after Kuster (1990), the Pegmatites around Kwara area and albitized granite plots in the zone of albitisation (Fig. 26). Norm calculations (Table 2) show an increasing Ab in the albitised granite, quartz-feldspar-pegmatite and quartz-muscovite-pegmatite with mean normative Ab values of 12.1, 30 and 42.8 respectively. This increase in normative Ab is indicative of albitisation (Kinnard et al. 1985). Albitisation occurs during sodic metasomatism and is characterised by the exchange of Na for Ca or K, and to a lesser extent Ca for Fe and Mg. In the albitisation process, hydrothermal fluids convert plagioclase and/or K-feldspar into nearly pure albite (Kaur et al., 2012). In the studied area, the effect of sodic metasomatic stage is represented by local albitization and local greisenization observed in the north-western portion of the studied area. Whitening of feldspars on the affected granitoid outcrops as is observed in the albitized granite, quartz-feldspar-pegmatite and muscovite granite is one of the notable megascopic

indicators for strong and pervasive albitisation and has commonly been observed in many other albitized granitoids (Baker, 1985; Charoy and Pollard, 1989; Petersson and Eliasson, 1997). The mineral assemblages generated during sodic metasomatism depend on the intensity of rock-fluid interaction, the strongly peralkali granites showing the greatest effect (Bowden and Kinnaird, 1984). Norm calculations by Kinnard et al. (1985) show that soda metasomatism is characterized by increasing Ab such as is observed in the albitised granite, bulk granite and muscovite granite which all show strong albitized signatures with mean normative Ab values of 12.1, 30 and 42.8 respectively. Subsequent work done by Kuster (1990) on a regional scale covering the study area, has made clear that these albites are the products of Na-metasomatism. In the albitized granitoids, the abundance of Na<sub>2</sub>O increases from 3.55 wt % in the quartz-feldspar-pegmatite to 7.0 wt % in the albitized granite, whereas K<sub>2</sub>O decreases from 5.38 wt % to 3.71 wt %, implying a K-Na exchange. The metasomatic transformation of K-feldspar and calcic plagioclase to albite causes severe depletion in Rb, Ba, Pb and Sr (Kaur et al., 2012) as observed in the albitized granite and pegmatites. The decrease in Rb abundances from 3399 ppm in the quartz-muscovite-pegmatite to 41.5 ppm in the albitized granite and 21.6 ppm in the quartz-feldspar-pegmatite respectively is also compatible with progressive albitisation of K-feldspar (Fig. 27) and loss of mafic phases, because Rb is rather compatible in K-feldspar, potassic hastingsite and biotite but highly incompatible in albite (Kaur et al., 2012). The plot of Rb vs Na/K (Fig. 27) shows the progressive depletion of Rb with increasing Na/K values (progressive albitisation of K-feldspar). It is however important to suggest that fractional crystallisation played an important role in the initial Rb concentration in the rocks and albitization only somewhat modifying the Rb concentration. The metasomatic process may have also led to the severe leaching of the REEs (mean  $\sum$ REE = Albitised granite-5.17, quartz-feldspar-pegmatite-15.82, muscovite

granite–5.07) and the conspicuous W-type REE tetrad effect observed in these rocks. The sodic metasomatic stage is characterized by the coexistence of crystals and supercritical fluid (El Hadek et al., 2016). This is supported by the existence of a W-type REE tetrad effect which indicates an open system, late stage, magmatic-hydrothermal interaction during the formation of the albitised rocks (Irber, 1999; Zhao et al., 2002). The REE depletion may be related to the transformation of accessory phases, such as monazite to apatite and thorite in peraluminous albitised granitoid (Boulvais et al., 2007). Also accompanying the albitisation process is the destruction of original Ti-Fe oxides, enrichment in uranium, and the introduction of columbite with minor cassiterite, thorite and xenotime (Obaje, 2009). The albitized granite, quartz-feldspar-pegmatite and quartz-muscovite-pegmatites have very low Fe and Ti concentrations ( $\text{Fe}_2\text{O}_3$  - 0.82 wt.%, 0.73 wt.% and 2.05 wt.%  $\text{TiO}_2$  0.003 wt%, 0.008 wt.% and 0.002 wt.% respectively). Albitisation also concentrates HFSE, especially Nb and Ta as observed in the albitized granite and pegmatites. While this may not be well pronounced in the albitized granitoids, it is however important to note that the albitized rocks have relatively notably elevated Nb and Ta concentrations compared to the other rocks in the study area (Table 3).

Sodic alteration is strongly fracture controlled (Battles, 1994), brecciation is well developed in the areas where the albitisation is well pronounced, especially in the albitised granite and quartz-muscovite-pegmatite. Hydrothermal fluids migrate to areas of low pressure and in regimes of extensional and strike-slip tectonics. It is not surprising that fluids concentrate into dilatant fault zones. In addition to the brecciation and cataclasis, it is widely observed that such fault zones are intensely silicified, sericitised, chloritised or show some other features of chemical or mineralogical change indicative of high fluid flux (Andy, 1998). In the Arum area, the albitised granite is well deformed and brecciated. Thin section study reveal that the

original K-feldspar has been albitized and there is a development of sericites along the mica grain boundaries. The albitisation is observed to be most pronounced along the NE-SW linearments in the north western flank of the study area characterised by high lineament densities.

Dillies and Einaudi (1992) suggests a depth 1 – 4km occurring at a low temperature ranging between 200 – 400<sup>0</sup>c. Fluid inclusions study done by El Hadek, (2016) reveals that albitization had taken place at high temperature (350°C - 410°C), and vapor-rich aqueous fluid. The shallow depth and low temperature characteristic of sodic metasomatism can account for the accompanying brittle deformation that is observed to affect the albitized rocks. Sodic metasomatism is economically important for the introduction of Nb-bearing ore minerals occurring as columbite in peraluminous biotite granites and as pyrochlore in the peralkali granites and, of less importance, as fergusonite in metaluminous hornblende biotite granites (Obaje, 2009). In the Nigerian province it is the albitized granites that have the highest uranium enrichment (Bowden et al., 1981), this is also manifested on a smaller scale in the study area as the albitised rock samples have elevated uranium concentration compared to the others. Uranium concentrations range from 1.9 to 23.4 ppm in the quartz-feldspar-pegmatite, 0.4 – 15 ppm in the quartz-muscovite-pegmatites and a mean value of 6.8 ppm in the albitized granite. All the albitized rocks have mean uranium concentration greater than the crustal abundance of 2.7 ppm (Taylor, 1964).

## **5.6 Petrogenesis**

The development of the Pan-African rare-metal pegmatites of central Nigeria is genetically related to post-kinematic, late-tectonic granite magmatism (Kuster, 1990). This plutonism is

characterized by its position after the major orogenic event, its multiple intrusive activity, its structurally controlled emplacement, and its geochemical specialisation patterns.

The peraluminous nature of the Pegmatites around Kwarra area is broadly interpreted as their derivation from intermediate to felsic crustal sources (Millerand Mittlefehldt., 1985, Chappell and White, 2001). Many experimental studies have shown that peraluminous granites are typically formed by melting of biotite + muscovitebearing metapelites (Gardien et al.,1995; Patino Douce and Harris, 1998). Based on the genetic subdivision of granitic rocks proposed by Chappell and White (1974), the Kwarra pegmatite fall into those extracted from sedimentary protoliths (S-type), which according to Chappell and White (2001) were formed by the melting of sedimentary and/or metamorphosed sedimentary or supracrustal rocks, such as metapelites. Kuster (1990), reported the occurrence of such metasedimentary rocks which are abundant in the high grade basement of the Wamba area and its surroundings, interpreted as metavolcano-sedimentary association of semipelitic sediments. This metapelitic rocks provide a source of appropriate composition for the LCT rare-metal pegmatite end-members (Černý, 1991).

Most LCT-type pegmatite fields are interpreted as the product of extreme granitic fractionation of melts ultimate sourced from sedimentary rocks (Černý , 1991; Martin and De Vito, 2005; London, 2008;Černý et al., 2012). Such a magmatic process is defined by fractional crystallisation leading to an increase of rare elements and fluxes in the residual melt with increasing distance from the consolidating parental granitic source (London, 2008, Trueman and Černý, 1982). Incomplete fractionation of mica-rich melts in collisional zones normally form LCT granitic pegmatites gives a high concentration of trace elements (Černý et al., 2012).

On the basis of the variations observed in A/CNK values, trace element patterns and mineralogy between the (rare-metal) quartz-muscovite-pegmatites and barren quartz-feldspar-pegmatites, it is reasonable to assume that different source materials were available for melting. It is assumed that the Pan-African continental collision and crustal thickening triggered the partial melting of the older crust and has led to the generation and intrusion of several magma batches, slightly differing in chemical composition and now representing major plutons (Kuster, 1990). The syn-collisional setting of the pegmatites supports their formation linked to the process of crustal thickening (Pearce, 1996). Partial melting of compositionally distinct protoliths can also produce wide compositional spectrum of granite magmas with the same degree of partial melting. This could be arising from the change mineralogy, trace element chemistry, mineral stability field of sheet silicates or accessory minerals and their content in the mineral/residuum phase, and metasomatic alteration of the source metasedimentary lithology (Shearer, C.K et al., 1992). Due to the multiphase nature of the late Pan-African magmatic activity and the ability of successive plutons to releasing residual, probably differently evolved pegmatitic melt, pegmatites, barren and mineralized have been produced from several parental granites (Kuster, 1990).

The REE trend of the quartz-muscovite-pegmatites indicates the effect of late stage metasomatic fluid in an open system magmatic-hydrothermal interaction during the formation of the rocks. The REE trend of the quartz-feldspar-pegmatite also indicate a similar melt-fluid interaction. The quartz-muscovite-pegmatite appear on average to be geochemically higher evolved than the quartz-feldspar-pegmatite. It show higher contents Rb, Cs, Mn, Ga, Tl, Sn and Ta whilst K/Rb, Fe/Mn, Ca, Ba, Sr, and Zr show a concomitant Decrease. This trend is observed in the quartz-muscovite-pegmatites attests to their highly fractionated nature (Kuster, 1990; Shaw et al., 2016). Highly fractionated nature of quartz-feldspar-pegmatite

may have led to the enrichment of incompatible elements in residual melts which may result in a co-existing magmatic-hydrothermal system. It seems therefore likely that the metasomatic replacement and mineralization processes have been generated from residual fluids of the pegmatite melts themselves and not by external fluid injections (Oyebamiji et al., 2018; Kuster, 1990). However, the notable depletion of REE, Ba and Sr with increasing Na/K ratios can also be attributed to metasomatic recrystallisation during albitisation and fluid interaction (Kaur et al., 2012). Trace elements more resistant to changes during postmagmatic alteration (Ti, Nb, Ta, Cs) are extremely depleted in the quartz-feldspar-pegmatite and less so in the quartz-muscovite-pegmatite and may represent original magmatic compositions more closely. The positive Eu anomaly in the quartz-feldspar-pegmatite and the negative Eu anomaly in the quartz-muscovite-pegmatite reflect strongly their derivation from different sources, probably lower crust and upper crust respectively (Rudnick and Gao 2003).

Structurally, the pegmatites are located in a highly strained zone, where the country rocks are highly deformed, foliated and affected by brittle – ductile shear zones. Lineament analysis and structural trends observed from the joints, faults, veins and foliation show NE-SW, N-S and NNE-SSW as the principal stress directions. The observable NE–SW (dextral) and NW–SE (sinistral) conjugate systems in the host rocks are due to Late Pan-African brittle deformation (Ball, 1980). The quartz-feldspar-pegmatite with majorly NW-SE and E-W direction are mostly found occurring in the migmatite gneisses while the quartz-muscovite-pegmatite predominantly trending NE-SW are populated in the banded gneisses and granite gneisses. The albitisation is observed to be most pronounced along the NE-SW lineaments in the north western flank of the study area characterised by high lineament densities. Brecciation is well developed in the areas where the albitisation is well pronounced, especially in the albitised granite and quartz-muscovite-pegmatite. The shallow depth and low

temperature characteristic of sodic metasomatism can account for the accompanying brittle deformation that is observed to affect the albitised rocks. A depth 1 – 4km occurring at a low temperature ranging between 200 – 400<sup>0</sup>c has been suggested for such sodic alteration (Dillies and Einaudi, 1992).

Based on the geochemistry, geological structures and mineralogy of the pegmatites, it is therefore suggested that the quartz-feldspar-pegmatite represent late-stage residual melts derived from less evolved granitic parent in the lower crust which have been derived by fractionation while the quartz-muscovite-pegmatite are products of highly fractionated late-stage magma derived from fertile granite at depth and modified by interaction with a coexisting hydrothermal phase during crystallisation beneath the amphibolite belt. The emplacement of these rocks was controlled by the reactivated ancient predominantly NE-SW, NNE-SSW and N-S trending fractures and minor NNW-SSE and E-W. No fertile granite was mapped in the study area, suggesting that it is either buried deep within the subsurface or have a rather distal relationship with the rare metal pegmatite. Trueman and Černý, (1982) noted that rare metal pegmatites are typically the most distant from their parent granites, having undergone increasing fractionation and concentration of rare elements and volatiles with increasing distance.

## CHAPTER SIX

### CONCLUSION AND RECOMMENDATION

#### 6.1 Conclusion

The study area was mapped in detail and a geological map was produced on a scale of 1:25,000. Locally, the main lithological units in the study area are migmatite-gneiss complex, Pan-African granitoids and the Younger Granites. The rock types in the area are amphibolite, migmatite gneiss, banded gneiss, granitic gneiss, albitised granite, alkali granite. Pegmatites and dolerites represent the minor rocks types in the study area. The quartz-feldspar-pegmatite are mostly hosted in the migmatite gneiss while quartz-muscovite-pegmatites are mostly found associated with the banded gneiss and granite gneiss and coincide with major lineaments in the study area, hence their deformed nature. The study area showed that structural lineaments were more concentrated in the migmatites, banded gneisses and amphibolites (Pre-Cambrian basement rocks) than in the Jurassic Younger Granites. The principal lineament trends are N-S, NE-SW, and NNE-SSW with minor ENE-WSW, E-W trends. The alkali granite is metaluminous while the albitized granite and pegmatites are peraluminous. Metamorphism in the rocks of the polycyclic basement is generally in the amphibolite facies grade with the characteristic hornblende-plagioclase mineral produced by medium pressure and temperature. There are two observable types of pegmatites in the study area: the rare-metal/muscovite rich quartz-muscovite-pegmatites and the barren/muscovite deficient quartz-feldspar-pegmatite. predominantly trending along NE-SW, NNE-SSW and N-S and minor NNW-SSE and E-W. The quartz-muscovite-pegmatites are observed to be trending mainly along the NE-SW trend while the quartz-feldspar-pegmatite predominantly along NW-SE and minor E-W trends. The syn-collisional setting of the pegmatites supports their formation linked to

the process of crustal thickening (Pearce, 1996) which is characteristic of the Pan-African orogeny (Kuster, 1990). The pegmatites are both peraluminous in nature ( $ASI > 1.0$ ) with the quartz-muscovite-pegmatite showing the strongest peraluminous signature ( $ASI = 3.01$ ). The quartz-muscovite-pegmatites appear on average to be geochemically higher evolved than the quartz-feldspar-pegmatite. They show higher contents Rb, Cs, Mn, Ga, Tl, W, Sn and Ta whilst K/Rb, Fe/Mn, Ca, Ba, Sr, and Zr show a concomitant decrease. This trend is observed in the quartz-muscovite-pegmatites which attests to their highly fractionated nature (Kuster, 1990; Shaw et al., 2016). The highly fractionated nature of quartz-feldspar-pegmatite may have led to the enrichment of incompatible elements in residual melts which may result in a co-existing magmatic-hydrothermal system as manifested by the conspicuous W-type REE tetrad effect displayed by the quartz-muscovite-pegmatites on the REE trend. The pegmatites plot in the field of albitized pegmatites in the plot of Ti-Sn-(Nb+Ta) modified After Kuster, (1990) further indicating the activity of hydrothermal fluid in the formation of the rocks. The concentration of Rb is observed to be progressively depleted as albitisation advances, showing that the albitisation process may have somewhat modified the Rb content of the pegmatites and albitised granite. The albitised rocks indicate that the sodic metasomatism may have increased the abundance of W, Na, Al, U and Sn while decreasing the concentration of Fe, Ti and REE. The quartz-muscovite-pegmatites in this study are enriched in rare-elements, particularly Sn, W, Rb, Be, and to a lesser extent Ta and Nb but depleted in REE, Sr and Ba. Mineral potential plot indicate that the rare-metal pegmatites are Li enriched and are of the LCT type. The LCT and peraluminous nature of the quartz-muscovite-pegmatite indicated that the rocks were ultimately sourced from the partial melting of sedimentary rocks probably metapelites. Based on the geochemistry and mineralogy of the pegmatites, it is therefore suggested that the quartz-feldspar-pegmatite represent late-stage residual melts of a less evolved granitic parent which have been derived by fractionation while the quartz-muscovite-pegmatite are products highly fractionated late-stage magma derived from

fertile granite at depth and modified by interaction with a coexisting hydrothermal phase during crystallisation beneath the amphibolite belt.

## **6.2 Recommendation**

Based on the observations from this research, I recommend that further study should be carried out on the Sn and W mineralization in the study area. Sn and W have high concentrations in the rare metal pegmatites and may have been concentrated by secondary processes in the area. Also, The extensive nature of metasomatic alteration and the deformed nature of the rocks in the area as expressed by fractures, joints and the lineament density, provides excellent conditions for the deposition of valuable hydrothermal minerals and will require amore robust geophysical and geochemical investigation to ascertain.

## **6.3 Contribution to Knowledge**

The major contribution of the work to knowledge are

1. The geological map of the study area has been updated at the scale of 1:25,000
2. The lineament map of the study area was produced
3. Petrographical and geochemical characterisation of the rocks in the study area.
4. The mineral potential of the rocks has been evaluated
5. Petrogenetic model of the rocks in the has been proposed

## REFERENCES

- Abdelfadil K.M. Asimow P.D. Azer, M.K. Gahlan H.A., (2016): Genesis and Petrology of Late Neoproterozoic Pegmatites and Aplites Associated with The Taba Metamorphic Complex in Southern Sinai, Egypt. *Geologica Acta*, Vol. 14, Pp 16.
- Adedoyin, A. D., Adekeye, J. I. D. And Alao, D. A. 2006. Trace element geochemistry of selected pegmatites from southwestern Nigeria. *Nig. Jour. Pure and Appli. Sci.*, 21: 2023 – 2035.
- Adetunji, A. and Ocan, O.O. (2010): Characterization and Mineralization Potentials of Pegmatites of Komu Area, Southwestern Nigeria. *Resource Geology* 60 (1): 87-97.
- Adetunji, A., Olarewaju, V.O., Ocan, O.O., Ganev, V.Y. and Macheva, L. (2016): Geochemistry and U-Pb Zircon Geochronology of The Pegmatites in Ede Area, Southwestern Nigeria: A Newly Discovered Oldest Pan- African Rock in Southwestern Nigeria. *Journal of African Earth Sciences* 115, 177- 190.
- Ajakaiye, D. E., Hall, D. H., Miller, T. W., Verheijen, P. J. T., Awad, M. B. and Ojo, S.B. (1986): Aeromagnetic Anomalies and Tectonic Trends in and Around The Benue Trough, Nigeria. *Nature*, 319, 582-584.
- Ajibade Ac, Rahaman Ma, Woakes M (1987): Proterozoic Crustal Development in The Pan-African Regime of Nigeria. Iip Working Group 3 Mid-Term Report
- Akintola O.F., and Adekeye J.I.D. (2008): Mineralization potentials of pegmatites in the Nasarawa area of central Nigeria [J]. *Earth Science Research Journal*. 12 (2), 213–234.
- Akintola A.I., Ikhane P.R., Okunlola O.A., Akintola G.O., and Oyebolu O.O. (2012 a): Compositional Features of Precambrian Pegmatites of Ago–Iwoye Area, Southwestern, Nigeria [J]. *Journal of Ecology and The Natural Environment*. 4 (3), 71–87
- Akintola A.I., Ikhane P.R., Okunlola O.A., Akintola G.O., and Oyebolu O.O. (2012 b): Geochemical features of the Precambrian Pan–African Pegmatites of Ijebu–Ifé Area, southwestern Nigeria [J]. *Environment, Ecology & Management*. 1 (1), 38–61
- Akoh, J.U., Ogunleye, P.O., (2014): Mineralogical and geochemical evolution of muscovite in the pegmatite group of the Angwan Doka area, Kokoona district: a clue to petrogenesis and tourmaline mineralization potential. *J. Geochem. Explor.* 146, 89-104.

- Akoh, J.U., Ogunleye P.O., Ibrahim A.A., (2015): Geochemical evolution of micas and Sn-, Nb-, Ta- mineralization associated with the rare metal pegmatite in Angwan Doka, central Nigeria. *Elsevier Journal of African Earth Sciences* 112, 24-36
- Ananaba, S.E. and Ajakaiye, D.E., (1987): Evidence of tectonic control of mineralization of Nigeria from lineament density analysis: a landsat study; *Int. Jour. Rem. Sensing*; vol.1, no.10;pp. 1445- 1453.
- Andy J. B. (1998): *Introduction to metamorphic textures and microstructures*. Second edition. Starnley Thornes Publishers Ltd. Pp 41 – 43.
- Anudu, G.K., Obrike, S.E., Iyakwari, S. and Ikpokonte, A.E. (2012): Preliminary structural study of Landsat imagery over Wamba and environs, Nasarawa State north-central Nigeria. *Research Journal of Applied Sciences*, Vol. 7, No. 1, Pp. 1-9.
- Baker, J. H. (1985): Rare earth and other trace element mobility accompanying albitization in a Proterozoic granite, W. Bergslagen, Sweden. *Mineralogical Magazine* 49, 107-115.
- Ball, E. (1980): An example of very consistent brittle deformation over a wide intracontinental area: The late Pan-African fracture system of the Tuareg and Nigerian Shield. *Tectonophysics* 61:363-379
- Ballouard, C., Poujol, M., Boulvais, P., Branquet, Y., Tartèse, R., Vignerresse, J-L., (2016): Nb-Ta fractionation in peraluminous granites: A marker of the magmatic-hydrothermal transition. *Geology* 44 (3), 231-234.
- Battles B.A. (1994): Arc-Related sodic alteration in the western United States. Ph.D. Thesis: Los Angeles, California, University of California, Los Angeles. Pp 120
- Beus A.A. (1966): Distribution of tantalum and Niobium in muscovite from granitic pegmatites [J]. *Geokhimiya*.10, 1216 –1220.
- Black R (1980): Precambrian of West Africa. *Episodes* 4:3–8
- Boulvais P., Ruffet G., Cornichet J., Mermet M (2007): Cretaceous Albitization and dequartzification of Hercynian peraluminous granite in the Salvezines Massive. *Lithos* 2007 – Elsevier
- Bowden, P. and Turner, D. C. (1974): Peralkaline and associated ring complexes in the Nigeria-Niger province, West Africa. In the alkaline rocks, 330-351. Sorensen, H. (editor). (*London: John Wiley and Sons.*).
- Bowden P, van Breemen O, Hutchison J, Turner DC (1976): Palaeozoic and Mesozoic age trends for some ring complexes in Niger and Nigeria. *Nature* 259:297–299
- Bowden P, Bennett JN, Kinnaird JA, Whitley JE, Abaa SI and Hadzigeorgiou-Stravakis P (1981): Uranium in the Niger-Nigeria Younger Granite Province. *Mineral Mag* 44:379–389

- Bowden P, Kinnaird JA (1984): Geology and mineralization of the Nigerian anorogenic ringcomplexes. *Geologisches Jahrb (Hannover)* B56, 3–65
- Burke KC, Dewey JF (1972): Orogeny in Africa. In: Dessauvage TFJ, Whiteman AJ (eds), *Africa geology*. University of Ibadan Press, Ibadan, pp 583–608
- Černý, P., and Burt, D. M. (1984): Paragenesis, crystallochemical characteristics, and geochemical evolution of Micas in granites pegmatites: In: Bailey, S. W. (Ed.), *Mica*. Mineralogical Society of America, *Reviews in Mineralogy* 13: 257- 297.
- Černý, P. (1982): Petrogenesis of granitic pegmatites. in *Granitic Pegmatites in Science and Industry* (P. Černý, edition). Mineralogical Association of Canada, *Short Course Handbook* 8: pp. 405-461.
- Černý P, Meintzer RE and Anderson AJ (1985): Extreme fractionation in rare-element granitic pegmatites: selected examples of data and mechanisms. *Canadian Mineralogist* 23: 381-421
- Černý, P. (1989): Exploration strategy and methods for pegmatite deposits of tantalum; Special Publication No. 7 of the society geology applied to mineral deposits. Pp 274 - 302
- Černý, P., (1991): Fertile granites of Precambrian rare-element fields: is geochemistry controlled by tectonic setting or source lithologies? *Precambrian Research* 51, 429-468.
- Černý P, London D, Novak M (2012): Granitic pegmatites as reflections of their sources. *Elements* 8, 289–294.
- Chappell BW, White AJR (1974): Two contrasting granite types. *Pacific Geol* 8:173–174
- Chappell BW, White AJR (2001): Two contrasting granite types: 25 years later. *Australian Journal of Earth Sciences* 48: 489-499
- Charoy, B. & Pollard, P. J. (1989): Albite-rich, silica-depleted metasomatic rocks at Emuford, northeast Queensland: mineralogical, geochemical, fluid inclusion constraints on hydrothermal evolution and tin mineralization. *Economic Geology* 84, 1850-1874.
- Chukwu-Ike I. M. (1977): Regional photogeological interpretation of the tectonic features of the central Nigerian Basement Complex - A satellite imagery based study. A Thesis submitted for the Degree of Doctor of Philosophy of the University of London. Department of Geology, Royal School of Mines, Imperial College, London, S.W.7,
- Collins, W. J., Beams, S. D., White, A. J. R. and Chappell, B. W., (1982): Nature and origin of A-type granites with particular reference to southeastern Australia. *Contributions to Mineralogy and petrology* 80, 180-200.
- Dada, S.S., Birck, J. L., Lancelot, J. R. and Rahaman, M. A. (1993): Archean migmatite-gneiss complex of North Central Nigeria: its geochemistry, Petrogenesis and crustal

- evolution. In: 16th International Colloquium on African Geology, Mbabane, Swaziland, Extended Abstracts, 1: pp. 97–102. Dada SS (2006): Proterozoic evolution of Nigeria. In: Oshi O (ed) The basement complex of Nigeria and its mineral resources (A Tribute to Prof. M. A. O. Rahaman). Akin Jinad & Co. Ibadan, pp 29–44
- Dada, S.S. (2008): Proterozoic Evolution of the Nigeria-Borborema Province,” In: R. J. Pankhurst, R. A. Trouw, B. B. Brito Neves and M. J. De Wit, Eds., West Gondwana: Pre-Cenozoic Correlations across the South Atlantic Region, Geological Society of London Special Publication, London, pp. 121-136
- Denies A. Battles and Mark D. Battle (2000): Arc-related sodic hydrothermal alteration in the western United State, Department of geology and geography, Georgia Southern University Stateboro, Georgia. Department of Geoscience, University of Arizona.
- Dillies J.H., and Einaudi, M.T., (1992): Wall rock alteration and hydrothermal flow path about the Ann Mason porphyry copper deposit, Nevada – A 6km vertical reconstruction: *Economic Geology*, v. 87, p. 1963-2001.
- Eby, G. N., (1992): Chemical subdivision of the A-type granitoids, petrogenetic and tectonic implications. *Geology* 20, 641-644.
- Eby, G. N., (2011): A-type granites: magma sources and their contribution to the growth of the continental crust. In: Molina, J. F., Scarrow, J. H., Bea, F., Montero, P. (Eds.), Seventh Hutton Symposium on granites and related rocks, Avila, Spain, Abstracts Book with Attendees Addresses, 50–51.
- Ekwueme, B.N. and Matheis, G. (1995): Geochemical and Economic Value of Pegmatites in The Precambrian Basement of Southeast Nigeria. In: R.K. Siwasta and R
- El Hadek H.H., Mohamed A. Mohamed, Galal H. El Habaak, Wagih W. Bishara, Kamal A. Ali (2016): Geochemical Constraints on Petrogenesis of Homrit Waggat Rare Metal Granite, Egypt: *International Journal of Geophysics and Geochemistry*; 3(4): 33-48
- El Hadek, H. H. (2016): Rare-metal granites and their related mineralization, Central Eastern Desert, Egypt. PhD thesis, Geology Department, Faculty of Science, Assiut University. (in press.)
- El-Bouseily, A.M. and El-Sokkary A.A (1975): The relationship between Rb,Sr and Ba in granitic rocks. *Journal of chemical geology* 16: pp. 207-219 *Elements* 8: 289-294
- Fernando Bea (2015): Geochemistry of the Lanthanide Elements Reunión de la Sociedad Española de Mineralogía Huelva 30 de junio al 3 de julio de 2015
- Ferre, E. C., Caby, R., Peucat, J. J., Capdevila, I. R., & Monie, P. (1998): Pan-African post-collisional ferro-potassic granite and quartz-monzonite plutons of Eastern Nigeria. *Lithos*, 45: pp. 255-278.

- Fitches, W. R., Ajibade, A. C., Egbuniwe, I. G., Hole, R. W., Wright, J. B. (1985): Late Proterozoic Schist belts and Plutonism in NW Nigeria. *Journal Geological Society London*, 142, 319 – 337.
- Frost, B. R., Barnes, C. G., Collins, W. J., Arculus, R. J., Ellis, D. J., & Frost, C. D. (2001): A geochemical classification for granitic rocks. *Journal of Petrology*, **42**, pp. 2033-048.
- Gandu AH, Ojo SB, Ajakaiye DE (1986): A gravity study of the Precambrian rocks in the Malumfashi area of Kaduna State, Nigeria. *Tectonophysics* 126:181–194
- Garba, I. (2003): Geochemical Discrimination of Newly Discovered Rare Metal Bearing and Barren Pegmatites in the Pan-African (600 +150 Ma) Basement of Northern Nigeria. *Applied Earth Science Transaction Institute of Mining and Metallurgy* 112. (13): pp. 287- 291.
- Gardien, V., Thompson, A.B., Grujic, D., Ulmer, P., (1995): Experimental melting of biotite + plagioclase + quartz ± muscovite assemblages and implications for crustal melting. *J. Geophys. Res.: Solid Earth* 100, 15581–15591.
- Gardner R. L., Piazzolo S., and Daczko N. R. (2015): Pinch and swell structures: evidence for strain localisation by brittle–viscous behaviour in the middle crust .*Solid Earth*, 6, 1045–1061, 2015
- Goldstein, A. G, (1988.): Factors affecting the kinematic interpretation of asymmetric boudinage in shear zones, *J. Struct. Geol.*, 10, 707– 715.
- Gordiyenko V.V. (1971): Concentration of Li, Rb, and Cs in potash feldspar and muscovite as criteria for assessing rare metal mineralization in granite pegmatites [J]. *International Geological Review*. 13, 134–142.
- Grant NK (1970): Geochronology of Precambrian basement rocks from Ibadan, South-Western Nigeria. *Earth Planet Sci Lett* 10:19–38
- Hanson G.N., (1978): The application of trace elements to the petrogenesis of igneous rocks of granitic composition. *Earth Planet. Sci. Lett.*, 38, 26-43
- Hanson G.N., (1980): Rare earth element in petrogenetic studies of igneous systems. *Ann. Rev. Earth Planet. Sci.* 8, 371-406
- Hofmann, A. (1972): Chromatographic theory of infiltration metasomatism and its application to feldspar. *American Journal of Science* 272, 69-90.
- Hugh R. R. (1993): Using geochemical data: evaluation, interpretation, presentation. Published by Pearson education Asia.in *Earth Sciences* 120, DOI 10.1007/978-3-540-92685-6 1, s C\_ Springer-Verlag Berlin Heidelberg

- Irber, W. (1999): The lanthanide tetrad effect and its correlation with K/Rb, Eu/Eu\*, Sr/Eu, Y/Ho and Zr/ Hf of evolving peraluminous granite suits. *Geochim.Cosmochim. Acta* 63, 489–508
- Jacobson RRE, Macleod WN (1977): Geology of the Liruei, Banke and adjacent Younger Granite ring complexes. *Geol Surv Niger Bull* 33:1–117
- Jacobson, R R. E. and Webb, J.S. (1946): The pegmatites of Central Nigeria.*Geol. Surv.Nigeria Bull.*17(61).
- Jatau, B. S. Temitope, O. L. Hanly Bingari (2012): Petrography and Structural Characterization of rocks around Ragga part of Kura sheet 189 SW North-Central Nigeria. A paper presented at 13RD AGM/Conference of the Nigerian Society of Mining Engineers held in Federal University of Technology Akure, Ondo State, Nigeria between 29thOctober and 1stNovember, 2013.
- Jolliff, B. L., Papike, J. J. and Shearer, C. K. (1989): Inter-and intro-crystal REE variations in apatite from the Bob Ingersoll Pegmatite, Black Hills, South Dakota. *Geochim.Cosmochim. Acta* 53, 429–441.
- Karche, J-P and Vachette, M. (1976.): Migration des complexes subvolcaniques a' structure annulaire du Niger. *Conse'quences.C.R. acad. Sci. Paris*, Vol. **282**, 2033-2036.
- Karche J. P., (1978): Age et migration de l'activite magmatique dans les complexes Paleozoique du Niger. *Consequences. Bulletin Society of Geology, France*, 20, 941-953.
- Kaur, P., Chaudhri, N., Hofmann, A. W., Raczek, I., Okrusch, M., Skora, S., Baumgartner, L. P., (2012): Two-stage, extreme albitization of A-type granites from Rajasthan, NW India. *J. Petrol.* 0, 1-30.
- Kinnaird JA (1984): Contrasting styles of Sn-Nb-Ta-Zn mineralization in Nigeria. *J Afr Earth Sci* 2:81–90
- Kinnaird JA, Bowden P, Ixer RA, Odling NWA (1985): Mineralogy, geochemistry and mineralization of the Ririwai complex, northern Nigeria. *J Afr Earth Sci* 3, 185–222
- Kuster D. (1990): Rare-metal pegmatites of Wamba, central Nigeria – their Formation in Lanthanides, tantalum and niobium, Springer-Verlag, New York, p.274-302.
- London, D., (1996): Granitic pegmatites. Royal Society Edition: *Journal of Earth Science* 87: pp. 305–319.
- London D. (2005): Granitic pegmatites: an assessment of current concepts and directions for the future. *Lithos* 80(2): pp. 281– 303

- London D. and Kontak D. J. (2012): Granitic Pegmatite: Scientific Wonders and Economic Bonanzas Elements, Vol. 8, pp. 257–261
- London, D., (2008): Pegmatites. Can. Mineral., Special Publication
- Martin, R.F., De Vito, C., (2005): The patterns of enrichment in felsic pegmatites ultimately depend on tectonic setting. Can. Mineral. 43, 2027–2048.
- Matheis G, Caen-Vachette M (1983): Rb-Sr isotopic study of rare-metal-bearing and barren pegmatites in the Pan-African reactivation zone of Nigeria. J Afr Earth Sci 1:35–40
- Matheis, G. (1987): Nigerian rare-metal pegmatites and their lithological framework. In: African Geology Reviews. Bowden, P. & Kinnaird, J.A., (Eds.), Geol. Journal, 22:271-291
- McDonough, W.F., Sun, S.S., (1995): The composition of the Earth. Chem. Geol. 120,
- McLennan, S. M. (1994) Rare earth element geochemistry and the “tetrad” effect. Geochim. Cosmochim. Acta 58, 2025–2033.
- Middlemost EAK 1985 Magmas and magmatic rocks. Longman, London
- Miller, C. F. and Mittlefehldt, D. F. (1985): Depletion of light rare-earth elements in felsic magmas. Geology 10, 129–133
- Milord I., Sawyer E.W., and Brown M. (2000): Formation of diatexite migmatite and granitic magmas during anatexis of semi-pelitic metasedimentary rocks: an example from St. Malo, France. Journal of Petrology, vol 4, no.3, pages 487-505
- Moller, P., and Morteani, G. (1987): Geochemical exploration guide for Tantalum pegmatites. *Economic Geology*, 42: pp. 185-187.
- Moody, J. D., Jenkins, J. O. & Meyer, D. (1985): An experimental investigation of the albitization of plagioclase. Canadian Mineralogist 23, 583-596.
- Murrell S. (1990): Deformation process in minerals rocks and ceramics. Published by the academic division of Unwin Hyman Ltd. Pp 109 – 130.
- Nakamura N (1974): Determination of REE, Ba, Fe, Mg, Na and K in carbonaceous and ordinary chondrites. Geochim Cosmochim Acta 38: 757-775.
- O’leary DW, Friedman JD, Pohn HA (1976): Lineament, linear, lineation: Some proposed new standards for old terms.’ Geol. Soc. Am. Bull., 87: 1463-1469.
- O’Connor, J. T. (1965): A classification for quartz-rich igneous rocks based on feldspar ratios. US Geological Survey, Professional Papers 52(5): pp. 79-84.

- Obaje, N.G. (2009): Geology and Mineral Resources of Nigeria, Lecture Notes
- Obiora, S.C. (2009): Field measurements in descriptions of igneous and metamorphic rocks. in Lambert-Aikhionbare, D.O. and Olayinka, A.I. (eds.) Proceedings of Field Mapping Standardisation Workshop, Ibadan University Press, Pp. 105-125.
- Okunlola, O.A., (2005): Metallogeny of Tantalum-Niobium Mineralization of Precambrian Pegmatites of Nigeria. *Mineral Wealth* 137: pp. 38-50.
- Olasehinde, P.I., Pal, P.C. and Annor, A.E. (1990): Aeromagnetic anomalies and structural lineament in the Nigerian Basement Complex. *Journal of African Earth Sciences*, Vol. 11, No. 3/4, Pp. 351-355.
- Olayinka AI (1992): Geophysical siting of boreholes in crystalline basement areas of Africa. *J Afr Earth Sci* 14:197–207
- Oyebamiji A. O., (2014): Petrography and Petrochemical Characteristics of Rare Metal Pegmatites around Oro, Southwestern Nigeria. *Asia Pacific Journal of Energy and Environment*, Volume 1, No 1: 70-88.
- Oyebamiji Abiola, Adeniyi JohnPaul Adewumi, Tehseen Zafar, Adegbola Odebunmi, Philips Falae, Oluwafemi Fadamoro, (2018): Petrogenetic and compositional features of rare metal Pan-African Post-Collisional pegmatites of southwestern Nigeria; A status review. *Contemp.Trennds. Geosci.*, 7 (2), pp 166-187
- Patiño Douce, A.E., Harris, N., (1998): Experimental constraints on Himalayan Anatexis. *J. Petrol.* 39, 689–710.
- Pearce J. A., Harris N. B and Tindle A. G. (1984): Trace element discrimination diagrams for the tectonic interpretation of granitic rocks. *Journal of Petrology*.25: pp. 956–983.
- Pearce J.A. (1996): Sources and Setting of Granitic Rocks. *Episodes* 19(4):pp. 120-125
- Petersson, J. & Eliasson,T. (1997): Mineral evolution and element mobility during episyenitization (dequartzification) and albitization in the postkinematic Bohus granite, southwest Sweden. *Lithos* 42, 123-146.
- Polard D. D., Fletcher RC, (2005): Fundamentals of structural geology. Cambridge University Press. The Edinburgh Building, Cambridge CB2 2RU, UK
- Rahaman MA, Emofurieta WO, Caen-Vachette M (1983): The potassic-granites of the Igbeti area: further evidence of the polycyclic evolution of the Pan-African belt in South-Western Nigeria. *Precambrian Res* 22:75–92

- Rahaman MA, Lancelot JR (1984): Continental crust evolution in SW Nigeria: constraints from U/Pb dating of pre-Pan-African gneisses. In: Rapport d'activite 1980–1984 – Documents et Travaux du Centre Geologique et Geophysique de Montpellier 4:pp 41
- Rahaman MA, Van Breeman O, Bowden P, Bennett JN (1984): Age migration of anorogenic ring complexes in Northern Nigeria. *J Geol* 92,173–184
- Rahaman, M. A., Ekwere, S. J., Azmatullah, M. and Ukpong, E. E. (1988): Petrology and Relation to late Pan-Africa granites. *Mineral Deposita*, 25: pp. 25–33.
- Rudnick, R. L. and Gao, S. (2003): Composition of the Earth Crust. Treatise on Geochemistry, Volume 3.pp. 659.ISBN 0-08-043751-6. Elsevier, 2003., p.1-64
- Samaila KI, Marcus ND, Kukwi JI (2011): The influence of wastewater on soil chemical properties on irrigated fields in Kaduna South Township, North Central Nigeria. *J. Sustain. Dev. Afr. Vol. 13(6): ISSN: 1520-5509.*
- Selway, J.B., Breaks, F.W., Tindle, A.G., (2005): A review of rare-element (Li-Cs-Ta) pegmatite exploration techniques for the Superior Province, Canada, and large worldwide tantalum deposits. *Explor. Min. Geol.* 14, 1–30.
- Shand, S J (1943): Eruptive rocks, 2nd ed. John Wiley, New York, pp 1-444
- Shaw R.A., Goodenough K.M, Roberts N M W, Horstwood M S A, Chenery S R, Gunn A G, (2016): Petrogenesis of rare-metal pegmatites in high-grade metamorphic terranes: A case study from the Lewisian Gneiss Complex of north-west Scotland. Elsevier, *Precambrian research* 281, pp 338-362.
- Shearer, C.K., Papike, J.J. and Jolliff, B.L. (1992): Petrogenetic Links among Granites and Pegmatites in the Harney Peak Rare-Element Granite-Pegmatite System, Black Hills, South Dakota. *The Canadian Mineralogist* , 30, 785.
- Slaby, E. (1992): Changes in the structural state of secondary albite during progressive albitization. *Neues Jahrbuch für Mineralogie, Monatshefte* 1992, 321-335.
- Smith, J.V. (1974): *Feldspar Minerals, Vol. 2, Chemical and Textural Properties.* Berlin: Springer, 690 p.
- Solomon S, Ghebream W (2006): Lineament characterization and their tectonic significance using Landsat TM data and field studies in the central highlands of Eritrea. *J. Afr. Earth Sci.*, 46: 371-378.
- Taylor, S. R. (1964): Trace element abundances and the chondritic Earth model. *Geochimica et Cosmochimica*: pp. 1989-1998
- Taylor, S. R. and McLennan, S. M. (1985): *The Continental Crust: its Composition and Evolution*". Blackwell Scientific Publications, 85: pp. 34-88

- Taylor S.R., Rudnick R.L., Mc Lennan S.C., and Eriksson K.A. (1986): Rare earth element patterns in Archean high- grade metasediments and their tectonic significance [J]. *Geochim.Cosmochim. Acta*, 50, 2267–2279.
- Terekhov E.N. Shcherbakova T.F. (2006): Genesis of positive Eu anomalies in acid rocks from the eastern baltic shield. *Geochemistry international*, vol 44, issue 5, pp 439-455
- Tischendorf G, Forster H. J. and Gottesmann B, (2001): Minor and trace element composition of trioctahedral micas: a review. *Mineralogical magazine*, April 2001, vol. 65(2), pp. 249-276
- Trueman, D.L. and Černý, P. (1982): Exploration for Rare- Element Granitic Pegmatites. *Granitic Pegmatites in Science and Industry*.P. Černý. Winnipeg, Mineralogical Association of Canada. 8.
- Tubosun IA, Lancelot JR, Rahaman MA, Ocan O (1984): U-Pb Pan-African ages of
- Turner DC (1983): Upper Proterozoic schist belts in the Nigerian sector of the Pan-African Province of West Africa. *Precambrian Res* 21:55–79  
two charnockite-granite associations from South-Western Nigeria. *Contrib Mineral Petrol* 88:188–195
- Van Breemen, O. and Bowden, P. (1973): Sequential age trends for some Nigerian Mesozoic granites. *Nature*, London, Vol. **242**, 9-11.
- Van Breemen O, Pidgeon RT, Bowden P (1977): Age and isotopic studies of some Pan-African granites from north central Nigeria. *Precambrian Res* 4:317–319
- Walker, R. W., Hanson, G. N., Papike, J. J., O’Neil, J. R. and Laul, J. C. (1986): Internal evolution of the Tin Mountain Pegmatite, Black Hills, South Dakota. *Am. Mineral.* 71, 440–459
- Whalen J B, Currie K L, Chappell BW (1987): A-type granites: geochemical characteristics,discrimination and petrogenesis. *Contrib Mineral Petrol* 95: 407-419.
- White W.M (2005): Trace elements. In: *Geochemistry*. Wiley-Blackwell. pp 258-278
- Winter J. D. (2014): *Principles of Igneous and Metamorphic Petrology*. *Pearason Education Limited*.Pp 165-172.
- Woakes M, Rahaman MA, Ajibade AC (1987): Some metallogenetic features of the Nigerian basement. *J Afr Earth Sci* 6:54–64
- Wright, J.B. (1970): Controls of Mineralization in the Older and Younger Tin Fields of Nigeria. *Economic Geology* 65: pp. 945-951

- Yassaghi A (2006): Integration of Landsat imagery interpretation and geomagnetic data on verification of deep-seated transverse fault lineaments in SE Zagros, Iran. *Int. J. Rem. Sens.*, 27: 4529-4544.
- Yurimoto, H., Duke, E. F., O'pape, J. J. and Shearer, C. K. (1990): Are discontinuous chondrite-normalized REE patterns in pegmatic granite systems the results of monazite fractionation? *Geochim.Cosmochim. Acta* 54, 2141–2145.
- Zhao, Y. X. (1988): Ore-forming mechanism of Qianlishan granite stock discussed from the relationship of Shizhuyuan W-polymetallic deposit with the
- Zhao, Z.H., Xiong, X.L., Han, X.D., Wang, Y.X., Wang, Q., Bao, Z.W., Jahn, B.M., (2002): Controls on the REE tetrad effect in granites: evidence from the Qianlishan and Baerzhe granites, China. *Geochemical Journal*, 36, 527-543.